The Use of Terrestrial Laser Scanners for 3-Dimensional Modelling and Quantification of the Effects of Competition and Phenology on Plant Structure with Fractal Analysis and Quantitative Structural Modelling Tools

By

Felipe Alencastro

A thesis submitted in partial fulfillment of the requirements for the degree of

Doctor of Philosophy

Department of Earth and Atmospheric Sciences

University of Alberta

Abstract

Terrestrial laser scanners (TLS) are active remote sensing sensors that use light to measure distances between the sensor and objects generating a three-dimensional dataset. This technology has been used in a diverse range of ecological studies measuring plant and vegetation properties. In the present dissertation, I used three-dimensional modelling algorithms on TLS derived point-clouds to assess plant structural parameters, plant competition, and the effects of plant phenological processes on tree structure.

Chapter 2 uses the Quantitative structure Model (QSM) to assess lianas and host-trees structural metrics in three different lianas infestation scenarios. The findings reveal that liana infestation impacts hosting trees differently. Lifeform structural metrics showed that lianas wood elements can reach much longer lengths than the elements of the host trees indicating a better space distribution. Also, the total wood volume proportion presented by each lifeform varies with the tree size and the level of liana infestation. In the end, two QSM derived metrics were proposed to evaluate liana infestation on trees of different sizes and ecosystems.

In chapter 3, fractal analysis was used to identify structural differences between trees living in forested and open-field environments. This study showed that the competition against neighboring plants in forested areas affects tree development and space occupancy. Trees living in open-field conditions occupy the space more efficiently and present more symmetric architecture than trees living in the forest, indicating less environmental stress.

The presence of leaves has a great impact on plant three-dimensional modelling, space occupancy, and tree architecture. In chapter 4, fractal analysis was used to explore the effect of the change of leave coverage on temperate broad-leaf tree species during the winter and spring seasons on tree architecture. The findings showed that trees occupy the space more efficiently during the leafed season. Last, Chapter 5 presents the summary of this thesis findings and provides directions for future research on three-dimensional modelling of plants using TLS point-clouds.

Preface

The chapters of this thesis are unpublished work. Chapters 2, 3 and 4 are being prepared for publication. I did the conceptualization of the research with the support of Dr. Arturo Sanchez-Azofeifa. I performed the data collection with the support of different field assistants. The data processing and analysis was performed by me. Antonio Jose Guzman Quesada provided text editions in the chapter 3. Dr. Arturo Sanchez-Azofeifa provided supervisory support and text editing during all the research process for the development of this dissertation. This research was partially funded by CAPES – Brazilian Education Agency.

Contents

Abstract ii
Preface iii
List of Tables vii
List of Figures viii
Glossary of Terms x
Chapter 1 - Introduction 1
1.1 - Motivation 1
1.2 - Objectives 3
1.3 - Scientific Background 4
1.4 - Thesis outline 8
Chapter 2 – Using Terrestrial Laser Scanner to analyze liana and hosting trees woody contribution. 11
2.2 - Methods 13
2.2.1 Study Site 13
2.2.2 Data Collection 14
2.2.2.a) Tree selection 14
2.2.2.b) TLS data collection 15
2.2.3- Registration 16
2.2.4- Pre-processing steps for Quantitative Structure Model (QSM) 16
2.2.5- Implementation of the Quantitative Structure Model (QSM) 17
2.2.6- Estimation of the liana's relative volume and load 19
2.3.1 - QSM performance on a complex vegetation point-cloud 20
2.3.2 Quantitative Structure Model (QSM) metrics 20
2.3.3 Relative volume and liana load 22
2.4 Discussion 23
2.4.1 Impact of plant lifeform interaction on dataset quality and QSMs modeling 23
2.4.2 QSM metrics to estimate RV and LL as tools for ecological assessment of infested trees 25
2.4.3 Limitations and uncertainties 28
2.5 – Conclusion 29
Chapter 3 Fractal Analysis on Forested and Open Field Trees 31
3.1 – Introduction 31
3.2 – Methods 33

3.2.1 - Site description 33
3.2.2 – Data Collection 33
3.2.3 – Registration 34
3.2.4 – Pre-processing procedures 34
3.2.5 – Fractal dimension 36
3.3 –Results 37
3.3.1- Fractal dimension 37
3.3.2 – Intercept 40
3.3.3 – Coefficient of determination 41
3.4 – Discussion 41
3.4.1 - Fractal dimension 42
3.4.2 – Coefficient of determination and developmental instability 43
3.4.3 – Intercept 45
3.4.4 – Light Competition and Tree Architecture 45
3.4.5 – Advantages and weaknesses of the method 46
3.5 - Conclusion 47
Chapter 4 – Using TLS and Fractal Analysis to Detect Structural Changes Caused by Phenology in Deciduous Trees 48
4.1 – Introduction 48
4.2. - Methods 50
4.2.1 Tree species 50
4.2.2 – Data collection 52
4.2.3 -Pre-processing procedures 53
4.2.4 – Fractal analysis 56
4.2.5 – Data analysis 57
4.3 – Results 57
4.3.1 – Fractal dimension 57
4.3.2 – Coefficient of determination (R square) 58
4.3.3 – Intercept 59
4.4 – Discussion 60
4.4.1 - Fractal dimension 60
4.4.2 - Coefficient of determination 61
4.4.3 - Intercept 62

4.4.4 - Methods advantages and limitations 62
4.5 - Conclusion 64
Chapter 5 – Concluding Remarks and Future Work 66
5.1 - Thesis key findings 66
5.2 – Future directions for three-dimensional modelling of vegetation 67
5.2.1 - Lianas Infestation 67
5.2.2 - Fractal Analysis of forested vs open field trees 68
5.2.3 – Fractal analysis of the phenological process in deciduous temperate trees 69
References 71

List of Tables

Table 2.1 - QSM Metrics derived for Tree and Liana components in the three study plots. Values in brackets represent DBH field measurements on trees and liana modelling values without the adjustments. All remaining values are derived from modeling after adjustments. ……21

Table 3.1. Fractal Metrics of Forest Trees at the RSNP-EMSS……38

Table 3.2. Fractal Metrics of Open Field Trees at the RSNP-EMSS ……..38

Table 4.1 Fractal analysis metrics for leaf-on and leaf-off tree point-clouds. ……57

List of Figures

Figure 2.1: Location of Santa Rosa National Park – Environmental Monitoring Super Site……14

Figure 2.2: Liana Infestation based on traditional approaches (number of liana stems, basal area, and canopy coverage). In red is presented the liana`s wood elements TLS point-cloud segmentation, whereas in green is presented the hosting tree TLS point-cloud. The segmentation between liana and tree datasets reached 12.2 meters for hosting tree 1; 11.5 for hosting tree 2; and 11.9 for hosting tree number 3. ……15

Figure 2.3: Sub-divided lianas datasets (Blue, red and green) from infested tree number 3. The QSM reconstructed individually in each subsection point-cloud and the metrics were combined to retrieve the total liana contribution. ……18

Figure 2.4: Lianas modeled using the QSM from tree number 3. Liana Stem diameter inconsistencies are indicated by red circles and were minimized by maintaining higher cylinder diameters within each QSM segment……19

Figure 2.5: Host tree number 1 presenting stem irregularities that caused QSM underestimation of tree DBH, and total wood volume. (A) In blue buttress; and (B) point-cloud horizontal cut on the trunk at DBH with non-cylindrical. Point to point calculations (72.5; and 73.1 centimeters) corroborate field measurement and contrast the model (72.5 vs 54.1). ……22

Figure 2.6: Liana infestation evaluation based on the liana load supported by each hosting tree…23

Figure 2.7: Tree and liana modelled elements distribution. It is possible to observe the hosting tree on plot 2 leaning towards the liana climbing elements, indicating structural stress due to the high liana load. ……27

Figure 3.1: Forested trees merged point-clouds with a spatial resolution of 0.01 meter. Tree colours represent the same living environment since the species was not gathered. Forested individuals were dominant emergent trees. The scale below each tree measures 10 meters. ……..35

Figure 3.2: Open-field trees merged point-clouds with a spatial resolution of 0.01 meters. In this figure, tree colors represent the same tree species. The scale below each tree measures 10 meters. ……36

Figure 3.3: Plot values of fractal dimension (top); intercept (centre); and coefficient of determination (down) of forested trees (green) and open-field trees (blue). ……40

Figure 3.4: Tree point-clouds divided in quarters using the trunk base and crown edges as reference and limits. Open-field trees (A to D) present higher symmetry than forested trees (E to H). Forested trees E and H present cells with rectangular shapes instead of the most commonly found square format. Open-field trees present their crown highest point aligned with their trunks. This behaviour is observed even when X, Y, and Z axes positions are dislocated (Open-field tree B), whereas in the forested trees F, G, and H the crown highest point is dislocated from the trunk center. The scale bar bellow trees represent 10 meters. ……41

Figure 4.1: Leaf-off tree point-clouds. Trees 1, 3, 5, and 7 present smaller size, and irregular crown shape due to their spatial arrangement with less sun light availability than trees 2, 4, 6, and 8. The former show a more symmetrical crown shape. Tree 9 is considerably larger than the other trees due its age. ……..52

Figure 4.2: Methodological procedures adopted in this study. In blue is the data acquisition, in orange the pre-processing procedures and in green the post-processing steps. ……..53

Figure 4.3: Structural differences between leaf-off (A, grey) and leaf-on (B, green) tree point-clouds. The leaf-off point-clouds permit the identification of individual branches, while the leaf-on datasets present higher point density on the crown region, hampering branch identification. 1A and 1B present a juvenile tree located on shadowed line (Tree number 1) with an irregular crown; in 1A is possible to observe disconnected points due to obstruction caused by the leaves on the top right of the crown. 2A and 2B presented juvenile tree from the illuminated line (tree number 4) with regular elliptical crown; the leafed point-cloud (2B) also showed some occlusion observed by the difference in point density on the top of the canopy. 3A and 3B present the mature tree (number 9) with prominent difference on the gap size on crowns of the two datasets. All leafed point-clouds (1B, 2B, and 3B) present leaf structures on the lower part of their trunks that were not detectable on the leaf-off datasets. ……..55

Figure 4.4: Violin graph representing the variability of fractal dimension values derived from TLS trees acquired during the leaf-on and leaf-off seasons. Points represent the values calculated for the two seasons. Mean for the leaf-off is 0.66 while the mean for the leaf-on is 0.68. ……....58

Figure 4.5: Violin graph representing the variability of the coefficient of determination values derived from TLS trees acquired during the leaf-on and leaf-off seasons. Points represent the values obtained for the two seasons. Mean for the leaf-off is 0.99 while the mean for the leaf-on is 0.98. ……..59

Figure 4.6: Violin graph graph representing the variability of intercept values derived from TLS trees acquired during the leaf-on and leaf-off seasons. Points represent the values for the two seasons. Mean for the leaf-off is 2.25 while the mean for the leaf-on is 2.32. ……..60

Glossary of Terms

ACG – Area de Conservacion Guanacaste

ALS – Airborne Laser Scanner

DBH – Diameter at Breast Height

*d*HB – Fractal Dimension from fractal geometry

FOV – Field of View

GLAS - Geoscience Laser Altimeter System

LiDAR- Light detection and Ranging

LL – Liana Load

NIR – Near InfraRed

PAI – Plant Area Index

PAVD – Plant Area Volume Density

QSM – Quantitative Structure Model

RMSE –Root Mean Square Error

R^2 – Coefficient of determination

SE – Standard Error

SOR – Statistical outlier removal

SRNP – EMSS - Santa Rosa National Park – Environmental Monitoring Super Site

SRTM – Shuttle Radar Topography Mission

TDF – Tropical Dry Forest

TLS- Terrestrial Laser Scanner

UAV – Unmanned Aerial Vehicle

3D- Three-Dimensional

Chapter 1 - Introduction

1.1 - Motivation

Forests are an important component of Earth's biosphere as they have a major influence on water, carbon, and energy cycles, affecting the global and regional climate (Rodriguez-Veiga et al., 2019; DellaSala, 2020, Fan et al., 2020). Forested ecosystems cover approximately one-third of the world`s land surface (Rodriguez-Veiga et al., 2019; DellaSala, 2020). These environments provide food and shelter to wildlife while supporting biodiversity (Fan et al., 2020). More than 40% of global forests are located in the tropics; temperate and boreal forests occupy around 25% each; and sub-tropical forests represent around 8% of the planet forested area (DellaSala, 2020). These ecosystems provide humans with food, wood for energy, shelter and tools. Humanity benefits economically from varied forest products as they also have important socio-cultural value with a myriad of uses from recreational to spiritual activities (Rodriguez-Veiga et al., 2019; DellaSala, 2020, Fan et al., 2020).

Forest ecosystems are composed of different elements, but one of the most important is their structure. Forest structure refers to the three-dimensional arrangement of plant elements (Kay et al., 2021; Annighofer et al., 2022). It reflects the environment complexity and influences forest productivity and dynamics, biodiversity, above and below carbon stocks, evapotranspiration, and forest resilience (Ali et al., 2020; Rago et al., 2021; Reich et al., 2021; Kay et al., 2021; Annighofer et al., 2022; Shimizu et al., 2022). Forest structure is affected by solar radiation, water availability, altitude, latitude, soil properties, human and natural disturbances (Candel-Perez et al., 2021, Rago et al., 2021). The effect of human interventions is reflected by different forest structure patterns that can be observed in the different successional stages after human interference (Kappelle et al., 1996; Gerwing, 2001; Faria et al., 2009; Sanchez-Azofeifa et al., 2009; Rodig et al., 2017; Sanchez-Azofeifa et al., 2017). Changes in atmospheric composition caused by human activities can affect forest dynamics leading to modification of the forest structure (Zotz et al., 2006). The increasing dominance of lianas in tropical forests is an example of these occurrences (Phillips et al, 2002; Zotz et al., 2006; Schnitzer and Bongers, 2011). The assessment of forest structure can be done by evaluating parameters such as basal area, canopy height, plant area index, number of forest strata, canopy openness, among others (Culvenor et al., 2014; Reyes-Palomeque et al., 2021).

At the tree level, structural complexity is known as tree architecture and reflects how each plant occupies a given space (Seidel et al., 2018; Seidel et al., 2019; Verbeeck et al., 2019; Shenkin

et al., 2020). Structural complexity is an important component in understanding leaves organizational arrangement which affects photosynthesis and gas exchange (Pickett and Kempf, 1980; Seidel et al., 2018; Rago et al., 2021). The tree height, the crown area, the branch order, the stem length, the diameter at the breast height (DBH), and leaf area are metrics commonly used to characterize tree architecture (Pickett and Kempf, 1980; Cote et al., 2011; Gulci et al., 2021). Tree basic metrics such as tree height and trunk diameter have been assessed to measure wood stock and forest growth since the beginning of rational use of forests to manage stock in forested areas (Andersen et al., 2006; Bragg, 2008). Throughout history, different methods and multiple tools were used to collect these parameters (Luoma et al., 2017; Wang et al., 2019; Jurjevic et al., 2020). Telescopic height poles and measuring ropes are examples to directly measure tree height that are still used (Wang et al., 2019; Jurjevic et al., 2020). Poles are manipulated from the ground whereas the ropes must be launched from the top of the tree until they reach the ground. These methods are time-consuming, inaccurate for tall trees, and involve some degree of risk for the survey team (Andersen et al., 2006; Jurjevic et al., 2020). Popular indirect field-based methods use trigonometric relationships between the distance and tangent angles formed by the observer and the measured tree crown top and stem base (Andersen et al., 2006; Luoma et al., 2017; Wang et al., 2019; Jurjevic et al., 2020). These indirect methods employ rangefinders, calipers and clinometers as tools to increase time efficiency compared to direct measuring methods (Andersen et al., 2006; Luoma et al., 2017; Wang et al., 2019; Jurjevic et al., 2020). Although these classic methods improve productivity over time, the intensive inventory on vast areas continues to be time-consuming and costly (Andersen et al., 2006, Shimizu et al., 2022). For this reason, the use of samples to model the population is an important strategy to understand forest behaviour (Wiant et al., 1996; Jurjevic et al., 2020).

Remote sensing has emerged as a fundamental technology to measure extensive forested areas since it can operate from diverse platforms, collecting data with different spatial and temporal resolutions in local and global scales (Lefsky et al., 2005; Sun et al., 2008; Sanchez-Azofeifa et al., 2017). LiDAR sensors produce high detailed three-dimensional information generated from a single or multiple points of illumination (Lefsky et al., 2002; Sun et al., 2008; Culvenor et al., 2014; Wilkes et al, 2017; Kay et al., 2021; Wang et al., 2021). In the past decades, LiDAR systems have been used extensively to assess tree and forest metrics from orbital platforms to field measurements (Lefsky et al., 2005; Calders et al., 2015; Brede et al., 2019; Wu et al., 2019; Kay et al., 2021; Zhang et al., 2022). Terrestrial laser scanners (TLS) have proved to measure plant structural metrics with unprecedented accuracy enabling great advances in tree and forest measurement and modelling

(Hosoi and Omasa, 2007; Raumonen et al., 2013; Calders et al., 2015; Seidel et al., 2018; Seidel et al., 2019; Brede et al., 2019).

1.2 - Objectives

The ability of Terrestrial Laser Scanners (TLS) to accurately assess tree and forest metrics in natural areas brings the opportunity to investigate plant structure in detail. In this thesis, I use TLS technology to understand how plants respond structurally to forest competition and environmental changes. The objectives of the present study are to address the following questions:

1 – What are the liana and host tree wood contributions in different degrees of parasitism in a liana-infested tropical dry forest?;

2 - Is fractal analysis capable of identifying structural differences in tree architecture of individuals living in the tropical dry forest and open-field environments?; and

3 – Is fractal analysis able of identifying structural differences caused by phenological processes in temperate deciduous trees?

To answer the first question, a group of liana-infested trees in the Santa Rosa National Park Environmental Monitoring Super Site SRNP-EMSS tropical dry forest was selected. I used a multiple point-of-view scan dataset and Quantitative Structural Model (QSMs) to assess liana and host tree structural metrics and space occupancy of each lifeform. I analyzed hosting trees and lianas segmented datasets individually to compare the different scenarios of infestation and its effects on the hosting trees.

For the second question, fractal analysis on TLS point-clouds generated from trees living in forested and open-field environments was employed to test the ability of voxels to identify modifications on the tree architecture caused by competition with neighbours' plants.

Last, I used two TLS datasets from a group of temperate deciduous trees, collected on two sequential phenological seasons. Fractal analysis was applied to the tree point-clouds with and without the presence of leaves to identify structural differences on these trees during one phenological cycle.

1.3 - Scientific Background

LiDAR (Light Detection and Ranging) is an active remote sensing method that uses laser light to measure the distance between the sensor and the objects. LiDAR uses the return travel time of light to define the range or distance between the sensor and the target. The range is half the return travel time multiplied by the speed of light (approximately 300,000 kilometers per second) (Dubayar and Dranke, 2000). The accuracy of this technology gives it a broad spectrum of uses in ecological, environmental, and forest structure studies. (Drake et al., 2002; Hopkinson et al., 2004; Castillo-Núñez et al. 2011; Rosell et al., 2012; Yang et al., 2013; Portillo-Quintero et al. 2014; Calders et al., 2015; Akerblom et al., 2017; Verbeeck et al., 2019).

There are two different measuring methods used today. The most commonly used in forestry is Time-of-Flight LiDAR which measures the distance using the time of the return of each laser signal emitted by the sensor (Drake et al. 2002). It can use discrete return systems, which record only the position of one contact between the laser beam and the target (Beland et al.,2014B), or full waveform systems, which record the full-time trace of the laser beam that is reflected by the object (Cifuentes et al., 2014 2014). The analysis of forest attributes using waveform LiDAR data can be done by decomposing the waveform into points and estimating structural metrics, analyzing the proportion of each forest strata present in the waveform dataset (Anderson et al., 2015; Disney et al., 2016). Both, high-density discrete return and full-waveform systems have been shown to provide similar forestry structural metrics (Van Leeuwen et al., 2010). The second method, the Phase-Based sensors, uses a constant laser with intensity-modulated at different frequencies, these systems can record with higher accuracy, but they are limited by the range that they can work, usually less than 100 meters (Cifuentes et al., 2014). They also have very high levels of data noise. For this reason, those systems are not commonly used for forestry and environmental studies (Cifuentes et al., 2014).

Since the 1930s, forestry was one the first disciplines to generate three-dimensional information from remote sensing data, mostly by using aerial photographs and stereoscopy to map vast areas of forest and also for measuring individual trees (Rosell et al., 2009). The use of LiDAR to study forestry was initially airborne, or Airborne Laser Scanning (ALS). Early studies that used ALS for forestry applications dated from the beginning of the 1980s. At the time, the Canadian Forest Service demonstrated the capacity of these sensors to measure stand heights, plant cover density and ground elevation (Lim et al., 2003). At the same time, LiDAR was used to map tropical forests in Central America (Lim et al., 2003). Most ALS research on forest environments focuses on ground and surface modelling to measure tree and forests heights (Hollaus et al, 2006; Klober et al., 2007;

Morsdorf et al., 2010, Wang et al., 2019). More recently studies are assessing detailed forest metrics (Yao et al., 2012; Pearse et al., 2018; Novotny et al., 2021), forest biomass (Nelson et al., 2017; Laurin et al., 2020), forest carbon storage (Hopkinson et al., 2016; Coomes et al., 2017; Jucker et al., 2018), and understory structural features (Jarron et al., 2020) on diverse forest environments.

LiDAR became an important tool for analyzing vegetation structure at various scales (Beland et al., 2014B). In 2003 NASA launched the Ice, Cloud and Land Elevation Satellite (ICESat) with its mounted sensor, the Geoscience Laser Altimeter System (GLAS). This LiDAR instrument is a full waveform system with a circular footprint of approximately 65 meters and a temporal resolution of 183 days. GLAS is the first LiDAR sensor for continuous global observation of the planet (Van Leeuwen et al. 2010). Lefsky et al. (2005) estimated tree height and forest biomass in temperate coniferous and deciduous forests in North America and tropical forests at the Amazon basin attesting the capacity of this data to assess forest structural metrics on different biomes. Boudreau et al. (2008) found that GLAS data can be used to access above-ground biomass at global scales. Sun et al. (2008) attested the geolocation and canopy height accuracies of this sensor by comparing GLAS data with radar (SRTM) and airborne LiDAR (LVIS) derived models. Nelson (2010) pointed out issues with GLAS heights and biomass calculations in areas with a low plant density in the Canadian boreal forest. The integration of GLAS with different remote sensing datasets was used to calculate mangrove height and biomass in Africa (Fatyinbo and Simard, 2013), and to estimate the amount and distribution of boreal forest biomass in North America (Margolis et al., 2015). Hajj et al. (2017) pointed out that integrating GLAS data with optical imagery increased the precision of biomass calculations in forests with high biomass concentration. The sensor is out of service since 2010, but its data are still being used to generate forest structure attributes (Kay et al., 2021).

From macro to micro scale, the use of Unmanned Aerial Vehicle (UAV) based LiDAR sensors to assess forest metrics at local scale became popular in the past decade (Wallace et al., 2012; Guerra-Hernandez et al., 2017; Wu et al., 2019; Lin et al., 2021, Zhang et al., 2022). LIDAR sensors operating from a UAV platform produce highly detailed point-clouds from above the forest canopy at a much lower cost than ALS and Satellites derived datasets (Wallace et al., 2012; Li et al., 2019; Hu et al., 2021; Zhang et al. 2022). The lower costs and high mobility of UAV-based LIDAR systems provide the possibility of temporal analysis of forest structure (Wallace et al., 2011; Guerra-Hernandez et al., 2017; Shrestha et al., 2021; Zhang et al., 2022).

Contemplating a reversed perspective from the LiDAR systems above, Terrestrial Laser Scanners (TLS) operate below the forest canopy (Liang et al., 2018; Shimizu et al., 2022) from the

ground and often stationary platform (Beland et al., 2011; Liang et al., 2018). TLS systems have a similar performance to ALS regarding operational wavelength, operational ranging and accuracy and pulse repetition frequency. TLS has the advantage of lower operational cost and freedom from limitations associated with ALS real-time georeferencing (Coveney and Fotheringham, 2011). Regarding the spatial resolution, airborne LiDAR systems present an average resolution varying between 0.1 and 1.0 meter. Ground-based scanners or terrestrial laser scanning (TLS) have a resolution that varies with the model and type of the equipment between 0.005 and 0.10 meter (Yang et al., 2013). For these characteristics, TLS sensors have great potential for describing forest structure with an unprecedented level of detail, while providing unique 3D fine-scale information of the distribution of plant elements (Van der Zande et al., 2009; Hosoi et al., 2013; Beland et al., 2014; Akerblom et al., 2017; Liang et al., 2018; Fan et al., 2020).

Point density and the field of view are essential characteristics of the sensor. Culvenor et al. (2014) developed an instrument that accesses forest structural properties with a scan geometry of 360° azimuths at a constant zenith angle (57.5°) that makes only 920 measurements. The field of view (FOV) of the instrument is what defines the space that will be scanned. Sensors with hemispherical FOV, such as TLS systems, can create a 3D point cloud of their surroundings from a static station and are fully automated; these datasets can have millions of measurements (Lichti and Jamtsho, 2006; Abbas et al., 2013; Shimizu et al., 2022). On the other hand, the point density of those point clouds is negatively correlated with the range, which means that objects closer to the sensor will be represented by a higher point density than objects located further, resulting in density differences in the representation of the 3D scene (Van der Zande et al., 2006, Lichti and Jamtsho, 2006; Beland et al., 2011; Cifuentes et al., 2014). Most sensors used in ecological and environmental applications have measure rates between 50,000 to 200,000 points per second (Abbas et al., 2013), generating datasets with tens of millions of points.

The intensity of the reflected laser signal is an important part of the information provided by TLS systems. It is related to the inclination at which the laser beam hits a target as well as the material interaction with the wavelength of the laser for a given instrument (Beland et al., 2011; Sun et al., 2014; Disney et al.,2015). For forestry studies, it is preferable to use near-infrared (NIR) lasers because in the NIR it is possible to separate wood and leaves (Rosell et al., 2012; Beland et al., 2014; Beland et al.,2014B). Thirty-two bands hyperspectral LiDAR sensors ranging from 309 to 914 nanometers proved to have the capacity to reveal biochemical parameters of the vegetation (Sun et al., 2014). There are many different TLS systems available on the market with different characteristics,

such as FOV, point density, laser wavelength, range and price. Understanding the advantages and limitations of them are important to help select the better one for each type of application.

Some limitations present in all TLS and other LiDAR systems are related to atmospheric conditions such as dust, wind, and humidity that can create ghost points, which are points without connection to any plant structure (Rosell et al., 2012; Beland et al., 2014B). Occlusion, or shadow effect, is another important issue of TLS measurements. This problem is related to plant density, and it is more prominent in forest environments with tall trees, high density of leaves, branches, and understory (Beland et al., 2011; Coveney and Fotheringham, 2011; Beland et al., 2014).

The use of data from multiple points of illumination created by positioning the TLS instrument at different locations in the forest, and merging the scans into a single dataset can create highly complex representations of vegetation structure (Beland et al., 2014, Wilkes et al., 2017, Liang et al., 2018). The process of merging point clouds from different stations is called registration. This procedure generates a complete three-dimensional dataset and helps minimize the occlusion effect improving the quality of the data. The negative effect is the accumulation of errors such as ghost points generated on individual scans (Van der Zande et al., 2006; Cifuentes et al., 2014; Wilkes et al., 2017). The point-cloud merging process can also generate undesirable consequences. Burt et al. (2013) found that a registration global error of 0.01 meter can lead to an error of 8.8% in biomass volume calculation.

The analysis of the TLS data for extracting forestry metrics has three main approaches: Voxel-based, Gap Probability-based vertical profile density methods, and Quantitative Structure Models. The voxel-based approach consists of the conversion of a LiDAR point cloud into voxel elements in a 3D arrangement to reproduce the plant features as a voxel model (Hosoi et al., 2013). Voxels are three-dimensional representations of a given volume such as pixels are the two-dimensional representation of a specific area. Voxel-based TLS models have been successfully used to calculate forestry parameters such as Leaf Area Density (Hosoi and Osama 2006; Hosoi and Osama 2007) and canopy gap fraction (Cifuentes et al., 2014). This method was also used to accurately estimate tree volume (Hosoi et al., 2013). The use of voxels is also employed in studies using fractal analysis of TLS point-clouds to retrieve plant structural information. These studies assessed the tree and stand volume and other structural metrics (Guzman et al., 2020), determining tree structural complexity (Seidel et al., 2018), and explored how environmental conditions affect tree architecture (Seidel et al., 2019).

The second approach, vertical profile density analysis, uses a Gap Probability theory, a similar approach to the full waveform LiDAR systems. This approach uses TLS point cloud data to model the forest structure by measuring plant density along with the forest vertical profile (Culvenor et al., 2014; Sanchez-Azofeifa et al., 2017). This methodology has been used to estimate Plant Area Volume Density (PAVD) which is a function of the vertical plant profile per volume unit and Plant Area Index (PAI) using data from different TLS sensors (Culvenor et al., 2014; Sanchez-Azofeifa et al., 2015; Rodriguez-Ronderos et al., 2016; Sanchez-Azofeifa et al., 2017). This approach has been used to understand the structural effects of liana removal on the forest (Rodriguez-Ronderos et al., 2016), to assess the effect of phenological processes on forest structure (Portillo-Quintero et al., 2014), and to identify structural differences on forests caused by local environmental conditions (Sanchez-Azofeifa et al., 2015; Sanchez-Azofeifa et al., 2017).

Quantitative Structure Models use a cylinder fitting approach to reconstruct tree woody elements retrieving structural metrics (Raumonen et al., 2013; Calders et al., 2015; Brede et al., 2019). It performs over single tree TLS datasets generated by multiple point-clouds from different illumination angles to create a complete three-dimensional view of the modelled tree (Burt et al., 2013; Raumonen et al., 2013; Calders et al 2015; Akerblom et al., 2017). From the QSMs one can compute tree height, diameter at the breast height (DBH), tree and trunk volumes and additional metrics fundamental to characterize tree architecture and complexity such as branch order, number of branches among others (Raumonen et al., 2013). Studies have shown its ability to accurately calculate tree wood volume and biomass (Burt et al., 2013; Raumonen et al., 2013; Kaasalainen et al., 2014; Calders et al., 2015; Brede et al., 2019) and tree species identification based on tree architectural parameters (Akerblom et al, 2017).

For its intrinsic characteristics and the variety of data analysis approaches available, TLS technology is an important tool for forestry and environmental research with proven ability in a myriad of plant structure assessment studies (Rosell et al., 2009; Palleja et al., 2010; Burt et al., 2013; Hosoi et al., 2013, Culvenor et al, 2014; Cifuentes et al., 2014; Calders et al., 2015; Sanchez-Azofeifa et al., 2015; Akerblom et al., 2017; Brede et al., 2019).

1.4 - Thesis outline

The chapters in this thesis use different three-dimensional modelling approaches to measure plant structure, plant competition, and the effect of plant phenology in tree structure. The chapters in this thesis dissertation were designed to be self-contained for publication in scientific journals;

therefore, some level of repetition should be expected. This redundancy is more present in chapters three and four since they use a similar methodology. Below is presented a summary of each chapter methodology and its relevance for the development of scientific knowledge of forest structure.

The interaction between two competing tropical forest plant lifeforms is explored in chapter 2. QSMs were used to measure structural metrics of lianas and host trees. This chapter investigated liana infestation in three different scenarios, from minor to high degrees of liana infestation. The woody material structural metrics were analyzed for each lifeform and infestation level to understand the dynamics and space occupancy and distribution pattern between lianas and host trees. The importance of this study relates to the increase of liana infestation on tropical forests (Phillips et al., 2002; Schnitzer, 2005; Ingwell et al., 2010; Schnitzer and Bongers, 2011), and its implications to forest ecology (Schnitzer and Bongers, 2002; Hilje et al., 2017; Mohandass et al., 2017; Schnitzer, 2018), to forest structure (Sanchez-Azofeifa et al., 2009; Lobo-Catalan and Jimenez-Castillo, 2014; Rodriguez-Rondero et al., 2016; Sanchez-Azofeifa et al., 2017; Schnitzer, 2018), and to forest growth (Gerwing, 2001; Schnitzer, 2005; Meunier et al., 2020). Moreover, the comprehension of liana infestation dynamics, its effects on host trees, and the outcome in the infested ecosystems are fundamental since liana increasing dominance on tropical forests was described as an important fingerprint of climate change (Lewis et al., 2004).

In chapter 3, I used fractal analysis to identify structural differences in trees living in forested and open-field environments. The voxel size versus the number of voxels necessary to characterize a TLS point-cloud of single trees and linear regression is the key aspect of the methodology used in this chapter. Fractal analysis derived metrics reveal space occupancy, symmetry, and size of the analyzed organisms (Escos et al., 1995; Alados et al., 1996; Alados et al., 1999; Escos et al., 2000; Alados et al., 2008; Seidel et al., 2018; Seidel et al., 2019, Guzman et al., 2020). This information permits the understanding of the complexity of the trees (Escos et al., 1995; Alados et al., 1996; Alados et al., 1999; Escos et al., 2000; Alados et al., 2008; Seidel et al., 2019; Seidel et al., 2019) and developmental stability of the environments they are living in (Freeman et al., 1993; Escos et al., 1995; Escos et al., 2000; Alados et al., 2008; Seidel et al., 2018; Guzman et al., 2020). The goal of this chapter is to test the ability of a new TLS fractal dimension analysis tool to assess the structural differences of these two groups. The significance of this study is to understand structural differences between open-field individuals and trees living in the light-permeable tropical dry forest.

In chapter 4, I used the same fractal analysis method to detect structural differences caused by the presence of leaves on temperate deciduous trees during one phenological cycle. Plant

phenology is essential to tree development, competition and survival (Ghelardini et al., 2014; Richards et al., 2020, Fu et al., 2020). This process is especially important in environments that present fluctuation on the availability of plant vital resources, such as nutrients, water, photoperiod, solar radiation intensity, and/or temperature (Ghelardini et al., 2014; Peaucelle et al., 2019; Fu et al., 2020). The main aspect of this chapter was to test if fractal analysis is capable to identify the structural modification on trees caused by the presence of leaves as a consequence of their phenological cycle. The importance of this study is to understand the structural transformation observed in dormant and growing seasons, and how those changes reflect on tree space occupancy efficiency.

In chapter 5, the thesis dissertation findings are summarized, while a set of new questions that emerged from our research are presented. Directions to new studies regarding plant modelling were also presented in this final chapter to improve the knowledge, the use, and the accuracy of TLS derived three-dimensional modelling of the vegetation.

Chapter 2 – Using Terrestrial Laser Scanner to analyze liana and hosting trees woody contribution.

2.1 - Introduction.

Lianas are a non-structural plant lifeform that parasitize trees by using them as structural support to reach the top of the forest canopy, while at the same time competing for resources and nutrients above and below the ground (Schnitzer et al., 2002). The abundance and diversity of lianas are driven by climate seasonality and forest disturbance (Schnitzer and Bongers, 2002; Schnitzer, 2005, Parolari et al., 2020; Waite et al, 2023). Recent studies have shown that lianas are extending their dominance in tropical forests (Phillips et al., 2002, Schnitzer and Bongers, 2011; Reis et al., 2020). Moreover, liana stems can represent approximately 25% of the total woody stems in many tropical forests (Schnitzer and Bongers, 2002). This dominance has been identified as one of ten key environmental change fingerprints in tropical environments (Lewis et al., 2004).

The detrimental effects of liana infestation on trees are well documented. Lianas are known to increase tree mortality, decrease tree growth and leaf productivity, impact forest structure along the path of ecological succession, and change tree architecture (Laurance et al., 2014; Matthews et al., 2016; Sanchez-Azofeifa et al. 2017; da Cunha Vargas et al., 2021). Recently, liana removal experiments conducted to understand this lifeform's contribution to forest structure found that lianas represent approximately 20% of the forest Plant Area Index (PAI) (Rodriguez-Rondero et al. 2016). The impact of lianas on host trees is also observable at the stand level. Liana infestation is responsible for increasing forest gaps by inducing tree mortality and decreasing forest regeneration. (Schnitzer and Bongers, 2002; Meunier et al., 2021; da Cunha Vargas et al., 2021 ; Estrada-Villegas et al., 2022). Lianas are also more dominant in disturbed areas of the forests such as forest borders and canopy gaps (Gerwing, 2001; Waite et al.,2023), therefore changing their environment`s dynamics by reducing the forest net growth, carbon uptake and biomass accumulation (Van der Heijden et al., 2015; Estrada-Villegas et al., 2020; Meunier et al., 2021; da Cunha Vargas et al., 2021; Estrada-Villegas et al., 2022; Waite et al., 2023). Despite these adverse impacts, the presence of lianas also provides benefits to tropical ecosystems. Lianas provide food and shelter to local fauna by attracting animals to infested areas (Hilje et al., 2017; Mohandass et al., 2017) and create connections between tree crowns, increasing wildlife mobility (Hilje et al., 2017). The quantification of liana infestation is challenging due to its structural arrangement and the connectivity to the host trees. Most methods

use manual approaches to measure stem frequency, liana basal area and host tree crown coverage by lianas (Perez-Salicrup and Meijere, 2005; Visser et al., 2018; Reis et al., 2020).

Since lianas do not invest in support structures to reach the top of the canopy, their stems rarely reach diameters with more than 10 centimeters (Schnitzer et al., 2012), and lianas with stem diameters inferior of 2 centimeters are able to reach the superior strata of the forest (Kurzel et al., 2006). Using trees as support structure to access the forest canopy allows lianas to present less Although lianas have fewer leaf layers, they often present a larger leaf area/stem diameter relation than trees (Medina-Vega et al., 2021). These unique morphologic characteristics of lianas make this plant lifeform difficult to study using traditional ground-based methods (van der Heijden et al., 2022). In the past decade, the use of a myriad of remote sensing instruments and methodologies are being used to expand our understanding about this important plant lifeform (van der Heijden et al., 2022). Recent advances brought relevant information about canopy infestation by lianas and spectral differences between trees and lianas leaves (Guzmán et al., 2018; Visser et al., 2021). New non-destructive approaches are allowing measurements of lianas structure on single liana stem (Moorthy et al., 2020).

The Quantitative Structure Model (QSMs) is a recognized approach to process Terrestrial Laser Scanner (TLS) derived point-clouds. QSMs reconstruct single trees to assess structural metrics such as volume, tree height, diameter at breast height (DBH), branch order, and wood elements' total length (Raumonen et al. 2013). The QSM uses cylinders to build plant wood elements since this geometrical form resembles tree trunks and branches (Raumonen et al., 2013). The implementation of a QSM follows two steps: 1) the algorithm segments the tree point cloud into the stem and branches, and 2) it fits cylinders over these wood elements, calculating the volume and other structural metrics. QSMs have been used successfully to calculate tree metrics in several studies (see Calders et al., 2014; Akerblon et al., 2017; Brete et al., 2019).

Until today, the use of TLS applied to lianas systems has focused more on the extraction of liana stems from their host trees (Moorty et al. 2019, 2020,), without focusing on the use of this information to characterize how much volume lianas are occupying on a given tree and the total length of woody biomass in comparison with its host tree. As such, the objective of this study is to use QSMs derived from TLS point-clouds to compare structural metrics values from lianas and their host trees on competitive tropical forest environment. I hypothesize that in cases of high liana infestation, this lifeform stems can present similar values of the hosting tree`s structural elements.

2.2 - Methods

2.2.1 Study Site

Data collection for this study was conducted at the Santa Rosa National Park Environmental Monitoring Super Site (SRNP-EMSS) (10°48'53" N, 85°36'54" W). Today the SRNP-EMSS is part of a mosaic of protected areas that makes up the Area de Conservacion Guanacaste (ACG), Guanacaste, Costa Rica (Figure 2.1). The climate is characterized by rainfall seasonality with annual precipitation varying from 900 to 2500 millimeters (mean of approximately 1750 mm). The dry season extends from November to May (Kalacska et al., 2007; Castro et al., 2018). The dry season is characterized by high temperatures, low relative humidity, and the incidence of intense air movements causing frequent wind gusts (Claudino-Sales, 2018). The park's ecological importance is reflected in its biodiversity of plants and wildlife dispersed over nine habitats characterized by different forest structures and species compositions, such as evergreen forest, deciduous forest, tropical dry forest, and mangroves (Kalacska et al., 2007; Claudino-Sales, 2018).

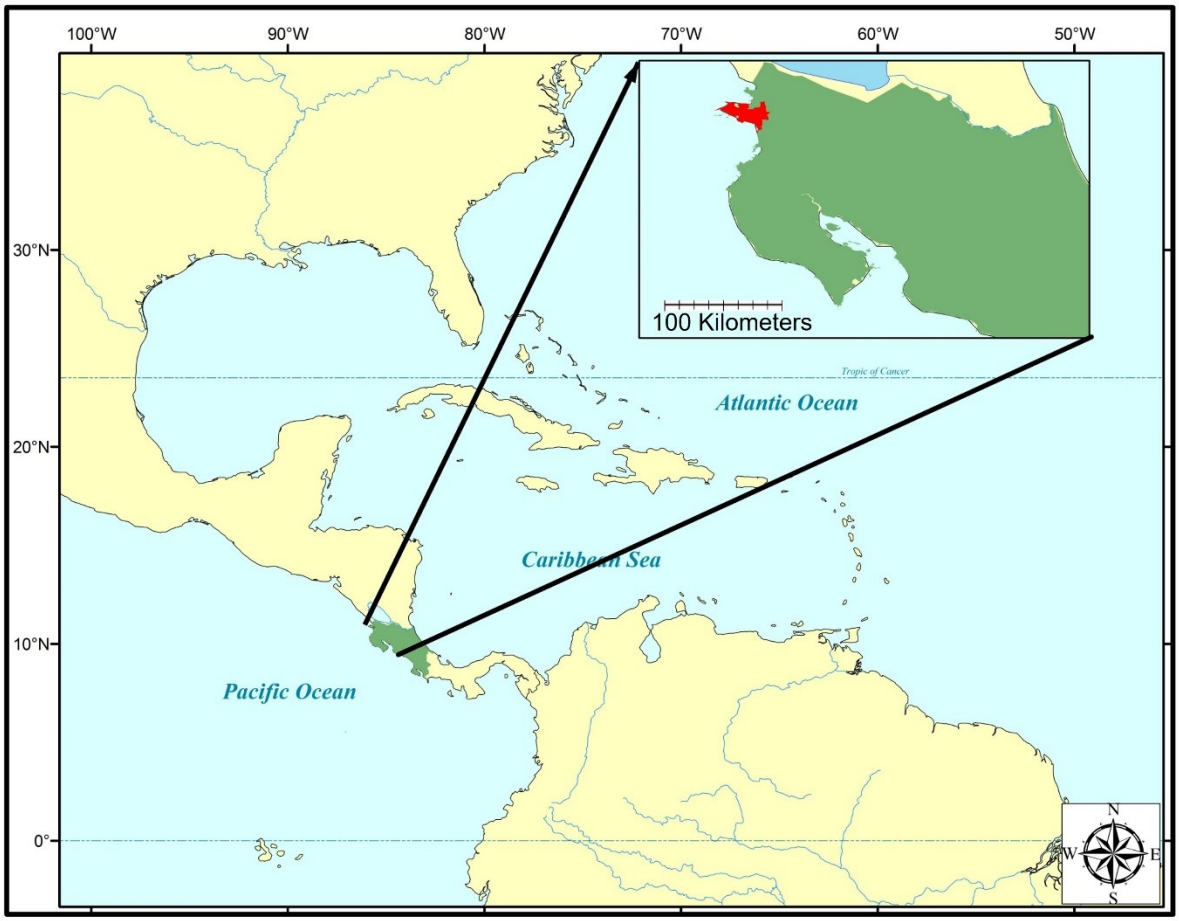

Figure 2.1: Location of the Santa Rosa National Park – Environmental Monitoring Super Site.

2.2.2 Data Collection

2.2.2.a) Tree selection

Studies at SRNP-EMSS have found that liana infestation is more prevalent on trees living in intermediate successional stages than in the early and late stages (Sanchez-Azofeifa et al., 2009; Sanchez-Azofeifa et al., 2017). For this reason, set of liana-infested trees was selected in areas of intermediate forests following the land cover classification of Kalacska et al. (2007). This classification is based on forest structure and plant diversity. Three trees with different levels of infestation were selected for the analysis. These trees represent the range of liana infestation for this type of forest; therefore, our results can be interpreted in a broader context. The level of liana infestation on the selected trees varied from a single stem climbing the host tree to reach the canopy, to over 20 liana stems climbing the host tree in the higher infestation scenario (Figure 2.2). The selected trees were located in low-density forest understory to minimize occlusion in the point cloud.

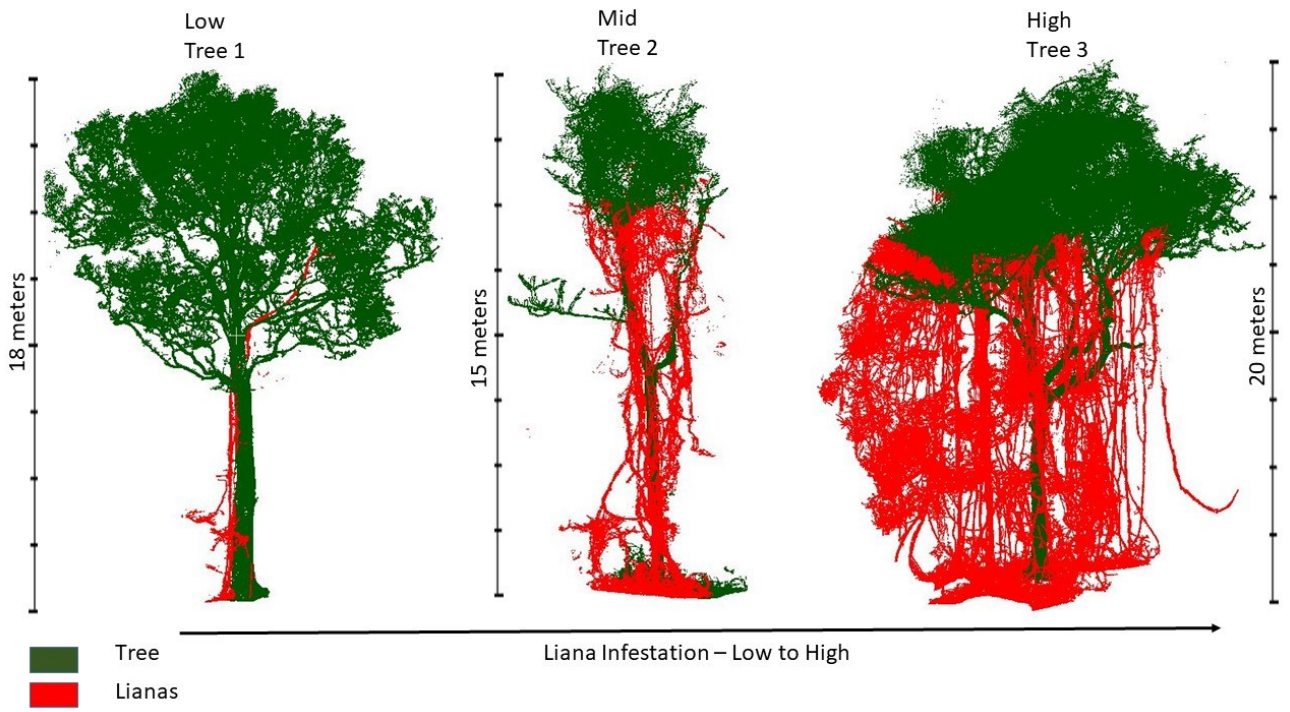

Figure 2.2: Liana Infestation based traditional approaches (number of liana stems, basal area and canopy coverage). In red is presented the liana`s wood elements TLS point-cloud segmentation, whereas in green is presented the hosting tree TLS point-cloud. The segmentation between liana and tree datasets reached 12.2 meters for hosting tree 1; 11.5 for hosting tree 2; and 11.9 for hosting tree number 3.

2.2.2.b) TLS data collection

The TLS data was collected at the end of the dry season (May/June 2015) when trees were without leaves. The data collection was done to minimize the occlusion effect caused by leaves and maximize scan coverage of the lianas and wood elements as well as the architecture of the host trees. Point cloud datasets were collected using a Leica C10, a single return TLS system that operates with visible green light at 532 nanometers (Green LiDAR) and presents a field-of-view of 360° azimuth and 270° zenith. Resolution was set to medium, producing 0.1-meter resolution datasets of objects located 100 meters from the sensor (Abbas et al., 2013).

The plot design positioned the infested target tree in the center with four scan stations on the corners approximately ten meters distant from it. Six to eight retro-reflective targets were placed in each plot for the co-registration of the point clouds. The number of reflective targets exceeds the minimum number of control points (four) suggested by Wilkes et al (2017) to ensure a full three-dimensional coverage of the target feature. the scan measurements were conducted on sunny, clear days with minimal wind to minimize the presence of ghost points caused by dust, aerosols and plant movement that negatively affect TLS derived tree metrics (Vaaja et al., 2016). The Diameter at Breast

Height (DBH) of the infested trees was measured to compare against the DBH (1.3 m) calculated by the QSM.

2.2.3- Registration

The co-registration of the individual point clouds, collected for each tree (4 per tree), was done using the retro-reflective targets placed in the field as control points and an automatic registration tool contained in the Leica Cyclone® (2021) software. Following co-registration, the four-point clouds for each infested tree were merged into a single point cloud. This process produces a highly detailed three-dimensional representation of vegetation structure for each tree, thus improving data quality and minimizing the occlusion effect (Beland et al., 2014, Cifuentes et al., 2014). The mean absolute error of the individual point cloud for the low, intermediate, and high infested trees were 0.002 meters, 0.005 meters, and 0.003 meters, respectively.

2.2.4- Pre-processing steps for Quantitative Structure Model (QSM)

The first step after the point-cloud registration was the extraction of the dataset to be modelled by the algorithm started with the liana infested tree extraction from the merged point-clouds. Next, since I selected dominant trees living in complex forest environment, the dense understory plant elements (forest regeneration, suppressed trees, shrubs, grass, and other plants) were manually cleaned to produce a point-cloud containing only elements from lianas and the analyzed trees.

The segmentation of lianas and the infested tree elements were also done manually to produce point-clouds of each plant lifeform. Since there are no existing algorithms for automatic liana segmentation due to the complexity of liana-infested point cloud, a manual segmentation of woody elements of the liana and tree system was conducted. Furthermore, since the mixture of woody elements from trees (branches) and lianas (stems) in the upper part of the canopy are quite similar making it impossible to separate liana stems and tree branches, I had to limit the segmentation to a height of 12.2 m out of 17.7 m for tree one, 11.5 m out of 14.9 m for tree two, and tree 11.9 m out of 19.3 m for tree three. Finally, since a three-dimensional modelling requires a dataset with an equal point density, and due to changes in TLS spatial resolution as a function of distance from the laser source, I subsampled the point clouds to a 0.01m spatial resolution. Last, a Statistical Outlier Removal (SOR, k-nearest neighbor of 10 and the standard deviation of 2) was used on each tree point cloud to eliminate isolated ghost points (Guzman et al., 2020).

2.2.5- Implementation of the Quantitative Structure Model (QSM)

The QSM of the woody component of the liana and tree point-clouds was done using TreeQSM in the Computree® software. The Minimum Diameter Path parameter was set as 1 centimeter as the point-clouds were subsampled to this spatial resolution. The Maximum Diameter Path was set as the DBH value measured for each tree. I created a minimum of five models of each infested tree, and the best model was chosen by visual comparison with the merged point-clouds.

Since TreeQSM was developed to follow a more deterministic stem/branch segmentation and sub-segmentation, the algorithm performed well on datasets that follow this architectural arrangement. Lianas, which present a more stochastic architectural arrangement, are a challenge for the model. To address some of the issues observed when the liana point clouds were implemented in the TreeQSM algorithm, several adjustments were made. First, I subdivided the liana dataset from tree number two into three sub-datasets due to the high number of liana stems (Figure 2.3). The former allowed for each portion of the point-cloud to be modelled individually, and the resultant models were merged and their metrics combined. The second adjustment was to keep constant the diameter of cylinders contained in the same segment. This approach was adopted after I observed undesirable variation of cylinder diameter within the modelled segments. This behavior was not consistent with either direct observation of the point cloud or the natural morphology of a given liana individual (Figure 2.4). For this adjustment, I used the largest diameter observed on a given segment and applied the same value to all the neighbor cylinders within the same segment.

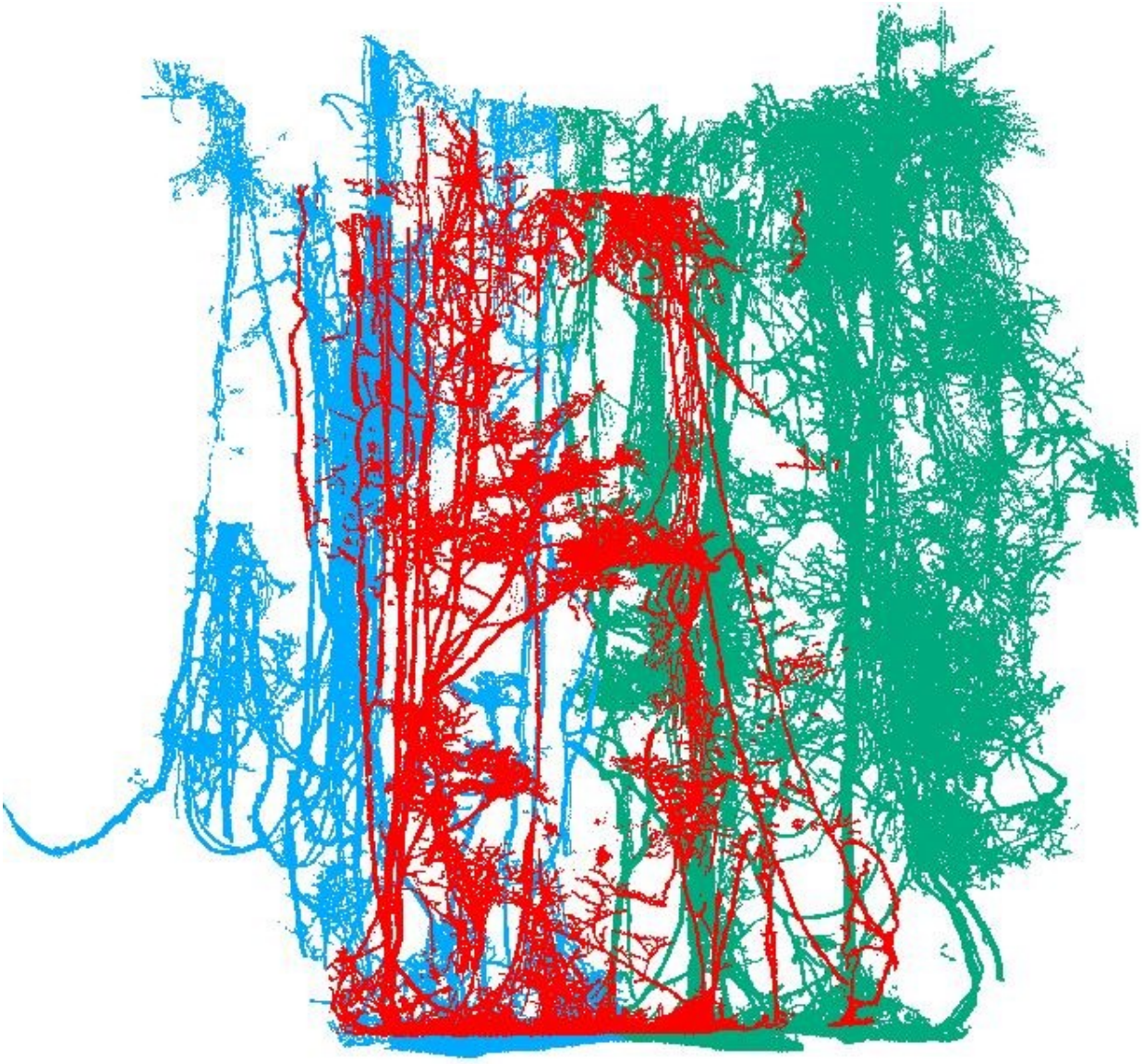

Figure 2.3: Sub-divided lianas datasets (Blue, red and green) from infested tree number 3. The QSM reconstructed individually in each subsection point-cloud and the metrics were combined to retrieve the total liana contribution.

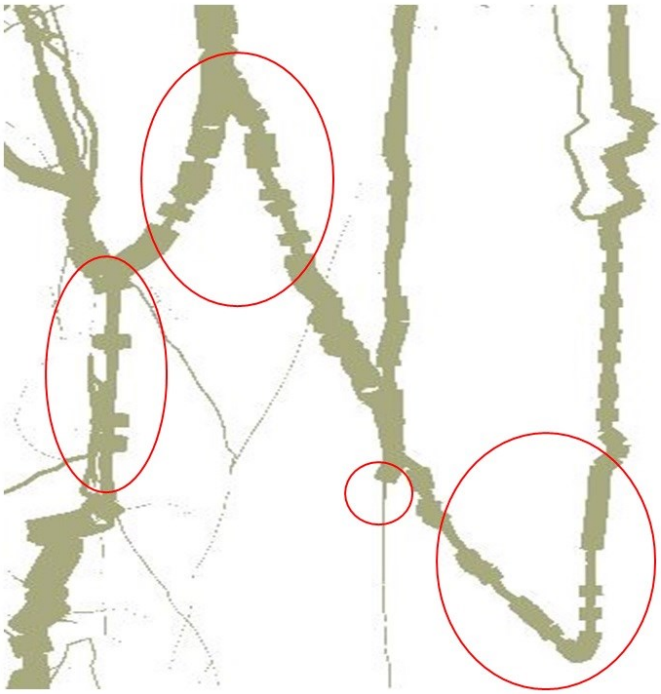

Figure 2.4: Lianas modeled using the QSM from tree number 3. Liana Stem diameter inconsistencies are indicated by red circles and were minimized by maintaining higher cylinder diameters within each QSM segment.

2.2.6- Estimation of the liana's relative volume and load

To compare the severity of liana infestation and wood volume/biomass contribution two metrics were used to quantify the liana occupancy of the three-dimensional space, and the degree of liana infestation of each tree: 1) the *Relative Volume (RV)* occupied by each lifeform on the three-dimensional space, and 2) *the liana load (LL)* as the ratio between the liana wood volume to tree wood volume calculated by the QSM algorithm. The Liana Load (LL), measures the ratio of liana wood elements that are supported by the hosting tree in function of its size, therefore normalizing the volume of liana infestation. The former allows a better understanding of the relation between host and parasite at the tree level.

Because the modelling ended at the intermediate strata of the liana infested tree crown (See section 2.2.4), I used the point-cloud cutting height and the crown projection of each analyzed tree to estimate the total occupied volume and from there the RV for each tree and liana system was estimated. The LL was estimated here as the percentage of liana's wood elements in relation to the wood volume for the hosting tree. This metric helps us better understand the level of liana infestation in each tree and to compare liana infested trees of different sizes and areas.

2.3 – Results

2.3.1 - QSM performance on a complex vegetation point-cloud

Cylinders, the basic unit of QSMs, are grouped into segments that are then connected to form stems and branches. Plants with multiple branches, bifurcations, and curved stems require more and smaller cylinders and segments to be reconstructed. As a result, the number of cylinders and number of segments reflect the complexity to build the model. Tree 1 was the only place where the model presented higher building complexity than the model generated for the parasitizing liana. For this tree, the QSM algorithm used 295 segments formed by 1360 cylinders to build the hosting tree, whereas the single liana parasitizing it needed 81 segments from 432 cylinders. Tree number 2 needed 218 segments from 932 cylinders to build the hosting tree, and 568 segments created by 2773 cylinders to reconstruct the lianas wood component. In tree number 3, the supporting tree was modelled by 136 segments generated from 705 cylinders, while the infesting lianas wood elements were reconstructed by 6255 segments integrated by a total of 29351 cylinders.

2.3.2 Quantitative Structure Model (QSM) metrics

Tree wood volume was estimated to be 2.60 m^3, 0.4 m^3, and 2.46 m^3 for tree 1, 2 and 3, respectively. The liana's volume before cylinder diameter adjustments was estimated to be 0.06 m^3, 0.28 m^3, and 0.91 m^3 for trees 1, 2 and 3 respectively. After adjusting the diameter values for the cylinders forming the same segment, these values changed to 0.07 m^3, 0.35 m^3, and 1.17 m^3 for trees 1, 2 and 3, respectively (Table 2.1). A comparison of QSM_{DBH} vs field measurements indicates values 0.54 m vs 0.72 m, and 0.20 vs 0.47, and 0.55 m vs. 0.56 m for trees 1, 2 and 3 respectively with a sub estimation of the QSM_{DBH} for trees 1 and 2. Figure 2.5 shows DBH miscalculation derived from the QSMs model caused by irregular shape of the tree trunk.

The liana total length was obtained by the sum of all lianas' elements infesting each host tree. The three samples used in this study presented great variation on this metric due to the different degree of infestation. The total length of the liana woody elements, estimated as the sum of stems and branches, indicate that tree 1 is the only one where this amount is lower than the length of the woody elements of the host tree. (37.3 m vs 147.1 m). Tree 2 shows a medium level of infestation (238.2 m vs 97.8), while Tree 3 shows a significant large amount of liana woody material than the host tree (2391.1 m vs 71.6 m). These values show that the amount of lianas stem using a single tree

as support can have enormous variation; and lianas stems can present higher total length values than their host trees even in intermediate liana infestation, such as tree number 2.

Table 2.1 - QSM Metrics derived for Tree and Liana components in the three study plots. Values in brackets represent DBH field measurements on trees and liana modelling values without the adjustments. All remaining values are derived from modeling after adjustments.

Plot	**Lifeform**	**Volume (m^3)**	**Length (m)**	**DBH (cm)**	**Crown Area (m^2)**	**Total Space (m^3)**	**Relative Volume (%)**	**Liana Load**
1	Tree	2.6	147.1	54.1 (72.5)	140.16	1,709.9	0.152	0.03
	Liana	0.07 (0.06)	37.3	NA	NA		0.004	
2	Tree	0.4	97.8	20.6 (47.5)	17.85	205.3	0.195	0.88
	Liana	0.35 (0.28)	238.2	NA	NA		0.17	
3	Tree	2.46	71.6	55.1 (55.5)	156.39	1,861.0	0.132	0.46
	Liana	1.17 (0.91)	2,391.1	NA	NA		0.063	

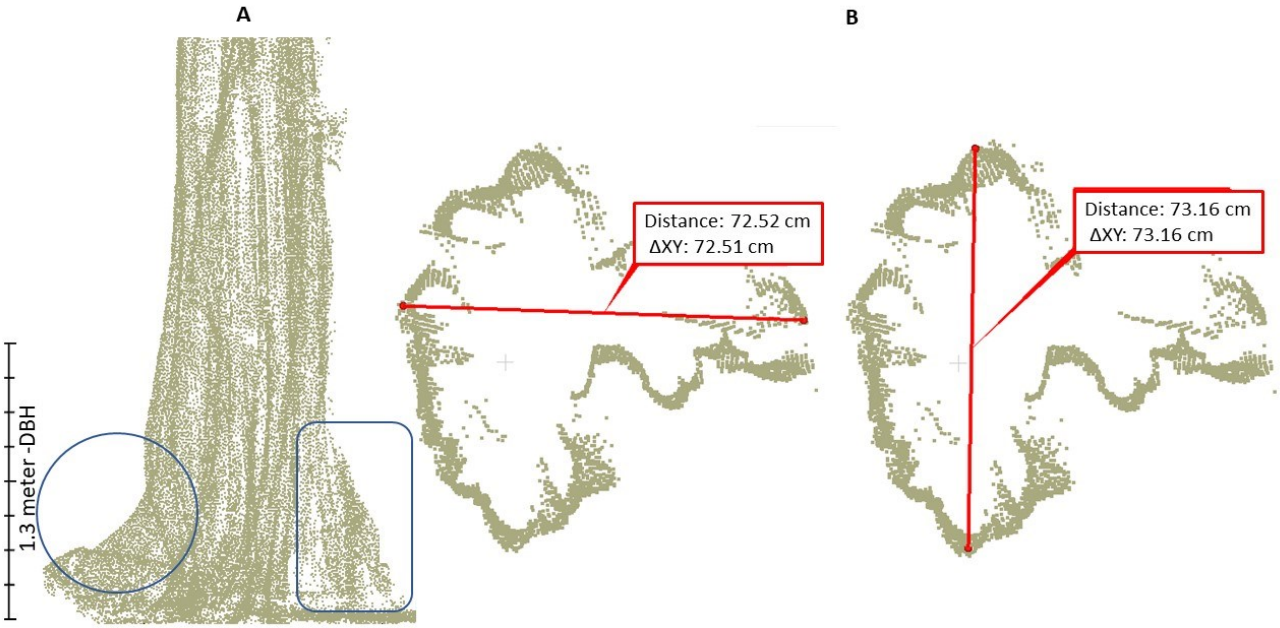

Figure 2.5: Host tree number 1 presenting stem irregularities that caused QSM underestimation of tree DBH, and total wood volume. (A) In blue buttress; and (B) point-cloud horizontal cut on the trunk at DBH with non-cylindrical. Point to point calculations (72.5; and 73.1 centimeters) corroborate field measurement and contrast the model (72.5 vs 54.1).

2.3.3 Relative volume and liana load

Since the relative volume (RV) is a function of the tree dimension, which in turn is especially affected by the host tree crown area, this variable was estimated for each tree at the cut-off height. As such, crown areas for our selected trees were estimated to be 140.2 m^2, 17.8 m^2, and 156.4 m^2 for trees 1, 2 and 3 respectively. Next, the total volume (V_t) available for each infested tree was 1,709.9 m^3, 205.3 m^3, and 1,861.0 m^3 for trees 1, 2 and 3 respectively. As such RV_t results for the QSM reconstructed trees are 0.15%; 0.19%; and 0.13%; for trees 1, 2 and 3 respectively. The QSM modelling of the lianas wood elements presented RV_l values of 0.004%, 0.170%, and 0.063% for trees number 1, 2 and 3 respectively.

Our results of LL were 0.03, 0.88, and 0.46 for trees number 1, 2 and 3 respectively. The former means that tree 3 supports half of its volume in lianas wood elements while tree 2 supports a higher degree of liana infestation of the trees analyzed in this study. This occurs due to the size of tree 2, which is considerably smaller than the other trees analyzed in this study. Therefore, the tree 2 supports a liana woody material representing almost 90% of its total volume. Figure 2.6 presents the liana load affecting the analyzed hosting trees.

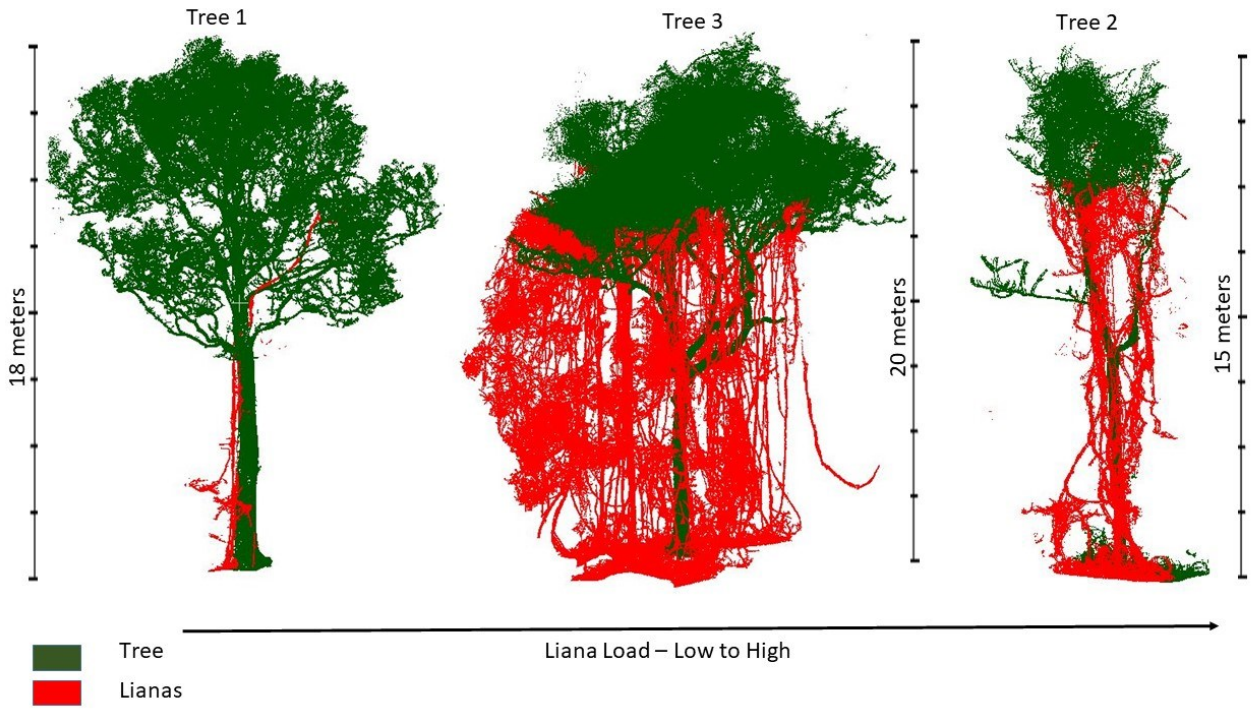

Figure 2.6: Liana infestation evaluation based on the liana load supported by each hosting tree.

2.4 Discussion

2.4.1 Impact of plant lifeform interaction on dataset quality and QSMs modeling

The ability of the QSM algorithm to assess structural metrics from TLS single tree point-clouds has been documented by numerous studies (Burt et al., 2013; Raumonen et al., 2013; Calders et al., 2014; Kaasalainen et al., 2014; Akerblom et al., 2017; Malhi et al., 2018; Brede et al., 2019). Its cylinder-fitting approach was developed based on the tree architecture elementary design of stem sub-dividing into branches of different orders that form the tree crown (Raumonen et al., 2013; Calders et al., 2014). Lianas present a dissimilar structural pattern where usually multiple liana stems climb the hosting tree (Gerwing, 2001; Schnitzer and Bongers, 2002; Perez-Salicrup and Meijere, 2005; Campanello et al., 2016; Smith-Martin et al., 2019), with their branches being arranged according to the local availability of light using the host tree as support (Schnitzer and Bongers, 2002; Meunier et al., 2021; Medina-Vargas et al., 2021). These characteristics created some challenges for modelling both lifeforms, and the errors occurred mainly for the following reasons: lianas have multiple stems; lianas have a diffuse spatial pattern; some liana stems climbing the hosting tree were attached to each other; and the parasite/host multiple contact points and proximity.

The interaction between parasite and host plant lifeforms affected the quality of the TLS point-clouds. The high density of liana stems climbing the same host tree increased the presence of occlusion of both lianas and tree point clouds. The presence of occlusion caused by plant elements is a common problem in TLS point-clouds from densely forested areas (Beland et al., 2011; Coveney et al., 2011; Beland et al., 2014), and it is known for decreased accuracy on the derived models (Burt et al., 2013; Kaasalainen et al., 2014, Malhi et al., 2018; Hu et al., 2021). The relation host/parasite increased the presence of occluded regions on both datasets due to the proximity between the two lifeforms. On the host trees, this issue was more problematic for trees 2 and 3 where the liana infestation was more intense.

The location of the liana elements also plays an important role in the modelling of the hosting trees, since in the infested tree 2, where the liana stems were located closest to the tree, the occlusion area occurs on the tree stem, affecting its volume calculation. In this case, the DBH calculation was less than half of the field measurement (table 2.1), corroborating the volumetric underestimation. On tree number 3 the inaccuracy was caused by the irregular form of the host tree's trunk, which presents buttresses and other irregularities at the DBH region (Figure 2.5), contrasting with the cylinder form used by the modelling algorithm. Since the algorithm reads the most external points on a stem as outliers, it fitted the stem cylinders based on the most internal points of the trunk (Raumonen et al., 2013; Hu et al., 2021), generating a DBH error of more than 15 cm, which certainly also affected the volumetric calculation accuracy for this tree.

The prolific liana abundance in tree number 2 created some distortion of this lifeform model, related to the contrast between its spatial arrangement and the tree architecture pattern used by the QSM algorithm. The QSM started modelling a given stem from the point cloud and merged the elements from other co-existing individuals as they were in contact with previously modelled elements. In this case, where multiple liana stems climb the host tree connected from the ground level, the model grouped these individuals to form the stem, which possibly caused an overestimation of the volume on this region of the model.

Since QSMs algorithms use cylinder fitting structure to model plant wood elements (Raumonen et al. 2013), the liana characteristics and morphology created some challenges. The high variation of cylinder diameters within the same modelled segment (illustrated in Figure 2.5) were adjusted to better depict the elongated liana stems with low variation in their diameter characteristics of this lifeform below the canopy level (Chen et al., 2015; Ichihashi and Tateno, 2015; Smith-Martin et al., 2019). This adjustment was done on all liana modelled segments by maintaining the higher

diameter value for all cylinders within each modelled segment for this lifeform as pointed out in the methods section. The number of cylinders necessary to model lianas elements was significantly higher than the number used to model the hosting trees in a high infestation scenario. The algorithm needed 433 cylinders to model the single liana stem infesting tree number 1, and 1,360 were used to model the tree that presented the lowest liana infestation level. On the other trees that presented a higher infestation (trees number 2 and 3) the number of cylinders used to model liana elements was superior to the cylinders needed to model the hosting trees. On host tree number 2, the model used 2,774 cylinders for the liana dataset and 932 cylinders for the tree point cloud. For tree number 3, the individual with the highest liana infestation, the algorithm used more than 29,351 cylinders to calculate the liana wood volume and 705 cylinders to calculate the tree volume. The high number of cylinders used by the QSMs to model the liana point-clouds expresses the complexity of modeling this lifeform.

2.4.2 QSM metrics to estimate RV and LL as tools for ecological assessment of infested trees

Our results corroborate Smith-Martin et al. (2019) findings that suggest lianas invest more in stems than previously assumed, and Sanchez-Azofeifa et al. (2009) found that liana presence increases Wood Area Index (WAI) in Tropical Dry Forest sites. On the other hand, liana volume and length values are much higher than those measured by Castellanos et al. (1992) on trees infested by single liana stems. This was expected since Castellanos et al. (1992) measured lianas infestation using traditional methods. They also focused on smaller trees (with canopies less than ten meters) where their measurements were more achievable. Using LiDAR and QSM, this study achieved measurements of liana infestation on trees over 15 meters high.

In this study, the liana infestation degree experienced by each host tree were different. Although the trees have similar height, the length of lianas stems infesting each host tree varied from 37.3 to 2391 meters. Previous studies that measured lianas stem lengths reported smaller values. Using a traditional field approach, Castellanos et al. (1992) measured lianas stem length values varying from 10 to 16 meters on single liana steam infestation on smaller trees. Moorthy et al. (2020) used a similar methodology with QSMs metrics derived from TLS point-clouds, and measure liana stem lengths varying from 25 to 135 meters infesting trees taller than the ones used in this study (van der Heijden et al., 2022).

The immense length values measured in this paper can be partially explained by the fact that I investigate hosting trees with multiple liana stems on highly infested trees, while previous studies

focused on single liana infestation scenarios; and by the fact that lianas stems can grow their stems between two to seven times more than trees in tropical dry forest (Schnitzer, 2005). These findings also bring light to the amount of liana stems that can be infesting individual trees can be much higher than previous studies have shown, and the implications of such high degree of infestation can generate on the infested tree structure.

The examination of the QSM derived metrics showed hosting trees suffering different levels of liana infestation, with LL ranging from 0.03 to 0.88. The fluctuation on the QSM values indicates a completely different relationship between the two lifeforms in our plots. Since lianas invest more in leaves than in stems and support structures compared with trees (Schnitzer and Bongers, 2002; Chen et al., 2015; Medina-Vega et al., 2021), I can infer that the liana infestation on these tree crowns would reflect the same pattern of the liana wood elements incidence with higher intensity. It is known that liana infestation decreases tree growth (Lobo-Catalan and Jimenez-Castillo, 2014; Schnitzer, 2018; Meunier et al., 2021), increases tree mortality (Ingwell et al, 2010; Schnitzer, 2018), affecting the carbon uptake by the forest (Schnitzer and Bongers, 2002; Van der Heidjen et al., 2013; Schnitzer et al., 2014; Meunier et al., 2021). In fact, hosting trees presenting highly liana infested crowns have a 100% higher mortality risk compared to trees that are not parasitized by lianas (Ingwell et al., 2010).

To better understand space occupancy efficiency of each lifeform, it is also necessary to observe its spatial configuration using variables such as the RV. Biological systems and organisms, in general, follow the same basic structural pattern (Stahl, 1962; Alados et al., 1996; Henkel et al., 2018). Regarding the spatial configuration of the liana and tree dynamics, I have noticed similarities with other biological arrangements. This arrangement is better observed for trees 2 and 3 (Figure 2.7), where the liana infestation was more severe, and it relates to how lianas use the hosting trees as support. Instead of the delivery of nutrients resembling our vascular system, lianas are efficiently competing with the parasitized tree for the same vital resources (Schnitzer et al., 2005; Alvares-Cansino et al., 2015; Collins et al., 2016; Dias et al., 2019; Meunier et al., 2021). The efficiency to better assess the available resources in the forest, by their capacity to better explore the three-dimensional space (Medina-Vargas et al., 2021), combined with their physiological traits (Andrade et al., 2005; Chen et al., 2015; Campanello et al, 2016; Collins et al., 2016; Chen et al., 2017; Marechaux et al., 2017; Schnitzer et al., 2018), is what provides lianas with their ability to efficiently compete with other lifeforms.

Figure 2.7: Tree and liana modelled elements distribution. It is possible to observe the hosting tree on plot 2 leaning towards the liana climbing elements, indicating structural stress due to the high liana load.

The second metric used, the liana load (LL), corroborates that the host tree number 2 is suffering the highest liana infestation. This tree was supporting almost its own wood volume in lianas stems, whereas the hosting tree number 3, where the abundance of liana stems was prolific, supported less than 50 percent of its own volume in liana wood elements. This occurs because of the dimensions of the trees and the total amount of infesting lianas supported by them. The tree number 3 presents higher total volume of lianas elements (1.17 cubic meters), while tree number 2 present significantly lower volume of liana wood material (0.35 cubic meters). Since tree 2 is much smaller than tree 3 (0.4 cubic meters vs 2.46 cubic meters), the amount of liana supported by this tree is proportionately superior to the amount supported by tree number 3. Therefore, the LL on tree number two is higher than the other two trees (0.88 for tree 2; 0.46 for tree 3 and 0.03 for tree 1). This degree of liana infestation generates structural responses from the host tree. It is possible to observe the tree with the highest liana load (tree number 2) leaning in the direction where most of the lianas wood elements are located (Figure 2.8). This behavior illustrates the conclusions by Schnitzer and Bongers (2002), that high liana infestation can mechanically affect the hosting trees due to its weight; leading to structural changes in their architecture to adapt to the high liana parasitism (Dias et al., 2017).

The liana load quantification allows a deep understanding of the relationship between parasite and host tree, predicting tree mortality and permitting the comparison of the liana infestation level on

trees of different sizes, living in any ecosystem. I found LL was the most efficient approach to evaluate liana infestation and parasitizing level on trees since it is unbiased by the infested tree size or by the number of liana stem climbing the hosting tree. The association between liana load and biomass and carbon accumulation from the two lifeforms is possible, but it is necessary to consider the lower density of liana stems in comparison with trees (Van der Sande et al., 2019) and wood compositional characteristics of each species.

2.4.3 Limitations and uncertainties

The QSMs are known to generate models of single trees that can have biomass and volumetric metrics calculated with accuracy above 90% (Burt et al., 2013; Calders et al., 2015; Brede et al., 2019; Damol et al., 2022). Lau et al. (2018) achieved volumetric accuracy of 97% when compared with traditional destructive measurements. This accuracy is not distributed uniformly along the tree point-cloud. The volume derived from modeled trunk is more accurate than the volume extracted from the reconstructed branches (Burt et al., 2013). This miscalculation can be caused by the presence of abnormal outliers that generate overestimation of the metric, or occlusion caused by the presence of leaves, high density of woody material at the tree crown area' and branch misalignment (Malhi et al., 2018; Disney et al., 2019; Hu et al., 2021; Demol et al., 2022). Moreover, the model accuracy varies with branch thickness (Lau et al., 2018; Demol et al., 2022). Lau et al. (2018) found that QSMs can rebuild more than 95% of the branches with diameters superior to 30 centimeters, while in the branches with diameters between 10 to 30 centimeters, the success rate was below 60%. The accuracy level decreases in the smaller diameter branches usually causing overestimation of the diameters and volume (Lau et al., 2018; Disney et al., 2019; Demol et al., 2022). This issue can cause branches with diameters below five centimeters to be accounted for more than 80% of the model volumetric miscalculation of trees (Demol et al., 2022). Since Lianas are characterized by their thin stems that usually do not reach more than ten centimeters (Schnitzer et al., 2012), the volumetric calculation of this plant lifeform needs to be accessed by field measurements to validate the values found in the present study.

The model also performs distinctly when reconstructing the length of branches of different diameter classes. The model underestimates lengths of branches with diameters inferior to 50 centimeters, and this misfit can lead to branch absolute underestimation of up 30% (Lau et al., 2018). In this context, it is possible to infer that liana total length values presented in this study is underestimated. It was measured more than two kilometers of lianas infesting a single tree in the site

used, and because of this model fitting issues, the total length extension of the liana infestation on the analyzed host trees might be greater than what was reported.

Our analysis was based on a small sample size of three liana infested trees located at SRNP-EMSS. This sample size does not allow us to understand or characterize the broad spectrum of liana relation with hosting trees and further studies are necessary for a better comprehension of the dynamics and competition of these key elements of tropical environments. Although this sample size is not sufficient to characterize the liana infestation in the TDF, it provides an example on how lianas parasite trees with different intensity. Our study also showed that liana infestation presents different spatial arrangement depending on the infestation level which generates diverse structural effect on the host trees. The proposed two metrics derived from three dimensional datasets provided important information about the liana infestation level on a host tree, and the space occupancy of each lifeform making it possible the comparison of the liana infestation on trees of different sizes.

2.5 – Conclusion

I used TreeQSM to calculate wood contribution and space occupancy of two plant lifeforms with different levels of liana parasitism on hosting. I found that despite common knowledge liana wood elements can reach space occupancy and wood volume close to tree wood volume in high infestation scenarios. I also found that due to their spatial arrangement, liana stems can extend to almost three kilometers long on a single hosting tree. This highlights the importance of a better understanding of this parameter and its importance for the forest structure and the dynamics between the host and parasite.

I proposed two QSMs derived metrics to evaluate liana infestation on trees of different sizes and environmental conditions. Space occupancy measures the proportion of the available three-dimensional space occupied by each lifeform. The liana load measures the ratio between the liana wood volume and the wood volume of the host tree. These metrics can be used to compare trees with different characteristics, sites, and infestation levels, or to monitor the infestation dynamics on trees along the time.

QSMs modelling of both lifeforms is challenging due to the parasite/host dynamics and proximity between the two lifeforms that increased occlusion and noise on the dataset. Further efforts need to be made to increase point-cloud segmentation to separate liana and tree datasets. The

modelling of the liana wood elements needs improvement since the single stem approach used by the QSM algorithm does not contemplate the liana natural occurrence.

Chapter 3 Fractal Analysis on Forested and Open Field Trees

3.1 – Introduction

The effects of plant density on trees and plant populations have been debated from different perspectives depending on the focus of interest. Several studies have explored the optimum tree density and spatial arrangement for maximizing stand wood (Alcorn et al., 2007, Antony et al., 2012) and tree fruit production (Paltineanu et al., 2016). In natural highly diverse and populated forested environments, light is the main factor driving tree growth and forest structure (Lang et al., 2010; Jucker et al., 2014, Ford, 2014), and the competition for water and nutrients happens underground while above-ground plants compete for canopy space that provides leaf surface used in photosynthesis and gas exchange processes (Nambiar et al., 1993; Grams and Andersen, 2007; Madsen et al., 2021). To survive and succeed in these environments, plants are capable of morphological changes in their architecture to adapt to the variation in space and illumination due to competition with neighbouring trees (Rouvinen et al., 1997; Thorpe et al., 2010; lang et al., 2010; Madsen et al., 2021). For example, Pickett and Kempf (1980) found that trees and shrubs in the understory of the forest have a branching rate inferior to the one without light restrictions. Morphological plasticity is the mechanism that allows broad-leaf tree species to shape their crowns according to the local environment and competition. Conifers trees on the other hand have their crown shape more stable reflected by their crown symmetry (Rouvinen et al., 1997). On broad-leaf tree species the crown shape is driven by abiotic factors (Rouvinen et al., 1997; Thorpe et al., 2010; Del Rio et al., 2014; Madsen et al. 2021). Sun light and competition are the main variable defining the shape of this group (Lang et al., 2010; Seidel et al., 2011; Jucker et al., 2014; MacFarlane and Kane 2017; Madsen et al., 2021). Light dependence varies by the species and successional group. Pioneer trees need a great amount of light to grow, whereas climax species are more shade tolerant and can be developed with much less sun light availability (Grams-Andersen et al. 2007).

Tree density and competition are important factors leading to morphological changes on crown structure (Del Rio et al., 2014; Ford, 2014; Seidel et al., 2017; Madsen et al., 2021). These variables, sunlight, competition, and plant density along with the morphological plasticity cause an irregular growth of the canopy and other plant structures, driven by the tree necessity to reach areas richer in vital resources, creating and irregular crown (Lang et al., 2010; Del Rio et al., 2024; Jucker et al., 2014; Condonnier et al., 2015; MacFarlane and Kane 2017; Madsen et al., 2021). Recent studies found that crown plasticity resulting from light competition is asymmetric, leading tree crowns to have irregular shapes (Lang et al., 2010; Siedel et al., 2011; Del Rio et al., 2014; Condonnier et al., 2015).

This phenomenon occurs because the light opportunities in the forest strata are dynamic, and plants must respond fast to occupy recently open gaps or find other light windows available, causing irregular branching patterns.

Plant growth and development are function of the availability of resources and environmental conditions of the site where they live (Grams and Andersen, 2007; Ford, 2014). Studies on plant developmental stability indicate that tree productivity peaks under a balance between ideal environmental conditions with the availability of resources, and a beneficial degree of competition that will vary accordingly with the specific demands of each species (Freeman et al., 1993, Escos et al., 2000, Alados et al.,2002 Seidel et al., 2019; Conn et al., 2019). Because of that knowledge, ideal densities on pure populations of fruit trees (Paltineanu et al., 2016) and trees for wood production (Arista et al., 1996; Alcorn et al., 2007, Antony et al., 2012) have been calculated based on the species demands and site characteristics aiming to improve volume and quality production. Also, forestry treatments such as thinning and liana removal have been developed to increase the productivity and use of resources based on the support capacity of the site and species demands (Gerwing, 2001; Xue et al., 2011; Cabon et al., 2018).

Fractals have been used to analyze trees (Seidel et al., 2011; Dorji et al., 2019; Guzman et al., 2020) and forest stand metrics (Guzman et al., 2020) from TLS derived point-clouds. Fractal analysis is the study of how the representation of an object behaves under the scale change of this object (Mandelbrot, 1983). The fractal dimension relates to how an object occupies the space measuring its structural complexity, which biologically is usually a beneficial trait (Alados et al., 1996; Escos et al., 2000; Seidel et al., 2017; Dorji et al., 2019). On plants, fractal analysis has been done to assess disease infestation on plants (Escos et al., 1995), plant stress (Alados et al., 1996; Alados et al., 2008), plant identification (Bruno et al., 2008), ecological succession (Alados et al., 2003), tree architecture (Alados et al., 1999; Seidel et al., 2017; Conn et al., 2019; Seidel et al., 2019), developmental stability (Freeman et al., 1993; Escos et al., 2000; Alados et al., 2002) and tree and stand metrics (Guzman et al., 2020). These studies have shown that under optimum conditions, plants have maximum space occupancy possible for their genotype; consequently, the degradation of these conditions due to environmental factors, disease or competition would cause the values of fractal dimension in these plants to decrease.

In this context, the objective of this study is to analyze the ability of fractal analysis to identify differences in tree architecture between trees living in open field conditions, without the presence of

other trees competing for light and other resources and trees living on a highly competitive but light-permeable tropical dry forest in Santa Rosa National Park, Guanacaste, Costa Rica.

3.2 – Methods

3.2.1 - Site description

This study was conducted at the Santa Rosa National Park – Environmental Monitoring Supersite, Costa Rica – SRNP-EMSS (10°48″ N, 85°36″ W), and The Guanacaste Conservation Area (Area de Conservacion Guanacaste - ACG) in Costa Rica. The ACG is located in the north portion of the Pacific coast and covers over 1630 km² of a mosaic of natural protected areas. The ACG extends from the sea level in the west to altitudes of 2000 meters on the volcanoes area in the east. The climate is tropical, with a dry and wet season with 1400 mm of average annual precipitation. It contains a high diversity of plant communities and forested habitats that includes mangroves, tropical wet forests, tropical dry forest and mountain cloud forest (Claudino-Sales et al., 2019).This study was conducted in the Tropical Dry Forest (TDF), which is a highly threatened ecosystem that in the Americas, occupies less than 35% of its original area (Portillo Quintero and Sanchez-Azofeifa, 2010). TDFs present high biodiversity of species as most of the tropical plant communities, and they also have high floristic endemism (Gentry, 1988; Kalacska et al. 2004). TDFs cover many different types of plant communities, which lead them to have different structural characteristics. Generally, they are smaller and less structurally complex than wet tropical forests. Canopy height is about half that of wet tropical forests, and basal area varies around 30 to 70% of what is commonly found in wet tropical forests (Murphy and Lugo, 1986). Also, tropical rain forests have at least three canopy strata, while many dry forests have only one or two (Murphy and Lugo, 1986).

3.2.2 – Data Collection

Three different TLS datasets were collected using a Riegl Vz400i and a Leica C10 TLS system. The open field trees dataset was collected in the dry season of 2017 using the Riegl VZ400i sensor. A total of nineteen trees were scanned using multiple scan positions. The data collection detailed description and open-field group dataset are available in Guzman et al. (2020). All five forested trees were collected in areas of late successional stage according to site classification proposed by Kalacska et al., (2007), and Li et al., (2018). One forest tree was scanned in the dry season of 2019 using the same instrument. The final four forest trees were scanned in May 2015 using the Leica C10 TLS system. All trees scanned as part of the forest group presented some degree of liana parasitism. Differently from the open-field trees, I did not gather information regarding tree species and genus in the forest group, but the trees are from different species. All five trees from the

forested environment were dominant individuals, presenting their crowns above the forest canopy. Both datasets, forested and open field were collected according to Wilkes et al., (2017). Each tree was scanned using a minimum of four scan positions located on cardinal coordinates between 5 to 15 meters from the interest tree. Retro-reflective targets were placed on the scan area to be used as control points on the registration process. This lack of species identification of the forest trees does not allow the present study to analyse the effects of the environment in individual species, but the study was designed to increase the understanding of the populations rather than individual tree species.

3.2.3 – Registration

The open field and the forest tree point-clouds collected using the Riegl sensor were registered on the RIEGL's RiSCAN PRO® software by applying the coarse co-registration using the common retro-reflective targets. Next, a multi-station adjustment procedure was used to correct rotation and translation errors on the single point-clouds until the accuracy of the registration was below five millimetres. When this accuracy was reached, a common coordinate system was applied to all point-clouds, and a file containing the merged information of all point-clouds was created and exported as a text file. The trees scanned using the Leica C10 sensor were registered using the Leica Cyclone® software, where on each tree project, all individual scan position point-cloud had its coordinate system adjusted for the first scan performed on the project. This approach generated registration accuracy below 5 millimetres on the four trees. A merged point-cloud containing all information on the project was created and exported as a text file.

3.2.4 – Pre-processing procedures

Subsequently to the registration, I performed a manual segmentation of the point-clouds to extract the trees of interest. This step was more complex on the forest dataset since the crown of these trees merged with other tree crowns, creating confusion in these regions and increasing the time of the segmentation. After the tree segmentation, a Statistical Outlier Removal (SOR) was performed on each remaining point-cloud using a k-nearest neighbour of 10 and the standard deviation of 2 to eliminate noise caused by ghost points not connected to the tree elements (Guzman et al., 2020). TLS tree modelling presents better performance using a dataset with equal point density (Brede et al., 2019). Therefore, the last pre-processing procedure was to subsample the data to a one centimeter spatial resolution to eliminate different spatial resolutions between the datasets caused by differences in the instruments or in the data collection procedures. This step was necessary since the two instruments used different spatial resolutions but also because in hemispherical field-of-view

instruments the spatial resolution decreases with the distance of the sensor, generating diverse spatial resolutions within the dataset (Lichti and Jamtsho, 2006). The manual segmentation of the trees, the application of the statistical outlier removal, and the subsampling of the point-clouds were executed on the CloudCompare® software (2021). The individual point-clouds generated after the pre-processing procedures are presented in figure 3.1 with the forested trees and in figure 3.2 with the individuals living in an open-field environment.

Figure 3.1: Forested trees merged point-clouds with a spatial resolution of 0.01 meter. Tree colours represent the same living environment since the species was not gathered. Forested individuals were dominant emergent trees. The scale below each tree measures 10 meters.

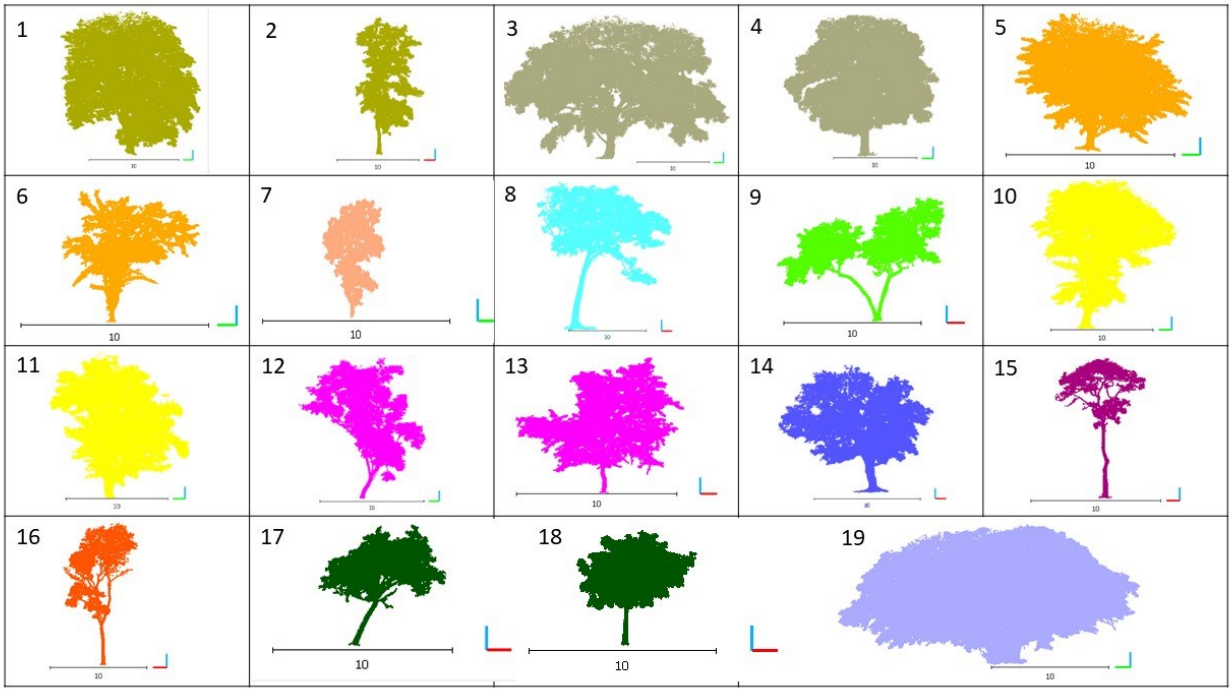

Figure 3.2: Open-field trees merged point-clouds with a spatial resolution of 0.01 meters. In this figure, tree colors represent the same tree species. The scale below each tree measures 10 meters.

3.2.5 – Fractal dimension

The fractal dimension measures the structural complexity of objects analyzing how it fills the space (Escos et al., 1995; Alados et al., 1996; Escos et al., 2000). In general, structural complexity is biologically beneficial (Alados et al., 1996) and on plants represents tree architecture (Siedel et al., 2019), This concept is related to the plant light exposure area, and photosynthetically active surface, which also regards to the plant area available to gas exchange processes (Escos et al., 1995; Seidel et. al, 2017). For this reason, the fractal dimension can be used as an important indicator of plant productivity, health and functionality (Alados et al., 2006; Seidel et al., 2017).

In this study, the fractal dimension was calculated for the tree point-clouds to analyze how the change on the scale affects the Euclidean distances between points, which represent the architectural structure of trees (Seidel et al., 2017; Guzman et al., 2020). I used the box-counting method, developed by Minkowski-Bouligand, where the algorithm counts the number of pixels needed to cover an image along with the variation of the number versus the size of the pixels when changing the scale of the image (Guzman et al., 2020). Since I was working with a three-dimensional dataset, voxels were used instead of pixels to evaluate the fractal dimension. I used a fixed grid of cubes to generate

the voxels and applied it on the tree point-clouds calculating the number of voxels necessary to cover each tree while changing the spatial resolution (Guzman et al., 2020).

For each tree point-cloud the voxels were created and analyzed using the "voxel-counting" function from the rTLS package (Guzman et al., 2020a) that analyzes how a given point-cloud can be covered using voxels of different sizes, the full description of the methods is presented in Guzman et al., (2020); and Guzman et al., (2020a). In summary, as the number of voxels increases as a power function, a positive fractal dimension (*d*HB) can be calculated using a linear model where the *d*MB is the slope of the model. The coefficient of determination reflects the self-similarity of the point-cloud (Guzman et al., 2020) and self-similarity on tree architecture (Seidel et al., 2017). The rTLS presents values of dHB between 0 and 1, where values increase with the structural complexity; for example, a tree with a single stem and no branches would present a lower dMB in comparison with a multi-layered canopy tree. I set up the minimum distance (Emin or cutoff) where voxels could be created at 0.01 meter, the same subsampled distance on the point-cloud) to avoid quantization errors generated when Emin is lower than the spatial resolution of the dataset.

To analyze the differences and compare the forested and open-field datasets I performed a t-test in each fractal dimension derived metrics. The use of large samples to understand differences between groups is always preferential over small samples since the second might not embrace all diversity of a population. Despite this preference, due to the finite nature of time and resources available to collect data, the t-test is a valid tool to differentiate populations in uneven sample sizes; unequal variances, and skewed population distribution even when applied on extremely small sample scenarios (N < 5) (de Winter, 2013). In this study, a fixed significance level of 95% to analyze all metrics was used.

3.3 –Results

3.3.1- Fractal dimension

The fractal dimension reflects the structural complexity of tree architecture. In our study, the point-clouds derived from forested and open field trees presented a different range of fractal dimension values. Of the five trees living in forested environment, the values of fractal dimension varied from 0.55 to 0.62 (Table 3.1, Figure 3), with a mean value of 0.59. Of the trees located in open areas without direct competition from other trees the fractal dimension values ranged between 0.64 to 0.73 (Table 3.2), a mean value of 0.69. The p-value measured for the fractal dimension for the two groups was 3.55E-08 confirming that the open field and forested trees are two statistically different

groups. According to Muff et al. (2022), p-values lower than 0,001 provide very strong evidence of the statistical difference of populations.

Table 3.1. Fractal Metrics of Forest Trees at the RSNP-EMSS

Forested Tree ID	intercept	slope	R2	Height (m)
1	2.27	0.59	0.98	15.9
2	2.99	0.62	0.94	18.7
3	2.66	0.59	0.96	17.6
4	2.77	0.61	0.96	19.3
5	1.99	0.55	0.97	14.5

Table 3.2. Fractal Metrics of Open Field Trees at the RSNP-EMSS

Open Field Tree ID	intercept	slope	R2	Height (m)	Genus
1	3.13	0.71	0.98	16.1	Ateleia
2	2.63	0.68	0.99	16.9	Ateleia
3	3.49	0.71	0.99	20.1	Cedrela
4	3.21	0.73	0.98	17.1	Cedrela

5	2.11	0.68	0.99	7.0	Crescentia
6	2.57	0.71	0.99	8.2	Crescentia
7	1.79	0.69	0.99	5.5	Curatella
8	3.00	0.67	0.99	18.6	Enterolobium
9	2.47	0.68	0.99	9.0	Gliricidia
10	3.01	0.69	0.99	14.6	Guazuma
11	2.86	0.72	0.99	14.3	Guazuma
12	2.49	0.70	0.99	8.4	Psidium
13	2.65	0.69	0.99	13.5	Psidium
14	2.85	0.71	0.99	12.1	Quercus
15	2.10	0.64	0.99	10.8	Simarouba
16	2.45	0.65	0.99	14.7	Trichilia
17	2.13	0.71	0.99	6.7	Swietenia
18	2.05	0.73	0.99	6.1	Swietenia
19	3.37	0.72	0.99	11.8	Ficus

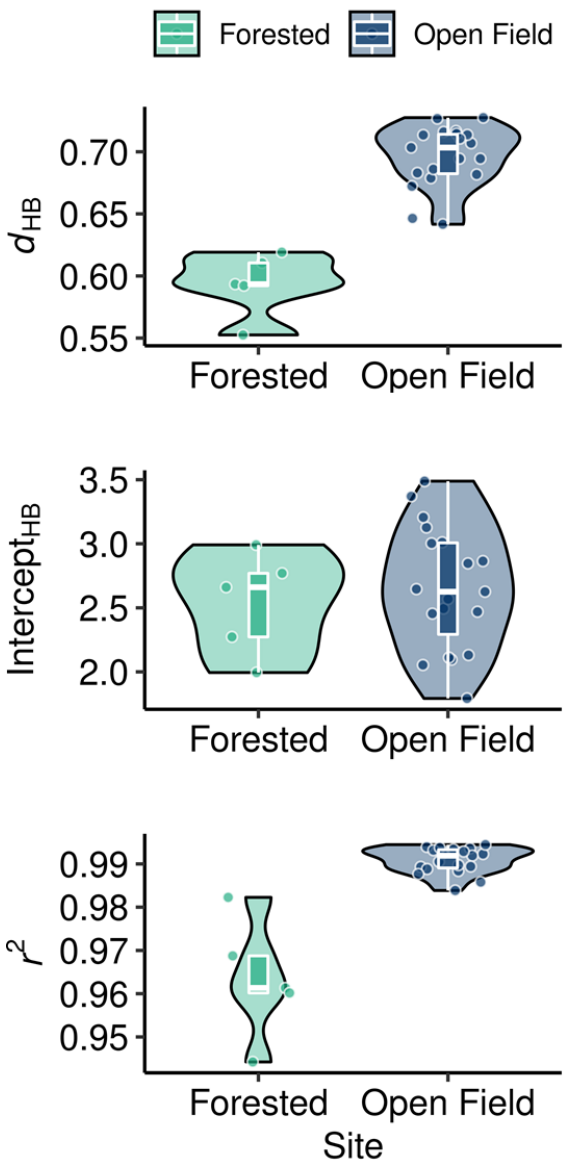

Figure 3.3: Plot values of fractal dimension (top); intercept (centre); and coefficient of determination (down) of forested trees (green) and open-field trees (blue)

3.3.2 – Intercept

The intercept of linear regression on the fractal analysis has proven to be a good predictor of tree size metrics (Dorji et al., 2019; Guzman et al., 2020). In our study, both tree groups presented similar values. The TLS point-clouds from the open field trees presented interceptMD variation between 1.79 and 3.49 (Table 3.2, Figure 3.3) with a mean value of 2.65, whereas the values obtained by the point-clouds of the forested trees ranged from 1.99 to 2.99 (Table 3.1, Figure 3.1) presenting a mean value of 2.53. The p-value calculated for this metric was 0.63, which indicates that the two populations are statistically similar.

3.3.3 – Coefficient of determination

The two datasets presented different ranges of the coefficient of determination. The tree from forested areas had values ranging from 0.94 to 0.98 (Table 3.1 and Figure 3.1) with a mean value of 0.96, while the trees from open areas presented values between 0.98 and 0.99 (table 3.2 and Figure 3.3), and a mean value of 0.99. The p-value for this metric was 2.54E-08 indicating a statistical difference between the two groups. This parameter reflects the self-similarity of objects (Seidel et al., 2017), which is related to plant developmental stress (Escos et al., 2000; Alados et al., 2008; Dorji et al., 2019). Figure 3.4 highlights some examples of the self-similarity differences observed on the forest and open-field trees.

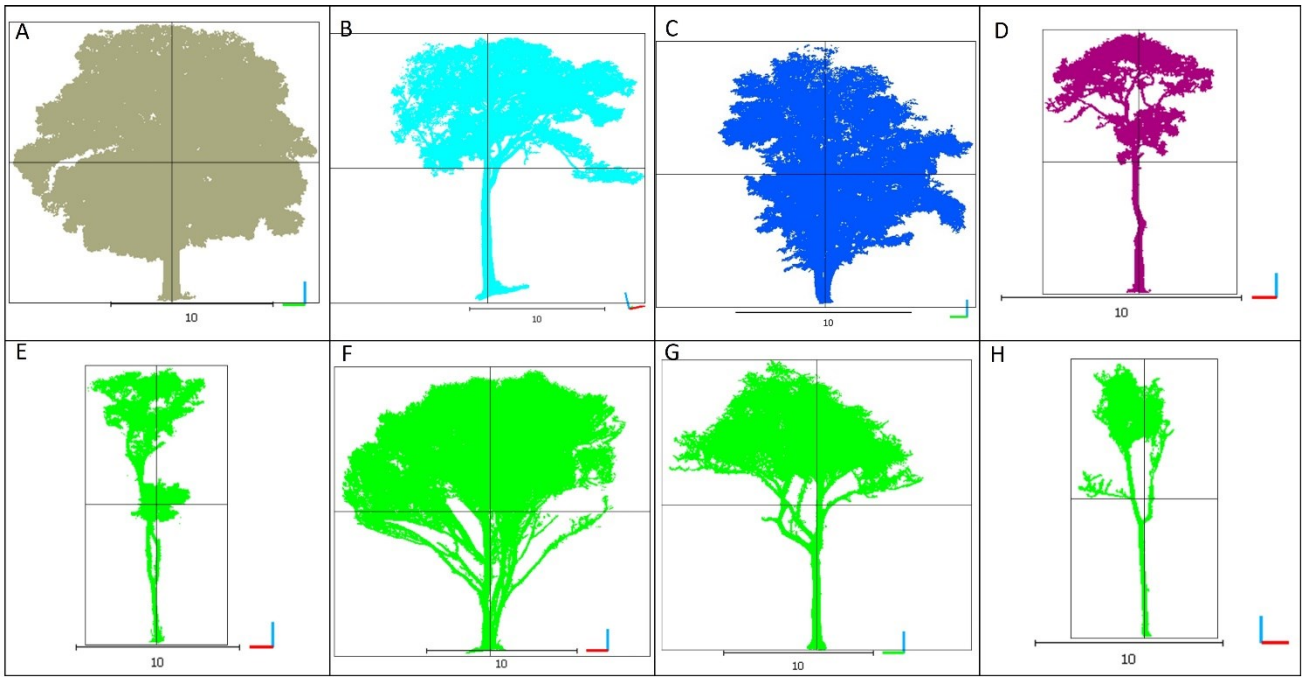

Figure 3.4:Tree point-clouds divided in quarters using the trunk base and crown edges as reference and limits. Open-field trees (A to D) present higher symmetry than forested trees (E to H). Forested trees E and H present cells with rectangular shapes instead of the most commonly found square format. Open-field trees present their crown highest point aligned with their trunks. This behaviour is observed even when X, Y, and Z axes positions are dislocated (Open-field tree B), whereas in the forested trees F, G, and H the crown highest point is dislocated from the trunk center. The scale bar bellow trees represent 10 meters.

3.4 – Discussion

Tree species can be classified by their functional, regeneration growing characteristics, strategies, and dynamics in the tropical forest (Poorter et al., 2006; Apgaua et al., 2017; Rubio and Swenson, 2022). Species from these functional groups present similar structural pattern adapted to take most advantage of the resources available in the guild that they are more efficient (Apgaua et al., 2017; Rubio and Swenson, 2022; Rubio and Swenson, 2023). Light demanding groups, including

pioneers that thrives in disturbed forests, are characterized by straight trunks, large leaves and usually monolayered canopies, while shade tolerant groups present multilayered wider crowns that allow these understory habitants capture light on the intermediate strata of the forest (Poorter et al., 2006; Adame et al., 2014). The study design of the present chapter did not contemplate the species identification of the forested trees. Although all forest trees used in this study are forest canopy dominant trees, the lack of species identification of this group of trees does not allow the analyse and comparison of the environment effect in a given species or functional group. For this reason, this chapter was designed to increase the understanding on how tree populations rather than individual tree species respond structurally to their diverse environments.

In the present chapter I found that open field trees presented higher fractal dimension values in comparison with the trees living in the forest. The higher values of the open-field group indicates that they have a more efficient space occupancy than the forested trees at the SRNP-EMSS. Our results show fractal analysis can detect tree architecture variation on trees living in an open field and forested environments at Santa Rosa National Park. The fractal analysis showed that trees in these two groups allocate plant structures differently and they present different fractal dimensions and coefficients of determination. These differences occur due to the differences in the tree architecture. Due to the small sample size used in this study, our findings are an indication of the behaviour of the two populations in the SRNP – EMSS only.

3.4.1 - Fractal dimension

Our results showed the open field trees and the forested trees are two different populations regarding the fractal dimension. This metric reflects how efficiently an object occupies the space, measuring its structural complexity (Alados et al., 1996; Escos et al., 2000; Seidel et al., 2017; Dorji et al., 2019). In plants, it measures the ability of branches, leaves and other structures to fill the space and indirectly reflects biomass production (Alados et al., 2008). The fractal dimension based on a box counting method used in this study is a powerful tool to measure tree architecture sensitive to tree shape and crown structures. In this approach, trees with a single steam and pole shape present low values of fractal dimension, while trees with a multi-layered wide, and spread crowns will present values approaching 1 (Seidel et al., 2017; Seidel et al. 2019, Guzman et al., 2020). The open field trees presented a higher fractal dimension than trees living in a forested environment indicating an effective occupancy of the space.

The capacity of filling the space reflects on the physiological processes of the trees and also reflect tree functional group characteristics (Apgaua et al., 2017; Rubio and Swenson, 2022). The branch structures increase contact between the tree and atmosphere allowing gases exchange and solar illumination (Escos et al., 1995, Alados et al. 1996, Escos et al., 2000; Ford 2014), therefore plants with larger fractal dimensions, such as our open field trees, are more efficient on the evapotranspiration process and to capture carbon dioxide (Alados et al., 1999; Seidel et al., 2017; Lau et al., 2018). Due to the more complex tree architecture indicated by the fractal analysis, individuals living in open field locations have more surface exposure to light, increasing photosynthesis efficiency (Escos et al., 1995; Ford, 2014). The main limitation for space-filling and consequently the increase of fractal dimension in trees living without competition for light and space is related to self-shading (Seidel et al., 2017), since it is not advantageous to trees to invest in structures that will not be functional and efficient (Grams and Andersen, 2007; Ford, 2014).

In tropical regions, forests have intense competition for resources and space due to the high density of individuals, where the competition for light is the main determinant for tree structure and growth (Lang et al., 2010; Jucker et al., 2014). Seidel et al. (2019) found that fractal dimension is affected by the light gradient. But the light is not the single factor affecting the fractal dimension of trees. Stress caused by diseases (Escos et al., 1995), lack of water (Escos et al., 2000; Alados et al., 2008), vegetation disturbance (Alados et al., 2005), and plant predation (Alados et al., 2008) are associated with change in plant structural development that affects their fractal dimension.

Also, it is important to point out that the SRNP-EMSS tropical dry forest is characterized by a high degree of liana infestation (Sanchez Azofeifa et al., 2009; Sanchez-Azofeifa et al., 2017). Liana parasitism is known to cause changes in tree architecture (Schnitzer and Bongers, 2002; Lobo-Catalan and Jimenez-Castillo, 2014) affecting the fractal dimension in the forested trees since all the individuals in this group presented some level of liana infestation.

3.4.2 – Coefficient of determination and developmental instability

In our fractal analysis, open field trees presented a higher coefficient of determination than the trees in a forested environment. This metric reflects the self-similarity of tree architecture; plants with a higher degree of architecture self-similarity present a higher coefficient of determination than plants with lower self-similarity (Escos et al., 1995; Alados et al., 2008; Seidel et al., 2017; Dorji et al., 2019).

Developmental stability relates to the conditions in which an organism`s grows. It is at a maximum under an ideal resourceful environment and decreases under suboptimum conditions or

disturbance of the previous scenario (Freeman et al., 1996). In our trees this reflects the higher values obtained by the open field trees living without direct competition from neighbours. The presence of environmental fluctuation, high level of competition, environmental disturbances and stress caused by lack of water and nutrients create a developmental instability stage in plants (Escos et al. 1995; Escos et al., 2000; Alados et al., 2008; Dorji et al., 2019).

This instability leads to morphological responses to the environmental conditions causing changes in plant symmetry (Escos et al. 1995; Alados et al., 2008, Ford, 2014; Jucker et al., 2015; Madsen et al., 2021). Under competition, there are two groups of morphological responses used by plants: first, size-symmetric competition occurs when the intake of resources is not dependent on the size of the plant, and second, size-asymmetric competition occurs where the intake of resources will depend on the size of the plant (Del Rio et al., 2014; Condonnier et al., 2015). Our forested trees live in a dynamic and competitive environment forcing them to adapt their shape constantly, which affect their self-similarity, reflecting on their lower coefficient of determination values. It is also Important to consider that trees respond differently to competition and environmental disturbance accordingly to their functional group traits, and some tree species more tolerant light restriction than others that need plenty of sunlight to be able to strive and develop (Apgaua et al., 2017; Rubio and Swenson, 2022). In this study the forested trees used were dominant top of canopy trees with more light availability than the ones in the understory strata.

Forests are highly dynamic environments where the competition for resources (Nambiar and Rogers, 1993; Grams and Andersen, 2007) and space (Thorpe et al., 2010; Madsen et al., 2021) is intense and constant, where light is the main driver for tree growth and structure (Lang et al., 2010; Jucker et al., 2014). Dispute for light induces size-symmetric competition since taller trees tend to overshadow smaller ones and trees can grow branches in recently open gaps in the forest (Lang et al., 2010; Seidel et al., 2011; Del Rio et al., 2014; Condonnier et al., 2015; Madsen et al., 2021) whereas competition for underground resources usually is size symmetric (Del Rio et al., 2014).In this study, since the open field trees are growing without competitors, their size hasn't been affected by the availability of light. This condition has enabled the symmetrical development of their crowns, which is demonstrated by their higher coefficient of determination values. The forested trees, on the other hand, are under competition with their neighbours, forcing them into a size-asymmetric growth (Figure 3.4). The developmental instability of the Santa Rosa National Park Forest is reflected in the lower coefficient of determination values of the group of trees living in this environment. These results corroborate the findings of Seidel et al. (2019) that light gradient affects the coefficient of determination. Moreover, the findings of this research support studies relating competitive and

instable environments with trees presenting higher degree of architectural asymmetry (Escos et al., 1995; Aldados et al., 1996; Rouvinen et al., 1997; Escos et al., 2000; Alados et al., 2002 Alados et al., 2008; Lang et al., 2010; Pretzsch et al., 2010; Seidel et al., 2011; Del Rio et al., 2014; Madsen et al., 2021).

3.4.3 – Intercept

In our study, the intercept of the fractal analysis presented similar values for trees living in both environments. The intercept is a predictor of the tree metrics related to size and crown dimensions (Dorji et al., 2019; Guzman et al., 2020). To conduct this study, I selected tree individuals with crowns above the forest canopy. Therefore, most of them were big dominant trees. The forested trees were dominant emergent trees. The open field individuals were prominent, long-living trees in pastures. These individuals were used as shadow refuge by cattle, and as food and rest resources by the local wildlife. The exceptions in this group were psidium trees (Trees 12, and 13) that were antique specimens but did not have an imposing stature due to their genotype, and juvenile individuals of the Swietenia genus (trees 17, and 18). Our results indicate that the trees used in this study have the same structural dimension, or same size. This behaviour can be explained by the fact that open-field trees presented the minimum (5.6 meters) and maximum (20.1 meters) tree height values. This is reflected in the intercept values of the open-field trees being more elastic and encompasses forested trees values that range from 14.5 to 19.3 meters in height.

3.4.4 – Light Competition and Tree Architecture

Light is acknowledged as one of the main factors influencing forest growth and tree architecture (Lang et al., 2010; Jucker et al., 2014; Poorter et al., 2021; Joshi et al., 2023). Light availability is unregular along the forest vertical profile (Thorpe et al., 2010; Fagundes et al., 2021), and presents temporal variability caused by constant changes on the environment, such as forest succession, disturbance, competition, and phenological process (Poorter et al., 2021; Matsu et al., 2021; Joshi et al., 2023). This dynamic mold the forest structure and species composition (Fagundes et al., 2021; Matsu et al., 2021), and shape tree architecture (Seidel et al., 2017; Matsu et al., 2021). Plant plasticity is what allow trees and other lifeforms to adapt to the changes on their environment (Jucker et al., 2015; Cushman and Machado, 2020), and tree functional groups respond differently to the conditions presented by the environment (Matsu et al., 2021; Rubio and Swenson, 2022). The results presented in this study corroborate the whole played by light availability in the tree architecture. The superior fractal dimension values achieved by the open field group of trees show that this category is occupying the space more efficiently than the forest group. The main limitation for the open-field

trees to increase their fractal dimension is self-shadowing (Seidel et al., 2017). The forested group, on the other hand, must compete with neighbour trees along the forest vertical profile to reach the available light (Fagundes et al., 2021; Matsuo et al., 2021) restricting their occupancy of the space and consequently their fractal dimension.

The coefficient of determination values presented in this study reflected how the different environmental condition where the groups life impacts their development and structure. Since this metric is affected by the physiologic challenges and instability that plants faced during their development (Alados and El Aich, 2008; Seidel et al., 2017). The open-field trees showed higher coefficient of determination numbers confirming that this group experienced less environmental stress than the forested group. It is important to note that in tropical dry forests, such as the SRNP, the drought is also an important factor of developmental instability that affects tree growth and architecture (Poorter et al., 2021), and influenced the coefficient of determination of both groups.

3.4.5 – Advantages and weaknesses of the method

In comparison with other remote sensing approaches to analyze plant structure and growth such as Leaf Area Indexes (LAIs), Plant Area Indexes (PAIs). and visual detection, the advantages of metrics derived from fractal analysis include the simplicity of the methods that uses the tree TLS merged point-cloud without the need of further point-cloud preparation such as classification of leaf and wood elements by algorithms or multitemporal measurements required on LAIs tools (Campo-Taberner et al., 2016; Bauer et al., 2019). It is also more practical and can be automated retrieve data fast from a great number of tree point-clouds with a minimum human interference, while the visual inspection requires detailed and time-consuming human manipulation, which make visual inspection methods difficult to be used in large TLS datasets. Moreover, the fractal analysis metrics bring knowledge of how efficiently trees occupy the space (Seidel et al., 2017; Dorji et a., 2019); information about self-similarity that reflects the environmental conditions that the plant have grown (Alados and El Aich, 2008; Dorji et al., 2029); and tree dimensions (Dorji et al., 2019; Guzman et al., 2020). These different aspects of plant structure bring the possibility of a much robust analysis of the tree, the environment where those plants live; and the developmental stress observed by individual trees or the population with same characteristics (Alados and El Aich, 2008; Seidel et al., 2017; Dorji et a., 2019; Guzman et al., 2020).

Some limitations of the fractal dimension that uses box counting regression-based methods is related to TLS point density. This approach is very sensitive to point-density along the TLS tree point-cloud (Brede et al., 2019; Liu et al., 2022), Differences in point coverage along the point cloud have

caused variation lower than 10% of fractal dimension values but is an important source of inconsistency on the methodology that needs to be assessed during the data collection with dense number of scanning positions per each tree, and pre-processing filtering to make the point-cloud density homogeneous on the point-cloud. These two possible sources of error were assessed and contemplated on the methodology of this study.

3.5 - Conclusion

This study showed that fractal analysis algorithm can identify structural differences in the architecture of forested and open-field trees in the Guanacaste Conservation Area. Since SRNP TDF`s are high light permeable forested environment, the capacity to differentiate the tree architecture of trees living in open and forested and open-field habitat indicated that fractal analysis is an important tool to measure and understand plant competition in different environmental conditions.

As expected, the open-field group presented higher fractal dimension values than the forest group, indicating that the first group occupies the space more efficiently in comparison to the group of trees living in the forested environment. This is because the only light limitation for trees in open-field environment condition was self-shadowing. On the other hand, trees growing in the forested environment are limited not only by self-shadowing but mainly by their neighbour competitors, which restrict their fractal dimension development.

The results also indicated that trees grown without neighbour competitors have better structural development than trees growing in a competitive forest environment. This is indicated by the higher coefficient of determination values presented by the open-field tree group which is characterized by more symmetric structures. This occurs since plant development in forests is limited by competition for resources and physical barrier by neighbours. This leads trees living in this environment to present crowns with more irregular shape than the trees living in open-field condition.

The small sample size especially in the forested group needs to be considered when interpreting our findings since only five trees were analyzed in this group in contrast with nineteen for the open-field group.

Chapter 4 – Using TLS and Fractal Analysis to Detect Structural Changes Caused by Phenology in Deciduous Trees

4.1 – Introduction

Trees are organisms that present irregular shape, and from the over three billion estimated individuals, it is unlikely that two trees are identical (Seidel et al., 2019). The crown structure is developed by the serial repetition of organs such as branches and leaves (Rouvinen et al., 1997). The tree architecture is the result of the plant`s genetic heritage and environmental conditions where the individual is located (Rouvinen et al., 1997; Thorpe et al., 2010; Seidel et al., 2017; MacFarlane and Kane 2017; Madsen et al., 2021). Different groups of trees present diverse strategies to succeed in challenging environments. Coniferous trees tend to keep their crown shape independent of the environmental conditions of their sites (Del Rio et al., 2014; Condonnier et al., 2015), whereas broad leaf species present a higher degree of morphological plasticity and can mold and adapt their shape to maximize resources intake (Del Rio et al., 2014; Condonnier et al., 2015). Pioneer tree species usually have low tolerance to shadow leading to an irregular growth of their crown under high competition of neighbour plants (O`Brien et al., 1995). Climax tree species, on the other hand, are much more shadow tolerant, and would keep their crown shape regular until they reach the forest canopy where they could use their morphological plasticity to explore the higher strata of the forest (O`Brien et al., 1995)

Perennial plants present growth and dormant periods to respond to seasonal changes in their environment caused by the annual climatic variation and seasons of the year (Ghelardini et al., 2014; Richards et al., 2020). This pattern of growth and dormancy is important for a plant to maximize growth in favorable periods when vital resources are available and minimize the risk of death in periods of extreme cold or drought, being essential for long term survival and plant competition (Ghelardini et al., 2014; Richards et al., 2020, Fu et al., 2020). Broad leaf trees use the deciduousness as strategy to survive during adverse periods of the year in tropical and temperate regions (Kikuzawa 1995, Fadon et al., 2020; Fu et al., 2020) These plants have adapted to pause or minimize their physiological activity during periods when the environmental conditions are extreme due to low temperature or lack of water, and could cause damage to plant tissue or result in death of the plant (Ghelardini et al., 2014; Richards et al., 2020).

Plant phenology is the study of the seasonal life cycle events driven by the periodic and annual variation in the climate (Ghelardini et al., 2014; Fu et al., 2020). Phenology analyzes the timing of

recurrent events in plants and plant communities, and the causes and intensity of these events regarding abiotic and biotic factors (Badeck et al., 2004). In individuals or at the species level, phenology describes the flowering and fruiting season, seed and leaf production timing (Manakasen et al. 1998; Bonnet, 2013). For commercial species, the understanding of their phenology is essential to guide planting of trees under ideal environmental conditions, and to predict harvest time and production volume and quality (Manakasen et al. 1998; Bonnet, 2013).

Since different environments present distinctive challenges for the plant community living in them, plant phenology is affected by diverse factors (Badeck et al., 2004; Polgar and Primack, 2011; Fu et al., 2020). In temperate regions, plant phenology is mainly affected by temperature, photoperiod, and sunlight intensity (Ghelardini et al., 2014; Peaucelle et al., 2019; Fu et al., 2020). Temperature variation is pointed to be the most influent factor affecting leaf production in these regions (Badeck et al., 2004; Ghelardini et al., 2014; Peaucelle et al., 2019; Fu et al., 2020). Photoperiod is another important driver to trigger phenological processes, such as leaf production and senescence in high latitudes (Polgar and Primack, 2011; Ghelardini et al., 2014, Chen et al., 2018; Fu et al., 2020), Peaucelle et al. (2019) argued that leaf production is more affected by solar radiation intensity than the change in the photoperiod in these regions. In tropical areas, the plant phenology is controlled by other factors, since solar radiation, temperature, and photoperiod do not present intense variation along the year (Badeck et al., 2004; Chen et al., 2018; Fu et al., 2020). The phenology of tropical plant species and communities is driven mainly by water availability (Fu et al., 2020).

Because of its importance for plant communities, plant phenology affects function and structure of terrestrial ecosystems by responding to seasonal climatic variations (Fu et al., 2020, Yang et al., 2022). In temperate regions, the carbon exchange between the broad-leaf forest and atmosphere is mainly controlled by deciduous trees phenology (Xia and Wan, 2012; Fu et al., 2020; Yang et al., 2022). The water cycle is also influenced by phenology due to plant evapotranspiration (Fu et al., 2020). The relations between plant and wildlife communities are deeply influenced by timing and intensity of phenological processes, since wildlife uses plants as food and shelter resources (Polgar and Primack, 2011). Due to the importance for ecosystems and human activities, phenological processes and timing have been well documented along the history, especially in temperate regions (Badeck et al., 2004). The predictability of phenology, and the long-term data available, make the study of the shift in the timing of phenological processes an important fingerprint of climate change (Badeck et al., 2004; Polgar and Primack, 2011; Li et al., 2019).

Fractal analysis examines how an object behaves under the change of its scale. Fractal dimension has been used over the past decades to assess plant structure, competition, and developmental stability (Escos et al., 1995; Alados et al., 1999; Escos et al., 2000; Alados et al., 2008; Seidel et al., 2017; Seidel et al., 2019). More recently, fractal analysis was employed to assess tree and forest stand metrics (Guzman et al., 2020). The main metric derived from fractal analysis, the fractal dimension, reveals the structural complexity of an organism and how efficiently it occupies space, being a good descriptor of tree architecture (Seidel et al., 2019). The structural complexity of plants is important since branch structure allows the contact between the tree and the atmosphere which provides sunlight and gases vital for them (Escos et al., 1995, Alados et al., 1999; Seidel et al., 2017). Another key metric extracted from fractal analysis is the coefficient of determination, since it reflects self-similarity which can be related to the environmental conditions affecting the plants, such as drought, disease, competition, and other stresses (Escos et al., 1995; Escos et al., 2000; Alados et al., 2008; Seidel et al., 2017).

In this chapter, I used terrestrial laser scanner (TLS) tree point-clouds to test the ability of fractal analysis to detect structural changes caused by phenological processes in deciduous trees. I also aimed to understand/explain the effects and causes of these structural changes.

4.2. - Methods

4.2.1 Tree species

To conduct this study, I selected a group of isolated young individuals of American elms (*Ulmus americana*) located at the University of Alberta campus. This species naturally occurs along the east coast of the United States and Canada spanning central west from Texas to Saskatchewan and Alberta (Bey, 1990). The precipitation across this area varies from 380 mm in its northwestern range to 1520 mm in the south of the US. Annual snow fluctuates from zero cm in Florida to 200 cm in some regions of Canada, and temperature can vary from -40”C in winter to +40”C in summer. They are more commonly found in areas with smooth topography and grow best on well-drained rich soils but they can be found in established communities on mountainous terrains and water-saturated soils (Bey, 1990). To survive across this diverse geographic area, the American elm needs to adapt to different climate and ecological conditions. A fundamental survival strategy to succeed in various biomes across North America, and explain its broad distribution is the deciduousness which allows the species to conserve energy during the winter months (Bey, 1990).

The American elm usually occurs in association with other species in mixed forests having an important ecological contribution to these ecosystems. It produces a great number of leaves annually

and its litter decomposes faster than most other species. Furthermore, it has a complex root system that can reach up to six meters deep. Although it is classified as an intermediate species, it has a long life cycle (>300 years). On a favourable site, it can reach heights of 35 to 40 meters with a diameter at breast height over 1.50 m. Its wood is moderately heavy and hard, presenting an interlocked fibre arrangement that is difficult to split. Its wood is prized for furniture, construction, flooring, and other noble uses (Bey, 1990).

I selected the American elm for this study because it shows strong deciduous and structural attributes such as broad crown and intense branch ramification. The former allows us to scan the same trees over a short period with the presence and absence of leaves, as well as with a variety in canopy structural complexity. Nine trees were selected in this study of which eight were juvenile individuals with ages ranging from 15 to 25 years. The ninth tree was a mature individual of over 50 years old. The ages of the studied trees are estimated based on their size and the age of the gardens where they are planted. The selected trees showed little variation in structure (other than variability associated with the presence/absence of leaves), such as branches lost, throughout the study period. The trees used in this study live in an urban/park environment without competition from other species. The spatial arrangement of the juvenile group affected the growth and tree architecture of the individuals. The eight juvenile trees were planted in two rows where one row has plenty of light while suppressing the second line. This condition caused the trees in the suppressed line (trees 1, 3, 5, and 7) to have lower stature and more irregular crown shape than the trees in the sunlight exposed row (trees 2, 4, 6, and 8) (Figure 4.1).

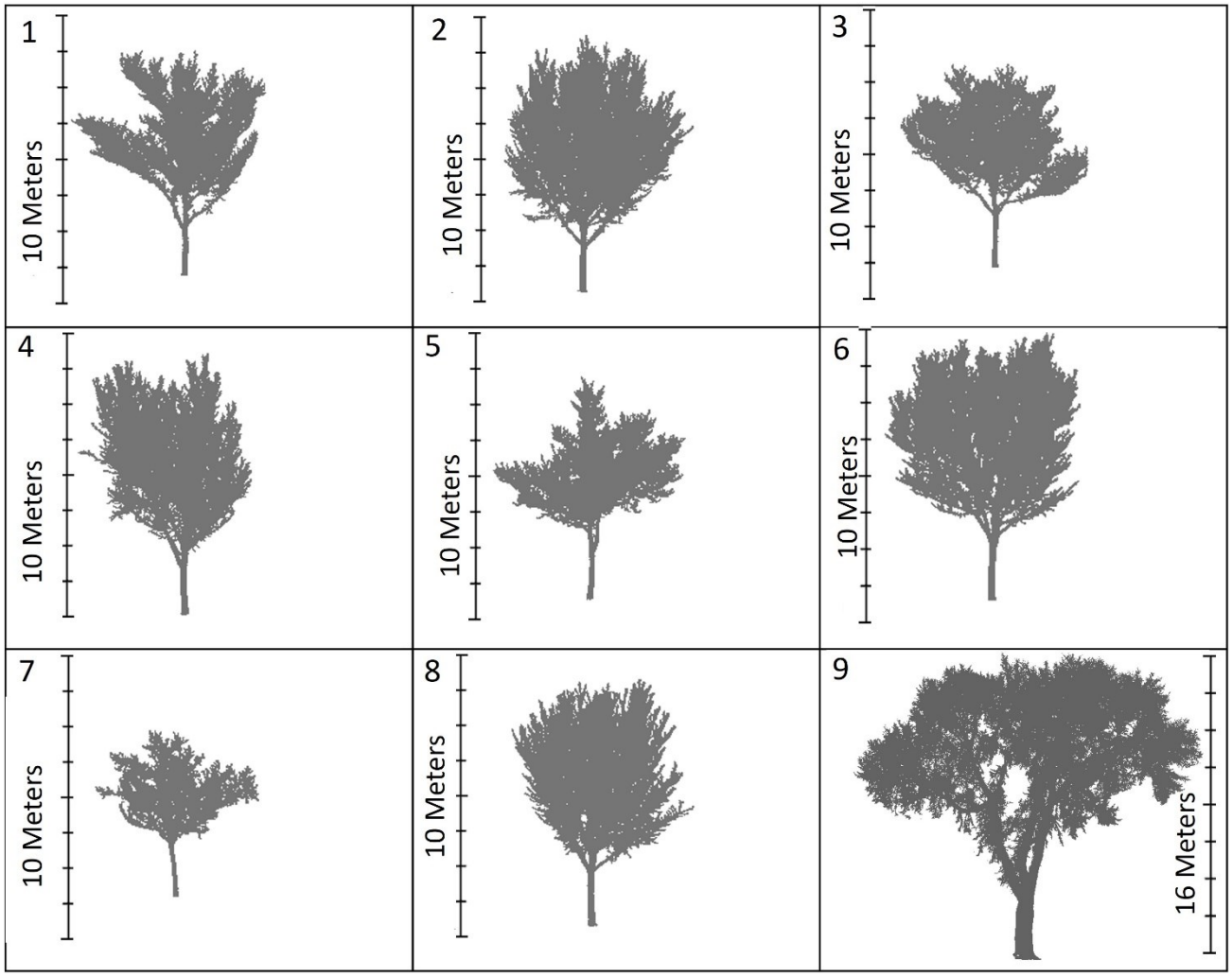

Figure 4.1: Leaf-off tree point-clouds. Trees 1, 3, 5, and 7 present smaller size, and irregular crown shape due to their spatial arrangement with less sun light availability than trees 2, 4, 6, and 8. The former show a more symmetrical crown shape. Tree 9 is considerably larger than the other trees due its age.

4.2.2 – Data collection

To produce the leaf-on/leaf-off datasets I had two data collections. The first took place on November 14, 2018 (leaf-off) and the second was on June 14, 2019 (leaf-on). I conducted the data collection on clear days to avoid ghost points caused by rain, snow, fog, dust, and aerosols. The scans were also performed without intense wind to minimize inaccuracies since wind can cause both underestimation and overestimation of TLS metrics in a single scan point-cloud (Vaaja et al., 2016).

In this study, I used a Riegl VZ 400i ® TLS sensor operating a near-infrared 1550nm laser beam. This instrument produces highly accurate data able to perform well when gaps are present in the canopy (Newnham et al., 2012), so it is commonly used for vegetation structure studies (Raumonen et al., 2013, Calders et al., 2014; Akerblom et al., 2017; Brede et al., 2019; Guzman et

al., 2020). The instrument operates at frequencies between 100kHz and 1200kHz and has a maximal effective measurement rate fluctuating from 42,000 to 500,000 points per second, and a maximum distance ranging from 250 to 800 meters. This sensor presents accuracies between 3 and 5 mm and operates at a 360º azimuth and 100º zenith field-of-view. I used the 600 kHz frequency set up, which measures up to 250,000 points per second with a maximum range of 350 meters.

Scans with multiple field-of-views were conducted around the targeted trees. A total of 12 positions were performed on the perimeter and on the inside of the areas of interest. The data collection layout was designed to maximize the number of trees each scan could assess. This approach provided a complete three-dimensional point-cloud of all scanned trees with at least three scans on each side of every tree. To minimize gaps in measurements due to the instrument`s zenith field-of-view, I conducted two measurements at each scan location; the first scan was done with the instrument in the vertical position, and on the second measurement I placed the sensor in the horizontal position to invert the zenith and azimuth field-of-view angles permitting full coverage of all trees of interest. This data collection design is similar to that of other TLS studies using the same instrument (Calders et al., (2014); Liang et al., (2016); Akerblom et al., (2017); Saarinen et al., (2017); Lau et al., (2018); Guzman et al., (2019); Brede et al., (2019)). Retro-reflective cylinder targets were mounted on metal poles at different heights and distributed throughout the area of interest. A minimum of four common targets are usually necessary to co-register each point-cloud with a high precision (Wilkes et al. 2017), therefore for each scan, I aimed to have a minimum of six retro-reflective targets.

4.2.3 -Pre-processing procedures

The order of all the pre- and post-processing methodological procedures performed in this study is presented in figure 4.2.

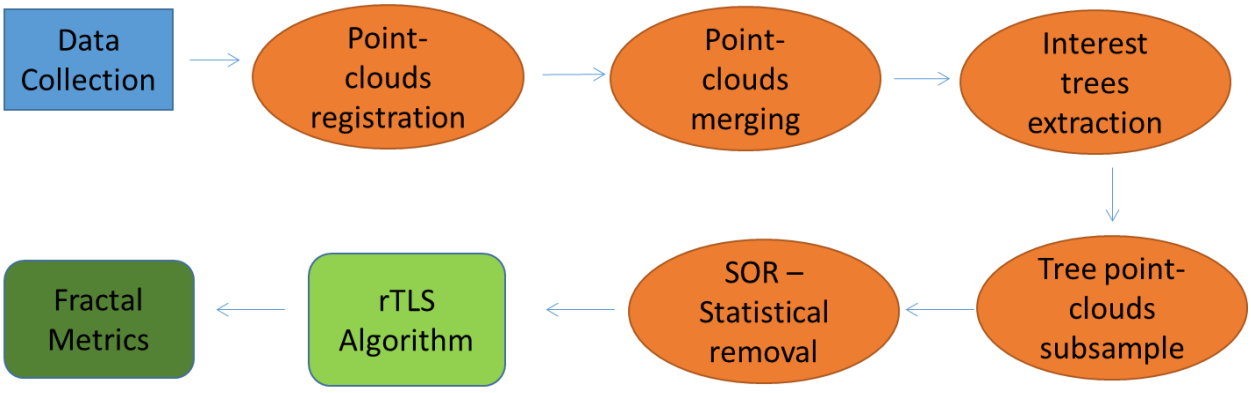

Figure 4.2: Methodological procedures adopted in this study. In blue is the data acquisition, in orange the pre-processing procedures and in green the post-processing steps.

The co-registration of the point-clouds was done using the Riegl RiscanPro software. I performed the semi-automatic registration using the reflective targets, and the sharp angles of the buildings surrounding the area of interest as control points. In this process, the software searches for the retro-reflective targets and urban features on the multiple point-clouds, giving them the same values on all point-clouds in a common coordinate system (Raumonen et al. 2013; Wilkes et al., 2017). The final procedure of this process is to adjust values of maximum distances for the same features to be located in the multiple point-clouds.

After the co-registration, all point-clouds of each tree were merged to create a single file. Here, I combined the information contained in each point-cloud to generate a full three-dimensional dataset of the selected trees (Wilkes et al., 2017; Lau et al. 2018). In this process, the final output contains all points detected in the single point-clouds. This resulting dataset can be assessed from all angles, permitting the three-dimensional modelling of the selected trees.

The following procedure was used to extract each tree point-cloud from the merged dataset. Segmentation of the trees was necessary since the fractal algorithm used in this study requires that each object (tree) be modelled as an individual dataset (Guzman et al., 2020), similarly to other algorithms used for three-dimensional modeling of trees that have the same prerequisite (Roumanen et al., 2013, Calders et al., 2014; Brede et al., 2019). Therefore, from the merged point-clouds from both, leaf-on and leaf-off datasets, I clipped the data of each tree manually in the CloudCompare software producing nine point-clouds from each season.

The next step was to subsample the point-clouds of each tree in the two periods. I selected a 1-centimeter-grid spatial resolution subsampling in the point-cloud. This step was fundamental to eliminate different spatial resolutions of the dataset, especially differences in the vertical profile caused by the sensor`s hemispherical field-of-view and scan distances (Lichti and Jamtsho, 2006). This step was also important to minimize redundant information and noise generated by the multiple scans. Lastly, a statistical outlier removal (SOR) was applied using a k-nearest neighbour of 10 and standard deviation of 2. This procedure was performed to eliminate non-connected points, and to avoid ghost points caused by dust and aerosols (Guzman et al., 2020). Figure 4.3 presents some examples of structural differences observed in the two datasets after all pre-processing procedures.

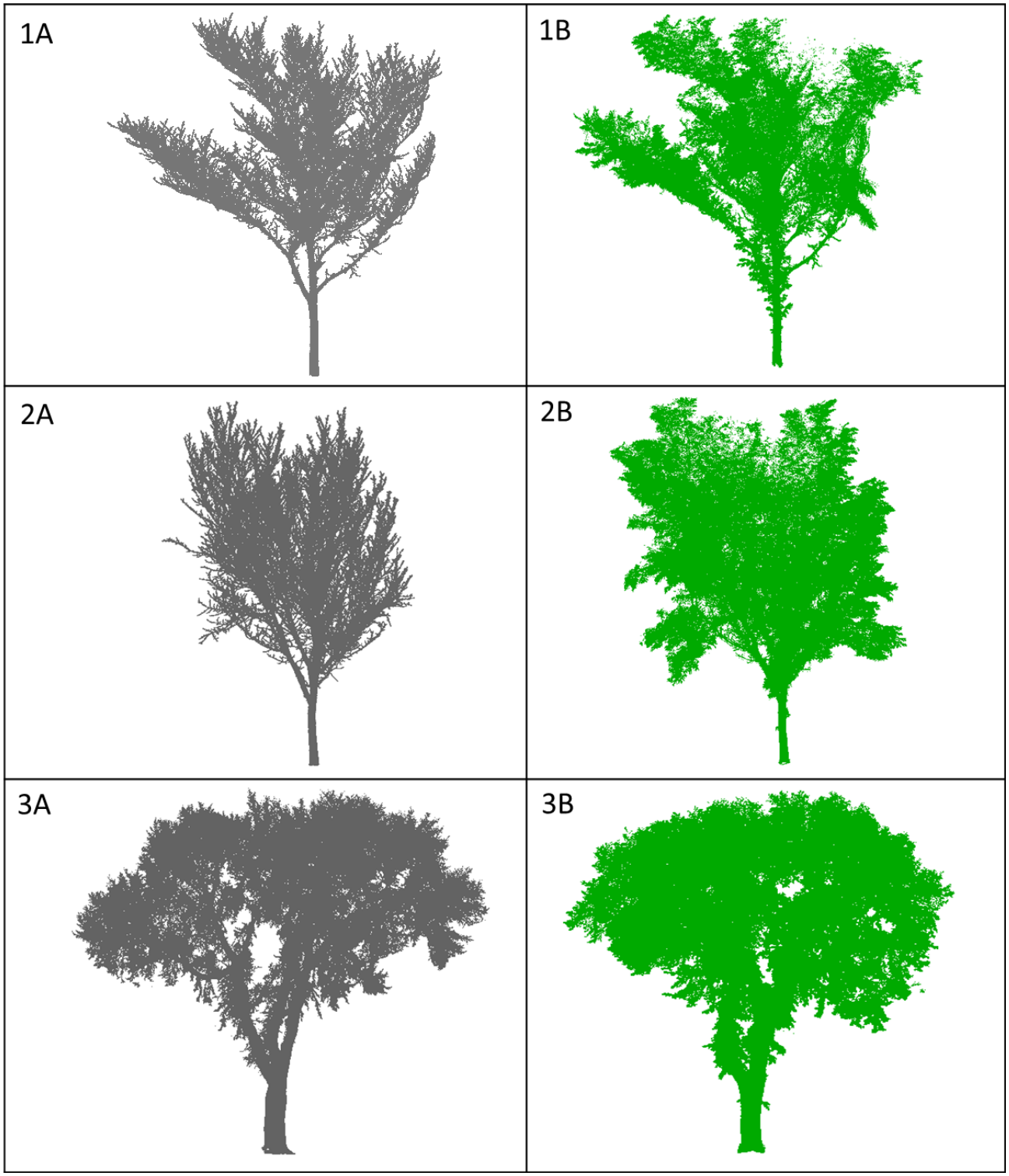

Figure 4.3: Structural differences between leaf-off (A, grey) and leaf-on (B, green) tree point-clouds. The leaf-off point-clouds permit the identification of individual branches, while the leaf-on datasets present higher point density on the crown region, hampering branch identification. 1A and 1B present a juvenile tree located on shadowed line (Tree number 1) with an irregular crown; in 1A is possible to observe disconnected points due to obstruction caused by the leaves on the top right of the crown. 2A and 2B presented juvenile tree from the illuminated line (tree number 4) with regular elliptical crown; the leafed point-cloud (2B) also showed some occlusion observed by the difference in point density on the top of the canopy. 3A and 3B present the mature tree (number 9) with prominent difference on the gap size on crowns of the two datasets. All leafed

point-clouds (1B, 2B, and 3B) present leaf structures on the lower part of their trunks that were not detectable on the leaf-off datasets.

4.2.4 – Fractal analysis

The fractal dimension reflects the structural complexity of objects describing how it fills the space (Escos et al., 1995; Alados et al., 1996; Escos et al., 2000). To biological organisms, structural complexity is often advantageous (Alados et al., 1996), and for trees it is reflected in their architecture (Siedel et al., 2019), The structural complexity is also associated with sun exposure, photosynthesis (Escos et al., 1995; Seidel et. al, 2017), and the capacity to exchange gas (Escos et al., 2000; Seidel et al., 2017). In this chapter, I used the fractal dimension from the tree point-clouds to analyze how the change in scale affects the Euclidean distance between points, which represent the architectural structure of trees (Guzman et al., 2020). I used the box-counting method, established by Minkowski-Bouligand, where the algorithm counts the number of pixels needed to cover an image along with the variation of the number versus the size of the pixels when changing the scale of the image (Guzman et al., 2020). Because I was working with a three-dimensional dataset, I used voxels instead of pixels to evaluate the fractal dimension. A fixed grid of cubes was used to generate the voxels and applied to the tree point-clouds of each season. This approach allowed measurement of the number of voxels necessary to cover each tree while changing the spatial resolution (Guzman et al., 2020).

The fractal analysis was done using the voxel-counting function from the rTLS package (Guzman et al., 2020a) where the point-cloud of each tree was analyzed, and metrics produced. This algorithm analyzes how a given point-cloud can be covered using voxels of different sizes. A full description of the method is presented in Guzman et al., (2020a); and Guzman et al., (2020). In essence, as the number of voxels increases as a power function, a positive fractal dimension (*d*HB) can be calculated using a linear model, where the *d*HB is the slope of the model. The rTLS presents values of dHB between 0 and 1, where values increase with the structural complexity.

The other two metrics derived from the linear model, the intercept and the coefficient of determination, are also important to understand the plant growing process. The intercept of the linear regression in the fractal analysis is an important predictor of tree metrics (Guzman et al., 2020). The coefficient of determination in fractal analysis reflects the self-similarity of the studied organism (Seidel et al., 2017), being an important parameter to assess the plant developmental stress (Escos et al., 1995; Escos et al., 2000; Alados et al., 2008).

In this fractal analysis I set up the minimum distance parameter for creating voxels (Emin or cutoff) to 0.01 meter to match the subsampled distance performed on the point-clouds, and avoid errors generated when Emin is lower than the spatial resolution of the dataset.

4.2.5 – Data analysis

To compare the leaf-on and leaf-off datasets and understand the effect of the phenology on the tree architecture I choose to use a t-test since the sample size used in this study is small (de Winter, 2013). I performed a paired t-test to compare single metrics derived from the fractal analysis of the leaf-on and leaf-off datasets. A t-test is commonly used to compare groups and identify different populations within the sample and can be used in extremely small sample scenarios (de Winter, 2013). The paired t-test is recommended when comparing differences between treatments when the samples were collected in pairs (Hsu and Lachenbruch, 2014; Hedberg and Ayers, 2015). In this study, I used a 95% of significance level for all metrics analyzed.

4.3 – Results

4.3.1 – Fractal dimension

In this study the point-clouds of the leaf-on trees presented a fractal dimension ranging from 0.65 to 0.70 with a mean of 0.68, median of 0.67, and a standard deviation of 0.014 (Table 4.1, Figure 4.4). The leaf-off trees presented a fractal dimension varying from 0.64 to 0.68 (Table 4.1, Figure 4.4) with a mean of 0.66, median of 0.65, and a standard deviation of 0.013. Tree number nine (mature tree) presents the lowest fractal dimension value for both phenological seasons. The two-tailed p-value calculated for the paired t-test was 0.0065 indicating statistical differences between the two datasets collected in differing phenological conditions.

Table 4.1 – Fractal analysis metrics for leaf-on and leaf-off tree point-clouds.

Tree ID	Fractal Leaf-On	Fractal Leaf-Off	R Square Leaf-On	R Square Leaf-Off	Intercept Leaf-On	Intercept Leaf-Off
1	0.68	0.66	0.99	0.99	2.14	2.08
2	0.68	0.68	0.98	0.99	2.40	2.27
3	0.67	0.67	0.99	0.99	2.01	2.03
4	0.70	0.66	0.99	0.99	2.41	2.26
5	0.68	0.66	0.99	0.99	2.16	2.08
6	0.69	0.68	0.98	0.99	2.36	2.25
7	0.67	0.65	0.99	0.99	1.86	1.82

8	0.68	0.67	0.98	0.99	2.37	2.26
9 -Mature	0.65	0.64	0.97	0.97	3.19	3.15
Mean	0.68	0.66	0.98	0.99	2.32	2.25
Median	0.67	0.65	0.986	0.991	2.36	2.25
St Dev	0.014	0.013	0.006	0.006	0.376	0.371

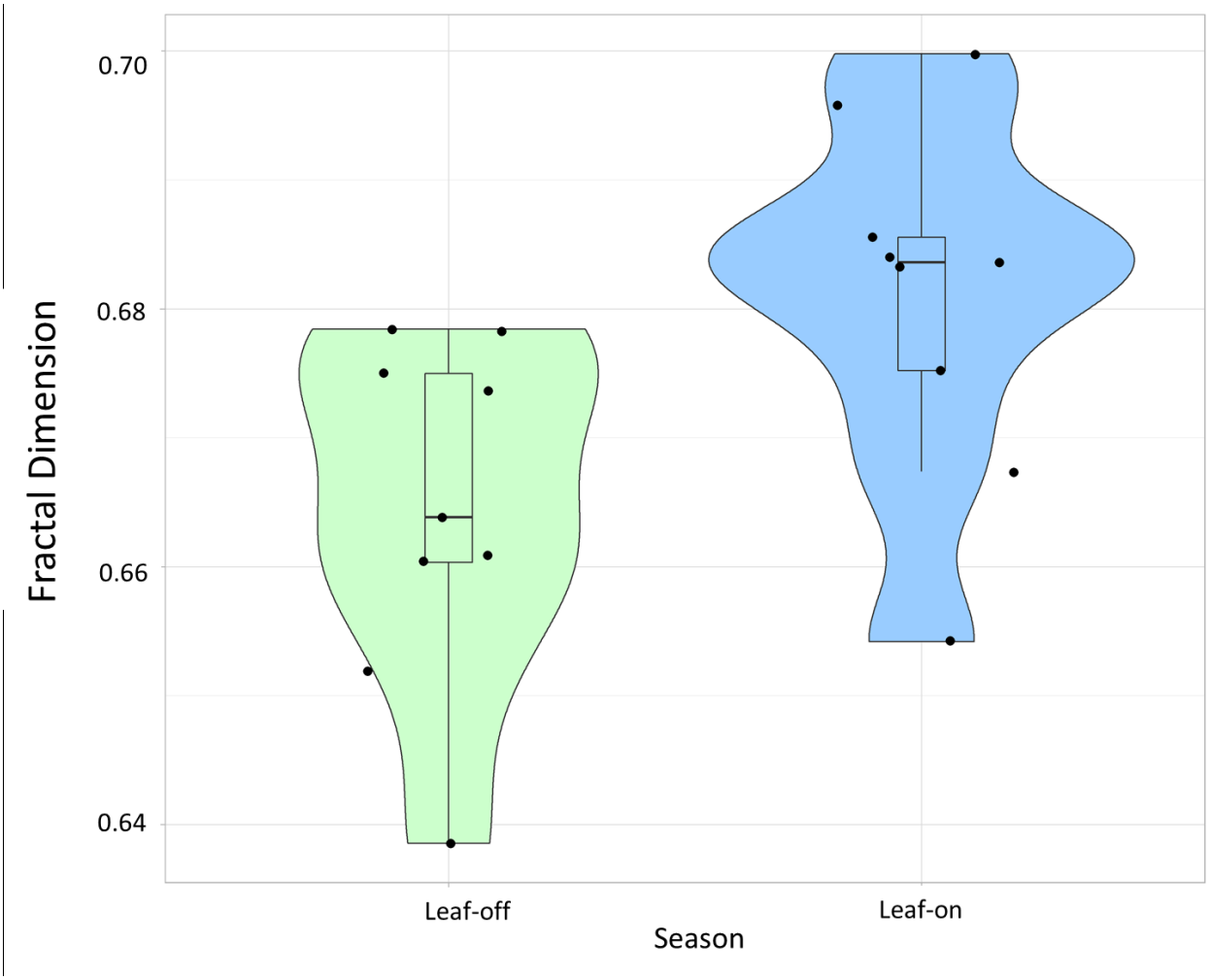

Figure 4.4: Violin graph representing the variability of fractal dimension values derived from TLS trees acquired during the leaf-on and leaf-off seasons. Points represent the values calculated for the two seasons. Mean for the leaf-off is 0.66 while the mean for the leaf-on is 0.68.

4.3.2 – Coefficient of determination (R square)

The point-clouds collected during the leaf-off season presented higher coefficient of determination values. The leaf-off values ranged from 0.97 to 0.99 with a mean and median of 0.99, and standard deviation of 0.006 (Table 4.1, Figure 4.5). Only the biggest and mature tree presented

a coefficient of determination lower than 0.99, which indicates a high degree of self-similarity. The point-clouds of the leaf-on season had coefficient of determination values ranging from the same absolute values (0.97 to 0.99) but the mean and median values for this group was 0.98, with a standard deviation of 0.006 (Table 4.1, Figure 4.5). The two-tailed p-value for this metric was 0.013 indicating that the two samples (leaf-on and leaf-off) are different.

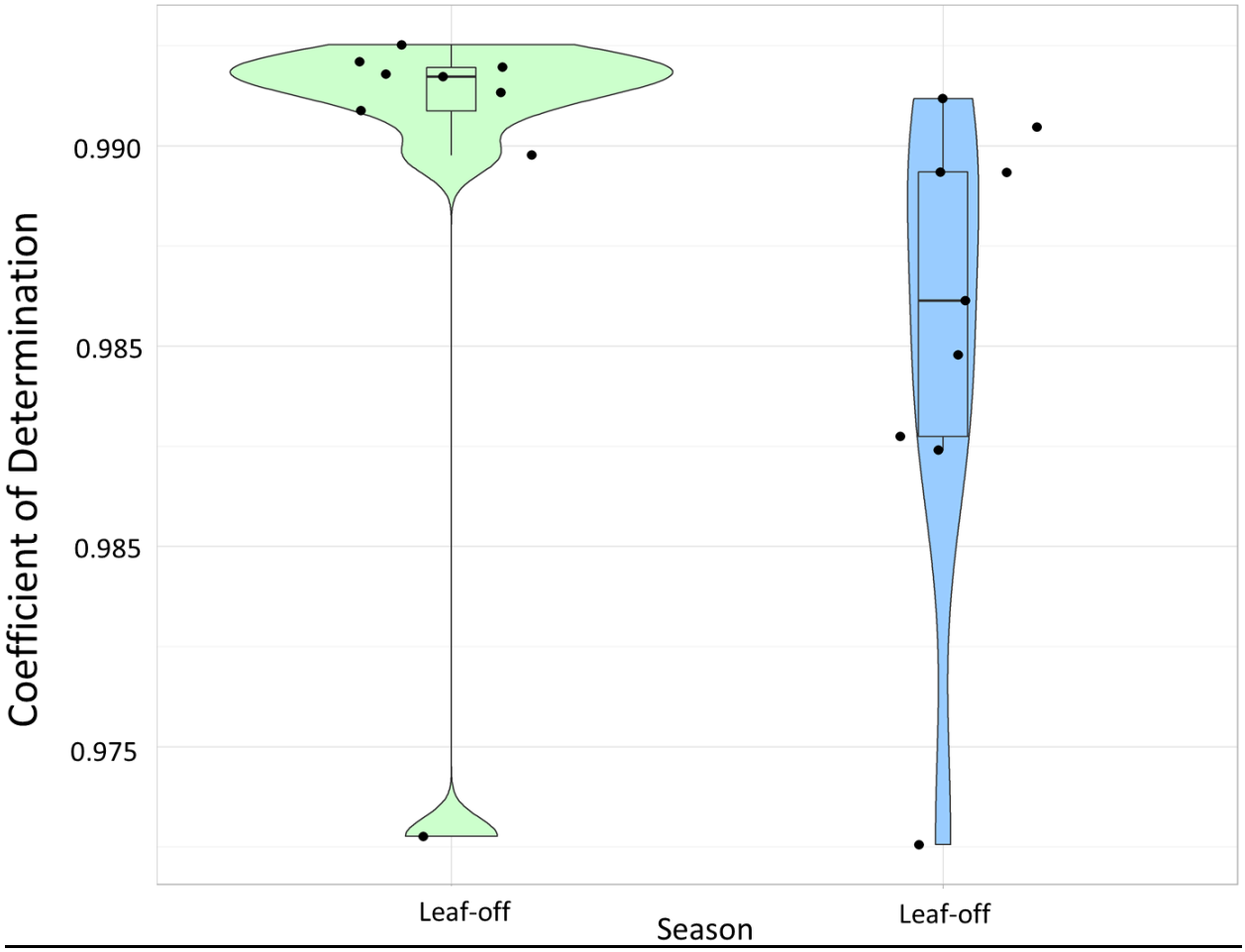

Figure 4.5: Violin graph representing the variability of the coefficient of determination values derived from TLS trees acquired during the leaf-on and leaf-off seasons. Points represent the values obtained for the two seasons. Mean for the leaf-off is 0.99 while the mean for the leaf-on is 0.98.

4.3.3 – Intercept

The point-clouds of trees presenting leaves have higher intercept values in comparison with the point-clouds of the same trees without leaves. The intercept for the leaf-on dataset ranged from 1.86 to 3.19 with a mean of 2.32, median of 2.36, and a standard deviation of 0.37 (Table 4.1. figure 4.6); while the leaf-off dataset presented values between 1.82 to 3.15 (Table 4.1, Figure 4.6) with a mean and median value of 2.25, and a standard deviation of 0.37. It is possible to observe from the

violin graph (Figure 4.6) that this metric presents a similar behavior during the leaf-off and leaf-on conditions. The two-tailed p-value for this metric was 0.007 indicating that the two datasets are statistically different.

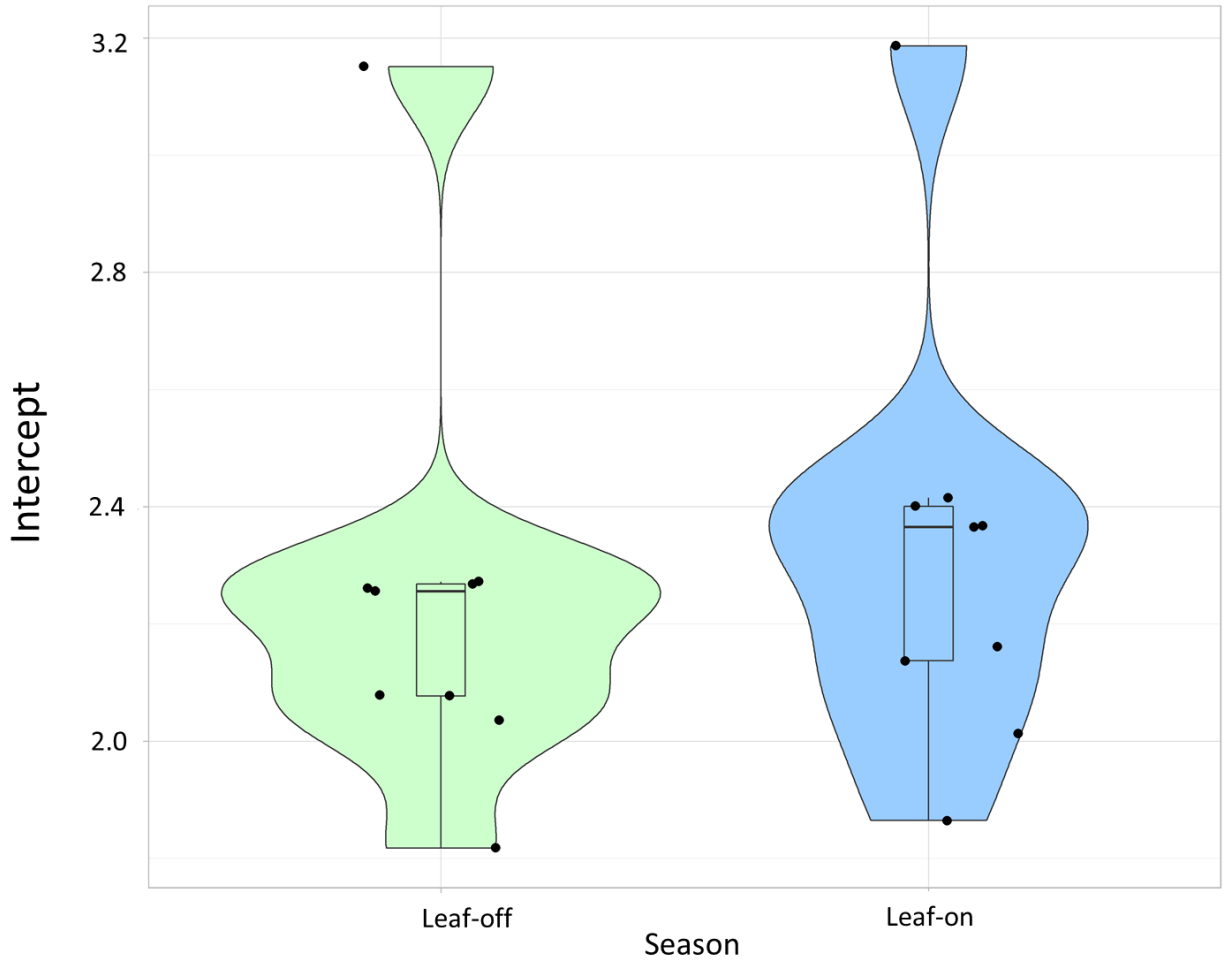

Figure 4.6: Violin graph graph representing the variability of intercept values derived from TLS trees acquired during the leaf-on and leaf-off seasons. Points represent the values for the two seasons. Mean for the leaf-off is 2.25 while the mean for the leaf-on is 2.32.

4.4 – Discussion

4.4.1 - Fractal dimension

In this study, the analyzed trees presented higher fractal dimension values in the leaf-on season in comparison with the leaf-off period. The fractal dimension measures the capacity of an organism to efficiently occupy the space reflecting its structural complexity (Alados et al., 1996; Escos et al., 2000; Seidel et al., 2017). This difference in fractal dimension between the two seasons demonstrates that fractal dimension is capable to detect structural differences in trees caused by the presence or absence of leaves driven by tree phenological processes.

The increase of the fractal dimension observed in the leaf-on season shows that trees can fill more efficiently the available space during this season. This occurs because plants have to maximize the use of the resources available in the growing season (Ghelardini et al., 2014; Fu et al., 2020; Richards et al., 2020). In temperate regions, temperature, photoperiod, and solar radiation intensity are the main factors triggering phenological processes because of their importance for plant growth and their uneven distribution along the year (Ghelardini et al., 2014; Peaucelle et al., 2019; Fu et al., 2020). The role of capturing light and gas exchange played by the leaves requires that the tree invest in them, modifying its structural arrangement to improve leaf surface exposure. These changes allow the trees to exploit these vital seasonal resources more efficiently (Ghelardini et al., 2014; Fu et al., 2020; Richards et al., 2020). Also, the decrease of fractal dimension of plants under stress has been reported (Alados et al., 1994; Escos et al., 1995), which corroborates the findings of the present study.

The spatial arrangement of the trees has influenced individual fractal dimension values. Trees located in areas of less sunlight availability (trees 1, 3, 5, 7) presented lower fractal dimension values than the other trees planted at the same time and place (trees 2, 4, 6, 8). The mature tree (tree 9) presented the lowest fractal dimension value in both scenarios. This lower fractal dimension value obtained by the mature tree may reflect the structural interventions on this tree over the years such as branches extraction due to its location in an urban park. Because their age and size, the juvenile trees suffered less structural interventions along their lives, what might reflect their higher fractal dimension in comparison with the mature tree.

4.4.2 - Coefficient of determination

The coefficient of determination is an important metric derived from the fractal analysis. It reflects the symmetry of the studied organisms (Escos et al., 1995; Alados et al., 2008; Seidel et al., 2017). In plants the study of this metric indicates developmental stress experienced by the individuals. In this study, the leaf-off dataset presented higher coefficient of determination values in comparison with the leaf-on. I hypothesise that this occurred because in the dormant period trees present their woody elements structure. This plant life stage is more stable than the dynamic growing season, when deciduous trees produce leaves, flowers and fruits and the changes occurs intensely and fast specially in high latitudes. (Fadon et al., 2020). This hypothesis needs to be better explored using multiple TLS measurements and fractal analysis during the growing season.

The mature tree presented the lowest coefficient of determination value from all analyzed individuals in both scenarios, behaving as an outlier in the group. This tree was also the only tree that maintained the same value for this metric in the leaf-on and leaf-off seasons. The smallest trees (1, 3, 5, 7) on the other hand, presented higher values than that of other trees from the same age. Since

this metric is related to self-similarity (Escos et al., 1995; Alados et al., 2008; Seidel et al., 2017), I interpret the lower coefficient of determination of the bigger trees to be due attributed to symmetry differences between the superior hemisphere (crown region) and the inferior hemisphere (trunk region). Also, the mature tree had been subject to many structural interventions in the past, such as branch removal, which changed its natural architecture. These structural interventions are common in trees living in park/garden environments, and they occurred mainly in the inferior branches.

I explain the fact of the mature tree maintain coefficient of determination value stable during the two seasons by its great dimensions. Its large size made the leaf coverage unable to modify its overall form. The juvenile trees present lower stature and their leaf coverage during the growing season was able to change the tree proportions, influencing its self-similarity and crown shape. This behavior observed for juvenile trees caused the decrease of the coefficient of determination values in the leaf-on season.

4.4.3 - Intercept

The intercept derived from the linear regression of the fractal analysis is related with the size and predictor of tree metrics (Guzman et al., 2020). This study showed the increase of intercept values during the leaf-on season. The presence of leaves in the trees generates an increase in space occupancy (increase in the fractal dimension), and increase of the individual volume, reflected in their intercept value. Also, for this metric the big mature tree presented outlier behaviour producing the highest intercept value. The trees positioned without light restrictions (2, 4, 6, and 8) showed higher values than the ones growing with light restrictions (1, 3, 5, and 7). These findings reinforce the relationship between the intercept of the linear regression and the tree size.

For both scenarios the two tree groups behave similarly. The violin graphic (figure 4.6) presents similar shape for the two seasons, with values increasing in the leaf-on period I hypothesise that this occurred due to the uniform leaf coverage on the trees due to the single species, and age of the studied group.

4.4.4 - Methods advantages and limitations

TLS point-clouds and tree 3-Dimensional modeling present multiple challenges and source of error`s and inaccuracies (Wilkes et al., 2017; Brede et al., 2019). Some of these issues is derived from data collection issues such and the target characteristics. Highly dense vegetation generates higher level of occlusion on the dataset. This can be partly addressed by increasing the number of scan positions to generate a better cover of the interested feature to achieve more homogeneous

point density along the point-cloud (Wilkes et al., 2017). Wind is also an important source of error`s by creating ghost point. All these inconsistencies cumulate in the point-cloud once you register multiple point-clouds into one merged dataset. Some of these error`s can be fixed such as the outliers ghost points using neighbourhood geometry filters (Guzman et al., 2020). Others, such as occlusion caused by highly dense vegetation or poor scan coverage presenting challenging solutions for modelling algorithms (Wilkes et al., 2017; Brede at al., 2019; Liu et al., 2022).

Different modelling algorithms respond to these dataset problems and characteristics according to how they were built. QSMs, for example, need that tree woody elements have full point coverage of their surface to perform (Calders et al., 2015; Brede ate al., 2019). Errors caused by lack of scan coverage and misfit of cylinder diameters are source of great under and over estimation of tree volume and other derived metrics (Burt et al., 2013; Brede et al., 2019) Fractal analysis methods do not require that high level of detail on all the plant point-cloud to generate valid results (Seidel et al., 2017; Dorji et al., 2019; Liu et al., 2022). Fractal dimension methods that are box-counting based methods present modest variation on their metrics due to point density change (Liu et al., 2022), This trait is an advantage of these algorithms in dense vegetated areas such as tropical forests and on the upper crown region of the trees where the occlusion is more problematic.

On the past decades, fractal have been used to address plant structure and developmental condition of the environment where they live. The methods are simple to apply, and their metrics are strong predictors of plant efficiency in filling the available space (Seidel et al.,2017; Guzman et al.,2020); developmental stress (Alados and El Aich, 2008; Seidel et al., 2017); and tree size (Dorji et al., 2019; Guzman et al., 2020). More recently, fractals are expanding their function and are being used to correct clumping effect in Leaf Area Indexes measurements. (Li and Mu, 2021; Liu et al., 2022). Moreover, due to its simplicity, fractal dimension analysis can be automated to measure large datasets, and on multi temporal data to compare the effects of the seasons or a new environmental condition experienced by the plants. Future efforts should be made to understand the relation between fractal dimension metrics and other structural parameters such as branch order and branch length.

The present study was conducted using a limited sample of only 9 individuals. A small sample is generally regarded as one size n<30. Small sample sizes are problematic to identify patterns (Vabalas et al., 2019), reducing the chance of detecting a real effect (Button et al., 2013). Another issue of concern with small sample size studies is that once a true effect is uncovered, they tend to overestimate the dimension of this effect, and the results can be difficult to reproduce (Button et al,

2013). Despite these problems, studies using a small number of samples are common (Button et al., 2013; Bacchelle, 2013; Vabalas et al., 2019), and there are situations when it is necessary to work with extremely small population (n<5) (Winter, 2013). In these scenarios, the t-test is an important tool to assess and identify patterns and differences (Winter, 2013; Poncet et al., 2016). Poncet at al. (2016) simulated normality and sample size concluding that they are not important when comparing two groups of the same size and variance. Winter (2013) attested that t-tests produce valid data analysis even in extremely small sample sizes (n=2). In this study a temporal comparison of the same individuals during two consecutive phenological seasons was performed, generating a similar dataset, which pointed to the use of the t-test (Winter, 2013; Poncet et al., 2016). Moreover, the paired t-test was used since the dataset was collected in pairs (Hsu and Lachenbruch, 2014; Hedberg and Ayers, 2015).

4.5 - Conclusion

The novelty of this study was to test the ability of fractal analysis to detect structural differences caused by deciduous phenology in trees in temperate region. My findings showed that this analysis can detect structural changes caused by annual phenological process in deciduous trees. This discovery is important since it shows that fractal dimension analysis can be used as a tool to measure plant phenological variation in time in each tree population. This finding allows the use of fractal dimension to compare the effects of phenology on the structure of different species of trees and plant communities.

This research showed that the presence of leaves increased the fractal dimension of trees, which indicates that during the growing season trees occupy the space more efficiently. This increase in fractal dimension values on leafed trees occurs due to their necessity to capture sunlight and gas during the growing season. The results of this study had the juvenile individuals presenting higher fractal dimension values than the mature tree. The coefficient of determination values of the two phenological seasons indicated that trees during the leaf-on period presented lower self-similarity indicating a higher developmental stress during the growing season.

Future efforts should focus on measuring the temporal variability/variation of the phenological process of deciduous trees. This effort will help to bring a better understanding of which climatic and environmental variables are more influent on the temporal variability of the phenology in plants, and plant communities. Another focus should be put on measuring how the fractal dimension varies along

the tree species life cycle, from seedling to its senescence, through the juvenile and mature forms, to understand which plant life stage is more efficient in occupying space.

Chapter 5 – Concluding Remarks and Future Work

5.1 - Thesis key findings

This dissertation explored three-dimensional modelling and quantification of plant structure using Terrestrial Laser Scanner derived point-clouds. A comparison of the structural metrics and dynamics between lianas and host trees was presented in chapter 2. Chapter 3 analyzed the structural differences between trees living in a competitive forested environment and trees growing without competition in open field habitats. Chapter 4 explored the structural differences generated by the presence/absence of leaves caused by plant phenology. The paragraphs below present the main achievements of this dissertation and their implications.

The structural dynamics of the competition for the three-dimensional space between lianas and hosting trees in Santa Rosa National Park was assessed in chapter 2. This chapter compared structural metrics derived from TLS point-cloud quantitative structural models from three liana-infested trees and described the relationship between lianas and host trees as a function of the infestation level. The trees presented different degrees of liana infestation. The chapter present metrics related to wood components of each lifeform and found that lianas can intensely invest in structural elements in high infestation scenarios. Here, I proposed new metrics to evaluate and compare liana infestation in trees that avoid biases present in popular methods that use liana stem abundancy, basal area and canopy/crown coverage.

Forests are environments where the competition for available resources is intense. In chapter 3, fractal analysis of TLS point-clouds was used to seek tree architectural differences caused by neighbourhood competition. I analyzed datasets of trees living in forested and open-field environments. Due to competition, trees living in forested areas are less symmetric and are less efficient in occupying the space than the individuals living in open-field habitats without the direct presence of competitors. The asymmetry observed in the forested trees was associated with developmental instability during the plant growth caused by light-related competition, while the superior efficiency to occupy the space by the open-field individuals was related to the unlimited space availability to trees living in these environments.

Plant phenology is essential to tree broad-leaf species in temperate environments. Chapter 4 used fractal analysis to investigate the structural effect of the presence/absence of leaves on

temperate deciduous trees caused by plant seasonal phenology process. The fractal analysis derived metrics from a group of trees during dormant and growing season were compared to test the ability of fractals to capture how plant structure changes as a consequence of plant phenology. During the leafed period, trees increased their fractal dimension indicating that they occupy space more efficiently during the growing season than in the dormant season. Plant symmetry is greater during the leaf-off season, indicating a higher developmental instability during the growing season.

5.2 – Future directions for three-dimensional modelling of vegetation

As with any doctoral thesis, during the development of each chapter, the observations generated a set of new questions. Here, these queries are presented along with possible approaches to solving some of the constraints encountered during this work. The observations presented in this section may or may not be exposed in each related chapter. Moreover, some of this future work might help to improve the accuracy and efficiency of TLS derived three-dimensional modelling, contributing to improve the quantification of plant biomass, and the understanding of plant competition dynamics, and its implication for forest structure and tree architecture.

5.2.1 - Lianas Infestation

As structural parasites, the dynamics of lianas and their host trees generate challenges for the point-cloud segmentation of each lifeform. In chapter 2 this segmentation was done manually and it was limited to the lower part of the hosting tree crowns. This process was time-consuming and computer power demanding since a very large number of files were created and merged until the final segmentation was achieved. Moorthy et al. (2019) presented a semi-automatic extraction of liana stems from TLS point-clouds, but it requires up to 30% of manual segmentation of liana wood elements mainly concentrated on the hosting tree crown region. This is the region where the manual segmentation is more time consuming and inaccurate due to occlusion and the dynamic between lifeforms. Therefore, an efficient and accurate automatic extraction of liana elements from TLS derived point-clouds is necessary to improve the three-dimensional modelling of this important lifeform. This liana segmentation tool will need to perform efficiently on TLS point-clouds of areas presenting dense understory since lianas are more prevalent in disturbed forests (Gerwing, 2001; Schnizer and Bongers, 2002; Schnitzer, 2005; Campbell et al., 2018).

In densely forested areas LiDAR sensors positioned at the ground level or under the forest understory such as Terrestrial Laser Scanners (TLS) are not able to reach the top of the canopy properly to make detailed measurements due to occlusion (Calders et al., 2015; Novotny et al., 2021).

The integration of TLS data with datasets from sensors positioned above the forest canopy such as drones can provide the coverage of the occluded regions. This combination of datasets assessing the forest from opposite perspectives would provide a complete three-dimensional view of the forest, minimizing occlusions caused by plant density and sensor positioning characteristics of datasets collected under or over the canopy.

The liana modelling using Quantitative Structure Model (QSMs) is challenging especially in tree infestation caused by multiple liana stems. Moorthy et al (2020) demonstrated the capacity of QSM metrics to assess liana single stem volume and biomass. The natural occurrence of liana infestation usually presents multiple lianas stems climbing hosting trees (Gerwing, 2001; Schnitzer and Bongers, 2002; Smith-Martin et al., 2019). This multiple stem occurrence characteristic of lianas is problematic for the QSM algorithm to solve since it was developed for a single stem modelling. A possible solution would be to segment the liana point-clouds into individual liana`s stem point-cloud. Another possibility would be analyzing TLS datasets containing only lianas using the voxel approach to evaluate the lifeform volume and structural contribution. Due to morphological characteristics, liana stems don`t present a great variation in stem diameter before reaching the top of the canopy (Castellanos et al., 1992; Chen et al., 2014). This constant stem diameter feature would increase the voxel modelling accuracy since the homogeneity of diameters would fit voxels more efficiently than in plants with more variable stem and branch diameters.

5.2.2 - Fractal Analysis of forested vs open field trees

The fractal analysis was able to identify structural differences in tree architecture of individuals of different species living in forested environments and open areas. These differences can be explained by the developmental instability experienced by trees in the forest caused by plant competition (Alados et al., 1996; Escos et al., 2000; Alados et al., 2002; Seidel et al., 2019). The Santa Rosa National Park Environmental Super Site (SRNP-EMSS) and the Area de Conservacion Guanacaste are a mosaic of ecosystems with diverse plant communities that present dissimilar structures varying from savannas to dry, wet and cloud forests (Claudino-Sales, 2019). Understanding the effect of plant density and abiotic factors on forest structure and tree architecture in each of these rich and diverse habitats is the next step I would take using the same approach used in chapter 3.

The liana infestation of tropical forested environments is well documented in the literature (Gerwing, 2001, Schnitzer and Bongers, 2002; Phillips et al., 2002; Ingwell et al., 2010; Marshall et al., 2020; Parolari et al., 2020; Reis et al., 2020). This phenomenon is more intense in tropical dry environments, and the SRNP-EMSS dry forest is an example of this infestation (Sanchez-Azofeifa et

al., 2009; Sanchez-Azofeifa et al., 2015; Sanchez-Azofeifa et al., 2017). The fractal analysis provides metrics related to the space occupancy and symmetry of objects. These metrics are associated to the organism structural complexity and developmental stability (Escos et al., 1995; Alados et al., 1996; Escos et al., 2000; Alados et al., 2002; Seidel et al., 2019). A further investigation would explore how liana infestation is affecting tree architecture and if the stress caused by lianas is increasing the developmental instability in the already demanding and competitive forested environments.

5.2.3 – Fractal analysis of the phenological process in deciduous temperate trees

The fractal analysis algorithm used in chapter 4 was able to detect the structural modification caused by the phenological process. Plant phenology is driven by environmental abiotic factors including climatic and plant nutritional variables (Ghelardini et al., 2014; Peaucelle et al., 2019; Fu et al., 2020). The dynamic of plant phenology has effects on energy, water, and carbon fluxes (Peaucelle et al., 2019; Richards et al., 2020; Yang et al., 2022). A further study would focus on understanding the temporal variability of temperate deciduous trees phenology by measuring annually the intensity of this process. Fractal analysis showed to be an important tool to measure the intensity of phenological process and it can be used to measure phenological variation caused by a given climatic anomaly at the tree and stand level.

Another study would explore whether the life stage of trees and other plant lifeform influences their structural arrangement and biomass allocation (McConnaughay and Coleman, 1999; Smith-Martin et al., 2019; Hu et al., 2020). From seedling to tree senescence, plants modify their structure to adapt to environmental changes in their habitat, such as gap opening; or to respond to their biological cycles (Jucker et al., 2014; Cabon et al., 2018; Madsen et al., 2021). How structural changes caused by plant phenology vary along tree life stages would be another crucial question to be answered using fractal analysis. Therefore, understand how plant life stage affect plant space occupancy is an interesting question to be assessed using fractal analysis.

The emerging outcome of this thesis dissertation is to display different TLS methodologies and applications for ecological analysis. The analysis and quantification of liana infestation in tropical forests using TLS point-clouds and QSMs was presented in chapter 2. In this chapter two main metrics were extracted from the analysis to compare different degrees of liana infestation. The structural effect of plant competition in trees was investigated in chapter 3 using fractal dimension and comparing trees living in forested and open-field environments in the Neo-tropics. Lastly, chapter 4 attests the ability of fractal analysis to detect structural changes caused by the phenological process in temperate

regions. All those findings would be useful to bring new remote sensing tools and a better understanding of tree architecture, forest structure, and forest ecological processes.

References

Abbas, M. A., Setan, H., Majid, Z., Chong, A. K., Idris, K. M., & Aspuri, A., 2013. Calibration and accuracy assessment of leica scanstation c10 terrestrial laser scanner. In *Developments in Multidimensional Spatial Data Models* (pp. 33-47). Springer, Berlin, Heidelberg.

Adame, P., Brandeis, T.J. and Uriarte, M., 2014. Diameter growth performance of tree functional groups in Puerto Rican secondary tropical forests. *Forest Systems*, *23*(1), pp.52-63.

Åkerblom, M., Raumonen, P., Mäkipää, R. and Kaasalainen, M., 2017. Automatic tree species recognition with quantitative structure models. *Remote Sensing of Environment*, *191*, pp.1-12.

Alados, C.L., Escos, J.M. and Emlen, J.M., 1996. Fractal structure of sequential behaviour patterns: an indicator of stress. *Animal behaviour*, *51*(2), pp.437-443.

Alados, C.L., Escos, J., Emlen, J.M. and Freeman, D.C., 1999. Characterization of branch complexity by fractal analyses. *International Journal of Plant Sciences*, *160*(S6), pp.S147-S155.

Alados, C.L., Giner, M.L., Dehesa, L., Escos, J., Barroso, F.G., Emlen, J.M. and Freeman, D.C., 2002. Developmental instability and fitness in Periploca laevigata experiencing grazing disturbance. *International Journal of Plant Sciences*, *163*(6), pp.969-978.

Alados, C.L., Pueyo, Y., Giner, M.L., Navarro, T., Escos, J., Barroso, F., Cabezudo, B. and Emlen, J.M., 2003. Quantitative characterization of the regressive ecological succession by fractal analysis of plant spatial patterns. *Ecological Modelling*, *163*(1-2), pp.1-17.

Alados, C.L., Pueyo, Y., Navas, D., Cabezudo, B., Gonzalez, A. and Freeman, D.C., 2005. Fractal analysis of plant spatial patterns: a monitoring tool for vegetation transition shifts. *Biodiversity & Conservation*, *14*(6), pp.1453-1468.

Alados, C.L. and El Aich, A., 2008. Stress assessment of argan (Argania spinosa (L.) Skeels) in response to land uses across an aridity gradient: Translational asymmetry and branch fractal dimension. *Journal of Arid Environments*, *72*(4), pp.338-349.

Alcorn, P.J., Pyttel, P., Bauhus, J., Smith, R.G.B., Thomas, D., James, R. and Nicotra, A., 2007. Effects of initial planting density on branch development in 4-year-old plantation grown Eucalyptus pilularis and Eucalyptus cloeziana trees. *Forest Ecology and Management*, *252*(1-3), pp.41-51.

Ali, A., Mattsson, E., Nissanka, S.P. and Wang, L.Q., 2020. Topmost trees and foremost species underlie tropical forest structure, diversity and biomass through opposing mechanisms. *Forest Ecology and Management*, *473*, p.118299.

Alonzo, Michael, Bodo Bookhagen, and Dar A. Roberts (2014). "Urban tree species mapping using hyperspectral and lidar data fusion." *Remote Sensing of Environment* 148: 70-83.

Álvarez-Cansino, L., Schnitzer, S.A., Reid, J.P. and Powers, J.S., 2015. Liana competition with tropical trees varies seasonally but not with tree species identity. *Ecology*, *96*(1), pp.39-45.

Anbarashan, M. and Parthasarathy, N., 2013. Diversity and ecology of lianas in tropical dry evergreen forests on the Coromandel Coast of India under various disturbance regimes. *Flora-Morphology, Distribution, Functional Ecology of Plants*, *208*(1), pp.22-32.

Andersen, H.E., Reutebuch, S.E. and McGaughey, R.J., 2006. A rigorous assessment of tree height measurements obtained using airborne lidar and conventional field methods. *Canadian Journal of Remote Sensing*, *32*(5), pp.355-366.

Andrade, J.L., Meinzer, F.C., Goldstein, G. and Schnitzer, S.A., 2005. Water uptake and transport in lianas and co-occurring trees of a seasonally dry tropical forest. *Trees*, *19*(3), pp.282-289.

Annighöfer, P., Mund, M., Seidel, D., Ammer, C., Ameztegui, A., Balandier, P., Bebre, I., Coll, L., Collet, C., Hamm, T. and Huth, F., 2022. Examination of aboveground attributes to predict belowground biomass of young trees. *Forest Ecology and Management*, *505*, p.119942.

Antony, F., Schimleck, L.R., Jordan, L., Daniels, R.F. and Clark, A., 2012. Modeling the effect of initial planting density on within tree variation of stiffness in loblolly pine. *Annals of forest science*, *69*(5), pp.641-650.

Apgaua, D.M., Tng, D.Y., Cernusak, L.A., Cheesman, A.W., Santos, R.M., Edwards, W.J. and Laurance, S.G., 2017. Plant functional groups within a tropical forest exhibit different wood functional anatomy. *Functional Ecology*, *31*(3), pp.582-591.

ARISTA, M. and TALAVERA, S., 1996. Density Effect on the Fruit-set, Seed Crop Viability and Seedling Vigour ofAbies pinsapo. *Annals of Botany*, *77*(2), pp.187-192.

Asner, G.P. and Martin, R.E., 2015. Canopy chemistry expresses the life-history strategies of lianas and trees. *Ecology of lianas*, pp.299-308.

Avalos, G., Mulkey, S. S., & Kitajima, K., 1999. Leaf Optical Properties of Trees and Lianas in the Outer Canopy of a Tropical Dry Forest1. *Biotropica*, *31*(3), 517-520.
Avery, T. E., & Burkhart, H. E., 2015. *Forest measurements*. Waveland Press.

Bacchetti, P., 2013. Small sample size is not the real problem. *Nature Reviews Neuroscience*, *14*(8), pp.585-585.

Bauer, J., Jarmer, T., Schittenhelm, S., Siegmann, B. and Aschenbruck, N., 2019. Processing and filtering of leaf area index time series assessed by in-situ wireless sensor networks. *Computers and electronics in agriculture*, *165*, p.104867.

Béland, M., Widlowski, J. L., Fournier, R. A., Côté, J. F., & Verstraete, M. M., 2011. Estimating leaf area distribution in savanna trees from terrestrial LiDAR measurements. *Agricultural and Forest Meteorology*, *151*(9), 1252-1266.

Béland, M., Widlowski, J. L., & Fournier, R. A., 2014. A model for deriving voxel-level tree leaf area density estimates from ground-based LiDAR.*Environmental Modelling & Software*, *51*, 184-189.

Béland, M., Baldocchi, D. D., Widlowski, J. L., Fournier, R. A., & Verstraete, M. M., 2014. On seeing the wood from the leaves and the role of voxel size in determining leaf area distribution of forests with terrestrial LiDAR.*Agricultural and Forest Meteorology*, *184*, 82-97.

Bey, C.F., 1990. Ulmus americana L. American elm. *Silvics of North America*, *2*, pp.801-807.

Boudreau, J., Nelson, R. F., Margolis, H. A., Beaudoin, A., Guindon, L., & Kimes, D. S., 2008. Regional aboveground forest biomass using airborne and spaceborne LiDAR in Québec. *Remote Sensing of Environment*,*112*(10), 3876-3890.

Bragg, D.C., 2008. An improved tree height measurement technique tested on mature southern pines. *Southern Journal of Applied Forestry*, *32*(1), pp.38-43.

Brede, B., Lau, A., Bartholomeus, H.M. and Kooistra, L., 2017. Comparing RIEGL RiCOPTER UAV LiDAR derived canopy height and DBH with terrestrial LiDAR. *Sensors*, *17*(10), p.2371.

Brede, B., Calders, K., Lau, A., Raumonen, P., Bartholomeus, H. M., Herold, M., & Kooistra, L. (2019). Non-destructive tree volume estimation through quantitative structure modelling: Comparing UAV laser scanning with terrestrial LIDAR. *Remote Sensing of Environment*, *233*, 111355.

e Brugnera, M. D. P., Fischer, R., Taubert, F., Huth, A., & Verbeeck, H., 2020. Lianas in silico, ecological insights from a model of structural parasitism. *Ecological modelling*, *431*, 109159.

Button, K.S., Ioannidis, J., Mokrysz, C., Nosek, B.A., Flint, J., Robinson, E.S. and Munafò, M.R., 2013. Power failure: why small sample size undermines the reliability of neuroscience. *Nature reviews neuroscience*, *14*(5), pp.365-376.

Burt, A., Disney, M. I., Raumonen, P., Armston, J., Calders, K., & Lewis, P., 2013. Rapid characterisation of forest structure from TLS and 3D modelling. In *2013 IEEE International Geoscience and Remote Sensing Symposium-IGARSS* (pp. 3387-3390). IEEE.

Cabon, A., Mouillot, F., Lempereur, M., Ourcival, J.M., Simioni, G. and Limousin, J.M., 2018. Thinning increases tree growth by delaying drought-induced growth cessation in a Mediterranean evergreen oak coppice. *Forest Ecology and Management*, *409*, pp.333-342.

Calders, K., Armston, J., Newnham, G., Herold, M., & Goodwin, N., 2014. Implications of sensor configuration and topography on vertical plant profiles derived from terrestrial LiDAR. *Agricultural and Forest Meteorology*, *194*, 104-117.

Calders, K., Newnham, G., Burt, A., Murphy, S., Raumonen, P., Herold, M., Culvenor, D., Avitabile, V., Disney, M., Armston, J. and Kaasalainen, M., 2015. Nondestructive estimates of above-ground biomass using terrestrial laser scanning. *Methods in Ecology and Evolution*, *6*(2), pp.198-208.

Campanello, P.I., Manzané, E., Villagra, M., Zhang, Y.J., Panizza, A.M., di Francescantonio, D., Rodriguez, S.A., Chen, Y.J., Santiago, L.S. and Goldstein, G., 2016. Carbon allocation and water relations of lianas versus trees. In *Tropical tree physiology* (pp. 103-124). Springer, Cham.

Campbell, M.J., Edwards, W., Magrach, A., Alamgir, M., Porolak, G., Mohandass, D. and Laurance, W.F., 2018. Edge disturbance drives liana abundance increase and alteration of liana–host tree interactions in tropical forest fragments. *Ecology and Evolution*, *8*(8), pp.4237-4251.

Campos-Taberner, M., García-Haro, F.J., Camps-Valls, G., Grau-Muedra, G., Nutini, F., Crema, A. and Boschetti, M., 2016. Multitemporal and multiresolution leaf area index retrieval for operational local rice crop monitoring. *Remote Sensing of Environment*, *187*, pp.102-118.

Candel-Pérez, D., Lucas-Borja, M.E., García-Cervigón, A.I., Tíscar, P.A., Andivia, E., Bose, A.K., Sánchez-Salguero, R., Camarero, J.J. and Linares, J.C., 2021. Forest structure drives the expected growth of Pinus nigra along its latitudinal gradient under warming climate. *Forest Ecology and Management*, p.119818.

Castellanos, A.E., Duran, R., Guzman, S., Briones, O. and Feria, M., 1992. Three-dimensional space utilization of lianas: a methodology. *Biotropica*, pp.396-401.

Castillo-Núñez, M., Sánchez-Azofeifa, G. A., Croitoru, A., Rivard, B., Calvo-Alvarado, J., & Dubayah, R. O., 2011. Delineation of secondary succession mechanisms for tropical dry forests using LiDAR. *Remote Sensing of Environment*, *115*(9), 2217-2231.

Castro, S. M., Sanchez-Azofeifa, G. A., & Sato, H., 2018. Effect of drought on productivity in a Costa Rican tropical dry forest. *Environmental Research Letters*, *13*(4), 045001.

Castro-Esau, K. L., Sánchez-Azofeifa, G. A., Rivard, B., Wright, S. J., & Quesada, M., 2006. Variability in leaf optical properties of Mesoamerican trees and the potential for species classification. *American Journal of Botany*, *93*(4), 517-530.

Cifuentes, R., Van der Zande, D., Farifteh, J., Salas, C., & Coppin, P., 2014. Effects of voxel size and sampling setup on the estimation of forest canopy gap fraction from terrestrial laser scanning data. *Agricultural and Forest Meteorology*, *194*, 230-240.

Chen, Y.J., Cao, K.F., Schnitzer, S.A., Fan, Z.X., Zhang, J.L. and Bongers, F., 2015. Water-use advantage for lianas over trees in tropical seasonal forests. *New Phytologist*, *205*(1), pp.128-136.

Chen, Y.J., Schnitzer, S.A., Zhang, Y.J., Fan, Z.X., Goldstein, G., Tomlinson, K.W., Lin, H., Zhang, J.L. and Cao, K.F., 2017. Physiological regulation and efficient xylem water transport regulate diurnal water and carbon balances of tropical lianas. *Functional Ecology*, *31*(2), pp.306-317.

Clark, D.B. and Clark, D.A., 1990. Distribution and effects on tree growth of lianas and woody hemiepiphytes in a Costa Rican tropical wet forest. *Journal of Tropical Ecology*, *6*(3), pp.321-331.

Claudino-Sales, V., 2018. *Coastal World Heritage Sites* (Vol. 28). Springer.

Collins, C.G., Wright, S.J. and Wurzburger, N., 2016. Root and leaf traits reflect distinct resource acquisition strategies in tropical lianas and trees. *Oecologia*, *180*(4), pp.1037-1047.

Cordonnier, T. and Kunstler, G., 2015. The Gini index brings asymmetric competition to light. *Perspectives in Plant Ecology, Evolution and Systematics*, *17*(2), pp.107-115.

Conn, A., Chandrasekhar, A., Rongen, M.V., Leyser, O., Chory, J. and Navlakha, S., 2019. Network trade-offs and homeostasis in Arabidopsis shoot architectures. *PLoS computational biology*, *15*(9), p.e1007325.

Coomes, D.A., Dalponte, M., Jucker, T., Asner, G.P., Banin, L.F., Burslem, D.F., Lewis, S.L., Nilus, R., Phillips, O.L., Phua, M.H. and Qie, L., 2017. Area-based vs tree-centric approaches to mapping forest carbon in Southeast Asian forests from airborne laser scanning data. *Remote Sensing of Environment*, *194*, pp.77-88.

Côté, J. F., Widlowski, J. L., Fournier, R. A., & Verstraete, M. M., 2009. The structural and radiative consistency of three-dimensional tree reconstructions from terrestrial lidar. *Remote Sensing of Environment*, *113*(5), 1067-1081.

Côté, J.F., Fournier, R.A. and Egli, R., 2011. An architectural model of trees to estimate forest structural attributes using terrestrial LiDAR. *Environmental Modelling & Software*, *26*(6), pp.761-777.

Coveney, S., & Stewart Fotheringham, A.. 2011. Terrestrial laser scan error in the presence of dense ground vegetation. *The Photogrammetric Record*,*26*(135), 307-324.

da Cunha Vargas, B., Grombone-Guaratini, M.T. and Morellato, L.P.C., 2021. Lianas research in the Neotropics: overview, interaction with trees, and future perspectives. *Trees*, *35*, pp.333-345.

Culvenor, D. S., Newnham, G. J., Mellor, A., Sims, N. C., & Haywood, A., 2014. Automated in-situ laser scanner for monitoring forest leaf area index. *Sensors*, *14*(8), 14994-15008.

Cushman, K.C. and Machado, J.L., 2020. Plasticity in branching and crown architecture helps explain how tree diversity increases tropical forest production. *The New Phytologist*, *228*(4), pp.1163-1165.

del Río, M., Condés, S. and Pretzsch, H., 2014. Analyzing size-symmetric vs. size-asymmetric and intra-vs. inter-specific competition in beech (Fagus sylvatica L.) mixed stands. *Forest Ecology and Management*, *325*, pp.90-98.

DellaSala, D.A., 2020. Forest Biome: Trees of Life.

Demol, M., Wilkes, P., Raumonen, P., Krishna Moorthy Parvathi, S., Calders, K., Gielen, B. and Verbeeck, H., 2022. Volumetric overestimation of small branches in 3D reconstructions of Fraxinus excelsior. *Silva Fennica*, *56*(1).

Dias, A. S., Dos Santos, K., Dos Santos, F. A. M., & Martins, F. R., 2017. How liana loads alter tree allometry in tropical forests. *Plant ecology*, *218*(2), 119-125.

Dias, A.S., Oliveira, R.S., Martins, F.R., Bongers, F., Anten, N.P. and Sterck, F., 2019. How do lianas and trees change their vascular strategy in seasonal versus rain forest?. *Perspectives in plant ecology, evolution and systematics*, *40*, p.125465.

Disney, M.I., Anderson, K., Hancock, S. and Gaston, K.J., 2016. Is waveform worth it? A comparison of LiDAR approaches for vegetation and landscape characterisation. *Remote Sensing in Ecology and Conservation*, *2*(1), pp.5-15.

Dorji, Y., Annighöfer, P., Ammer, C. and Seidel, D., 2019. Response of beech (Fagus sylvatica L.) trees to competition—New insights from using fractal analysis. *Remote Sensing*, *11*(22), p.2656.

Dorji, Y., Schuldt, B., Neudam, L., Dorji, R., Middleby, K., Isasa, E., Körber, K., Ammer, C., Annighöfer, P. and Seidel, D., 2021. Three-dimensional quantification of tree architecture from mobile laser scanning and geometry analysis. *Trees*, pp.1-14.

Drake, J.B., Dubayah, R.O., Clark, D.B., Knox, R.G., Blair, J.B., Hofton, M.A., Chazdon, R.L., Weishampel, J.F. and Prince, S., 2002. Estimation of tropical forest structural characteristics using large-footprint lidar. *Remote Sensing of Environment*, *79*(2-3), pp.305-319.

Dubayah, R.O. and Drake, J.B., 2000. Lidar remote sensing for forestry. *Journal of forestry*, *98*(6), pp.44-46.

Escós, J.M., Alados, C.L. and Emlen, J.M., 1995. Fractal structures and fractal functions as disease indicators. *Oikos*, pp.310-314.

Escos, J., Alados, C.L., Pugnaire, F.I., Puigdefábregas, J. and Emlen, J., 2000. Stress resistance strategy in an arid land shrub: interactions between developmental instability and fractal dimension. *Journal of Arid Environments*, *45*(4), pp.325-336.

Estrada-Villegas, S., Hall, J. S., Van Breugel, M., & Schnitzer, S. A., 2020. Lianas reduce biomass accumulation in early successional tropical forests. *Ecology*, *101*(5), e02989.

Estrada-Villegas, S., Pedraza Narvaez, S.S., Sanchez, A. and Schnitzer, S.A., 2022. Lianas significantly reduce tree performance and biomass accumulation across tropical forests: a global meta-analysis. *Frontiers in Forests and Global Change*, *4*, p.812066.

Fadón, E., Fernandez, E., Behn, H. and Luedeling, E., 2020. A conceptual framework for winter dormancy in deciduous trees. *Agronomy*, *10*(2), p.241.

Fan, G., Feng, W., Chen, F., Chen, D., Dong, Y. and Wang, Z., 2020. Measurement of volume and accuracy analysis of standing trees using Forest Survey Intelligent Dendrometer. *Computers and Electronics in Agriculture*, *169*, p.105211.

Fan, G., Nan, L., Dong, Y., Su, X. and Chen, F., 2020. AdQSM: A New Method for Estimating Above-Ground Biomass from TLS Point Clouds. *Remote Sensing*, *12*(18), p.3089.

Faria, D., Mariano-Neto, E., Martini, A.M.Z., Ortiz, J.V., Montingelli, R., Rosso, S., Paciencia, M.L.B. and Baumgarten, J., 2009. Forest structure in a mosaic of rainforest sites: the effect of fragmentation and recovery after clear cut. *Forest Ecology and Management*, *257*(11), pp.2226-2234.

Fatoyinbo, T.E. and Simard, M., 2013. Height and biomass of mangroves in Africa from ICESat/GLAS and SRTM. *International Journal of Remote Sensing*, *34*(2), pp.668-681.

Fedigan, L. M., & Jack, K. M., 2012. Tracking neotropical monkeys in Santa Rosa: lessons from a regenerating Costa Rican dry forest. In *Long-term field studies of primates* (pp. 165-184). Springer, Berlin, Heidelberg.

Ford, E.D., 2014. The dynamic relationship between plant architecture and competition. *Frontiers in Plant Science*, *5*, p.275.

Foster, J. R., Townsend, P. A., & Zganjar, C. E., 2008. Spatial and temporal patterns of gap dominance by low-canopy lianas detected using EO-1 Hyperion and Landsat Thematic Mapper. *Remote Sensing of Environment*, *112*(5), 2104-2117.

Freeman, D.C., Graham, J.H. and Emlen, J.M., 1993. Developmental stability in plants: symmetries, stress and epigenesis. *Genetica*, *89*(1), pp.97-119.,

Fu, Y., Li, X., Zhou, X., Geng, X., Guo, Y. and Zhang, Y., 2020. Progress in plant phenology modeling under global climate change. *Science China Earth Sciences*, *63*(9), pp.1237-1247.

Gentry, A.H., 1988. Changes in plant community diversity and floristic composition on environmental and geographical gradients. *Annals of the Missouri botanical garden*, pp.1-34.

Gering, L.R. and May, D.M., 1995. The relationship of diameter at breast height and crown diameter for four species groups in Hardin County, Tennessee. *Southern Journal of Applied Forestry*, *19*(4), pp.177-181.

Gerwing, J.J., 2001. Testing liana cutting and controlled burning as silvicultural treatments for a logged forest in the eastern Amazon. *Journal of Applied Ecology*, *38*(6), pp.1264-1276.

Gerwing, J.J., Schnitzer, S.A., Burnham, R.J., Bongers, F., Chave, J., DeWalt, S.J., Ewango, C.E., Foster, R., Kenfack, D., Martínez-Ramos, M. and Parren, M., 2006. A standard protocol for liana censuses 1. *Biotropica: The Journal of Biology and Conservation*, *38*(2), pp.256-261.

Ghelardini, L., Berlin, S., Weih, M., Lagercrantz, U., Gyllenstrand, N. and Rönnberg-Wästljung, A.C., 2014. Genetic architecture of spring and autumn phenology in Salix. *BMC Plant Biology*, *14*(1), pp.1-18.

Grams, T.E. and Andersen, C.P., 2007. Competition for resources in trees: physiological versus morphological plasticity. In *Progress in botany* (pp. 356-381). Springer, Berlin, Heidelberg.

Guerra-Hernández, J., González-Ferreiro, E., Monleón, V.J., Faias, S.P., Tomé, M. and Díaz-Varela, R.A., 2017. Use of multi-temporal UAV-derived imagery for estimating individual tree growth in Pinus pinea stands. *Forests*, *8*(8), p.300.

Guzmán Q, J. A., Rivard, B., & Sánchez-Azofeifa, G. A., 2018. Discrimination of liana and tree leaves from a Neotropical Dry Forest using visible-near infrared and longwave infrared reflectance spectra. *Remote Sensing of Environment*, *219*, 135-144.

Guzmán, J., Hernandez, R., Sanchez-Azofeifa, G., 2020. rTLS: Tools to process point clouds derived from Terrestrial Laser Scanning. rTLS: Tools to process point clouds derived from Terrestrial Laser Scanning. Zenodo, https://doi.org/10.5281/zenodo.3525573

Guzmán Q, J. A., Sharp, I., Alencastro, F., & Sánchez-Azofeifa, G. A., 2020. On the relationship of fractal geometry and tree–stand metrics on point clouds derived from terrestrial laser scanning. *Methods in Ecology and Evolution*, *11*(10), 1309-1318.

Hajj, M.E., Baghdadi, N., Fayad, I., Vieilledent, G., Bailly, J.S. and Minh, D.H.T., 2017. Interest of integrating spaceborne LiDAR data to improve the estimation of biomass in high biomass forested areas. *Remote Sensing*, *9*(3), p.213.

Harper, K.A., Macdonald, S.E., Burton, P.J., Chen, J., Brosofske, K.D., Saunders, S.C., Euskirchen, E.S., Roberts, D.A.R., Jaiteh, M.S. and Esseen, P.A., 2005. Edge influence on forest structure and composition in fragmented landscapes. *Conservation biology*, *19*(3), pp.768-782.

Harrison, D., Rivard, B., & Sanchez-Azofeifa, A., 2018. Classification of tree species based on longwave hyperspectral data from leaves, a case study for a tropical dry forest. *International journal of applied earth observation and geoinformation*, *66*, 93-105.

Hedberg, E.C. and Ayers, S., 2015. The power of a paired t-test with a covariate. *Social science research*, *50*, pp.277-291.

Henkel, R., Hoehndorf, R., Kacprowski, T., Knüpfer, C., Liebermeister, W., & Waltemath, D., 2018. Notions of similarity for systems biology models. *Briefings in bioinformatics*, *19*(1), 77-88.

Hicks, D.J. and Chabot, B.F., 1985. Deciduous forest. In *Physiological ecology of North American plant communities* (pp. 257-277). Springer, Dordrecht.

Hilje, B., Stack, S., & Sánchez-Azofeifa, A., 2017. Lianas abundance is positively related with the avian acoustic community in tropical dry forests. *Forests*, *8*(9), 311.

Hollaus, M., Wagner, W., Eberhöfer, C. and Karel, W., 2006. Accuracy of large-scale canopy heights derived from LiDAR data under operational constraints in a complex alpine environment. *ISPRS Journal of Photogrammetry and Remote Sensing*, *60*(5), pp.323-338.

Honda, H., 1971. Description of the form of trees by the parameters of the tree-like body: Effects of the branching angle and the branch length on the shape of the tree-like body. *Journal of theoretical biology*, *31*(2), pp.331-338.

Hopkinson, C., Chasmer, L., Young-Pow, C., & Treitz, P., 2004. Assessing forest metrics with a ground-based scanning lidar. *Canadian Journal of Forest Research*, *34*(3), 573-583.

Hopkinson, C., Chasmer, L., Barr, A.G., Kljun, N., Black, T.A. and McCaughey, J.H., 2016. Monitoring boreal forest biomass and carbon storage change by integrating airborne laser scanning, biometry and eddy covariance data. *Remote Sensing of Environment*, *181*, pp.82-95.

Hosoi, F. and Omasa, K., 2007. Factors contributing to accuracy in the estimation of the woody canopy leaf area density profile using 3D portable lidar imaging. *Journal of experimental botany*, *58*(12), pp.3463-3473.

Hosoi, F., Nakai, Y., & Omasa, K., 2013. 3-D voxel-based solid modeling of a broad-leaved tree for accurate volume estimation using portable scanning lidar. *ISPRS Journal of Photogrammetry and Remote Sensing*, *82*, 41-48.

Hsu, H. and Lachenbruch, P.A., 2014. Paired t test. *Wiley StatsRef: statistics reference online*.

Hu, M., Lehtonen, A., Minunno, F. and Mäkelä, A., 2020. Age effect on tree structure and biomass allocation in Scots pine (Pinus sylvestris L.) and Norway spruce (Picea abies [L.] Karst.). *Annals of Forest Science*, *77*(3), pp.1-15.

Hu, M., Pitkänen, T. P., Minunno, F., Tian, X., Lehtonen, A., & Mäkelä, A., 2021. A new method to estimate branch biomass from terrestrial laser scanning data by bridging tree structure models. *Annals of Botany*.

Hu, T., Sun, X., Su, Y., Guan, H., Sun, Q., Kelly, M. and Guo, Q., 2021. Development and performance evaluation of a very low-cost UAV-LiDAR system for forestry applications. *Remote Sensing*, *13*(1), p.77.

Ichihashi, R. and Tateno, M., 2015. Biomass allocation and long-term growth patterns of temperate lianas in comparison with trees. *New Phytologist*, *207*(3), pp.604-612.

Ingwell, L.L., Joseph Wright, S., Becklund, K.K., Hubbell, S.P. and Schnitzer, S.A., 2010. The impact of lianas on 10 years of tree growth and mortality on Barro Colorado Island, Panama. *Journal of Ecology*, *98*(4), pp.879-887.

Janzen, D. H., 1987. Insect diversity of a Costa Rican dry forest: why keep it, and how?. *Biological Journal of the Linnean Society*, *30*(4), 343-356.

Janzen, D.H., 1988. Tropical dry forests. The most endangered major tropical ecosystem, in: Wilson, E.O. (Ed.), Biodiversity. National Academy Press, Washington, DC, USA, pp. 130– 137.

Jarron, L.R., Coops, N.C., MacKenzie, W.H., Tompalski, P. and Dykstra, P., 2020. Detection of sub-canopy forest structure using airborne LiDAR. *Remote Sensing of Environment*, *244*, p.111770.

Jucker, T., Bouriaud, O., Avacaritei, D., Dănilă, I., Duduman, G., Valladares, F. and Coomes, D.A., 2014. Competition for light and water play contrasting roles in driving diversity–productivity relationships in Iberian forests. *Journal of Ecology*, *102*(5), pp.1202-1213.

Jucker, T., Bouriaud, O. and Coomes, D.A., 2015. Crown plasticity enables trees to optimize canopy packing in mixed-species forests. *Functional Ecology*, *29*(8), pp.1078-1086.

Jucker, T., Asner, G.P., Dalponte, M., Brodrick, P.G., Philipson, C.D., Vaughn, N.R., Teh, Y.A., Brelsford, C., Burslem, D.F., Deere, N.J. and Ewers, R.M., 2018. Estimating aboveground carbon density and its uncertainty in Borneo's structurally complex tropical forests using airborne laser scanning. *Biogeosciences*, *15*(12), pp.3811-3830.

Jurjević, L., Liang, X., Gašparović, M. and Balenović, I., 2020. Is field-measured tree height as reliable as believed–Part II, A comparison study of tree height estimates from conventional field measurement and low-cost close-range remote sensing in a deciduous forest. *ISPRS Journal of Photogrammetry and Remote Sensing*, *169*, pp.227-241.

Kaasalainen, S., Krooks, A., Liski, J., Raumonen, P., Kaartinen, H., Kaasalainen, M., Puttonen, E., Anttila, K. and Mäkipää, R., 2014. Change detection of tree biomass with terrestrial laser scanning and quantitative structure modelling. *Remote Sensing*, *6*(5), pp.3906-3922.

Kappelle, M., Geuze, T., Leal, M.E. and Cleef, A.M., 1996. Successional age and forest structure in a Costa Rican upper montane Quercus forest. *Journal of Tropical Ecology*, *12*(5), pp.681-698.

Kalacska, M., Sanchez-Azofeifa, G.A., Calvo-Alvarado, J.C., Quesada, M., Rivard, B., Janzen, D.H., 2004. Species composition, similarity and diversity in three successional stages of a seasonally dry tropical forest. Forest Ecology and Management 200, 227–247.

Kalacska, M., Sanchez-Azofeifa, G. A., Rivard, B., Caelli, T., White, H. P., & Calvo-Alvarado, J. C., 2007. Ecological fingerprinting of ecosystem succession: Estimating secondary tropical dry forest structure and diversity using imaging spectroscopy. *Remote Sensing of Environment*, *108*(1), 82-96.

Kobler, A., Pfeifer, N., Ogrinc, P., Todorovski, L., Oštir, K. and Džeroski, S., 2007. Repetitive interpolation: A robust algorithm for DTM generation from Aerial Laser Scanner Data in forested terrain. *Remote sensing of environment*, *108*(1), pp.9-23.

Krishna Moorthy, S. M., Calders, K., Di Porcia e Brugnera, M., Schnitzer, S. A., & Verbeeck, H., 2018. Terrestrial laser scanning to detect liana impact on forest structure. *Remote Sensing*, *10*(6), 810.

Kurzel, B.P., Schnitzer, S.A. and Carson, W.P., 2006. Predicting liana crown location from stem diameter in three panamanian lowland forests 1. *Biotropica: The Journal of Biology and Conservation*, *38*(2), pp.262-266.

Lai, Y., Mu, X., Li, W., Zou, J., Bian, Y., Zhou, K., Hu, R., Li, L., Xie, D. and Yan, G., 2022. Correcting for the clumping effect in leaf area index calculations using one-dimensional fractal dimension. *Remote Sensing of Environment*, *281*, p.113259.

Lang, A.C., Härdtle, W., Bruelheide, H., Geißler, C., Nadrowski, K., Schuldt, A., Yu, M. and von Oheimb, G., 2010. Tree morphology responds to neighbourhood competition and slope in species-rich forests of subtropical China. *Forest Ecology and Management*, *260*(10), pp.1708-1715.

Larjavaara, M. and Muller-Landau, H.C., 2010. Rethinking the value of high wood density. *Functional Ecology*, *24*(4), pp.701-705.

Lau, A., Bentley, L.P., Martius, C., Shenkin, A., Bartholomeus, H., Raumonen, P., Malhi, Y., Jackson, T. and Herold, M., 2018. Quantifying branch architecture of tropical trees using terrestrial LiDAR and 3D modelling. *Trees*, *32*(5), pp.1219-1231.

Laurance, W. F., Goosem, M., & Laurance, S. G., 2009. Impacts of roads and linear clearings on tropical forests. *Trends in ecology & evolution*, *24*(12), 659-669.

Laurance, W.F., Andrade, A.S., Magrach, A., Camargo, J.L., Valsko, J.J., Campbell, M., Fearnside, P.M., Edwards, W., Lovejoy, T.E. and Laurance, S.G., 2014. Long-term changes in liana abundance and forest dynamics in undisturbed Amazonian forests. *Ecology*, *95*(6), pp.1604-1611.

Laurin, G.V., Puletti, N., Grotti, M., Stereńczak, K., Modzelewska, A., Lisiewicz, M., Sadkowski, R., Kuberski, Ł., Chirici, G. and Papale, D., 2020. Species dominance and above ground biomass in the Białowieża Forest, Poland, described by airborne hyperspectral and lidar data. *International Journal of Applied Earth Observation and Geoinformation*, *92*, p.102178.

Lefsky, M.A., Cohen, W.B., Harding, D.J., Parker, G.G., Acker, S.A. and Gower, S.T., 2002. Lidar remote sensing of above-ground biomass in three biomes. *Global ecology and biogeography*, *11*(5), pp.393-399.

Lefsky, M.A., Harding, D.J., Keller, M., Cohen, W.B., Carabajal, C.C., Del Bom Espirito-Santo, F., Hunter, M.O. and de Oliveira Jr, R., 2005. Estimates of forest canopy height and aboveground biomass using ICESat. *Geophysical research letters*, *32*(22).

Lewis, S. L., Malhi, Y., & Phillips, O. L., 2004. Fingerprinting the impacts of global change on tropical forests. *Philosophical Transactions of the Royal Society of London. Series B: Biological Sciences*, *359*(1443), 437-462.

Li, J., Yang, B., Cong, Y., Cao, L., Fu, X. and Dong, Z., 2019. 3D forest mapping using a low-cost UAV laser scanning system: Investigation and comparison. *Remote Sensing*, *11*(6), p.717.

Li, W., Cao, S., Campos-Vargas, C., & Sanchez-Azofeifa, A., 2017. Identifying tropical dry forests extent and succession via the use of machine learning techniques. *International Journal of Applied Earth Observation and Geoinformation*, *63*, 196-205.

Li, W., Campos-Vargas, C., Marzahn, P., & Sanchez-Azofeifa, A., 2018. On the estimation of tree mortality and liana infestation using a deep self-encoding network. *International Journal of Applied Earth Observation and Geoinformation*, *73*, 1-13.

Li, W. and Mu, X., 2021. Using fractal dimension to correct clumping effect in leaf area index measurement by digital cover photography. *Agricultural and Forest Meteorology*, *311*, p.108695.

Lim, K., Treitz, P., Wulder, M., St-Onge, B. and Flood, M., 2003. LiDAR remote sensing of forest structure. *Progress in physical geography*, *27*(1), pp.88-106.

Lin, Y.C., Liu, J., Fei, S. and Habib, A., 2021. Leaf-Off and Leaf-On UAV LiDAR Surveys for Single-Tree Inventory in Forest Plantations. *Drones*, *5*(4), p.115.

Liang, X., Kankare, V., Hyyppä, J., Wang, Y., Kukko, A., Haggrén, H., Yu, X., Kaartinen, H., Jaakkola, A., Guan, F. and Holopainen, M., 2016. Terrestrial laser scanning in forest inventories. *ISPRS Journal of Photogrammetry and Remote Sensing*, *115*, pp.63-77.

Liang, X., Hyyppä, J., Kaartinen, H., Lehtomäki, M., Pyörälä, J., Pfeifer, N., Holopainen, M., Brolly, G., Francesco, P., Hackenberg, J. and Huang, H., 2018. International benchmarking of terrestrial laser scanning approaches for forest inventories. *ISPRS journal of photogrammetry and remote sensing*, *144*, pp.137-179.

Lichti, D.D. and Jamtsho, S., 2006. Angular resolution of terrestrial laser scanners. *The Photogrammetric Record*, *21*(114), pp.141-160.

Liu, X., Ma, Q., Wu, X., Hu, T., Dai, G., Wu, J., Tao, S., Wang, S., Liu, L., Guo, Q. and Su, Y., 2022. Nonscalability of Fractal Dimension to Quantify Canopy Structural Complexity from Individual Trees to Forest Stands. *Journal of Remote Sensing*, *2022*, p.0001.

Lobos-Catalán, P., & Jiménez-Castillo, M., 2014. Different patterns of biomass allocation of mature and sapling host tree in response to liana competition in the southern temperate rainforest. *Austral Ecology*, *39*(6), 677-685.

Loría-Naranjo, M., Samper-Villarreal, J., & Cortés, J., 2014. Structural complexity and species composition of Potrero Grande and Santa Elena mangrove forests in Santa Rosa National Park, North Pacific of Costa Rica. *Revista de Biología Tropical*, *62*(4), 33-41.

Luoma, V., Saarinen, N., Wulder, M.A., White, J.C., Vastaranta, M., Holopainen, M. and Hyyppä, J., 2017. Assessing precision in conventional field measurements of individual tree attributes. *Forests*, *8*(2), p.38. Madsen, C., Kunz, M., von Oheimb, G., Hall, J., Sinacore, K., Turner, B.L. and Potvin, C., 2021. Influence of neighbourhoods on the extent and compactness of tropical tree crowns and root systems. *Trees*, pp.1-14.

MacFarlane, D.W. and Kane, B., 2017. Neighbour effects on tree architecture: functional trade-offs balancing crown competitiveness with wind resistance. *Functional Ecology*, *31*(8), pp.1624-1636.

Madsen, C., Kunz, M., von Oheimb, G., Hall, J., Sinacore, K., Turner, B.L. and Potvin, C., 2021. Influence of neighbourhoods on the extent and compactness of tropical tree crowns and root systems. *Trees*, *35*(5), pp.1673-1686.

Malhi, Y., Jackson, T., Patrick Bentley, L., Lau, A., Shenkin, A., Herold, M., Calders, K., Bartholomeus, H. and Disney, M.I., 2018. New perspectives on the ecology of tree structure and tree communities through terrestrial laser scanning. *Interface Focus*, *8*(2), p.20170052.

Mandelbrot, B.B., 1983. The fractal geometry of nature. Freeman, New York.

Maréchaux, I., Bartlett, M.K., Iribar, A., Sack, L. and Chave, J., 2017. Stronger seasonal adjustment in leaf turgor loss point in lianas than trees in an Amazonian forest. *Biology letters*, *13*(1), p.20160819.

Margolis, H.A., Nelson, R.F., Montesano, P.M., Beaudoin, A., Sun, G., Andersen, H.E. and Wulder, M.A., 2015. Combining satellite lidar, airborne lidar, and ground plots to estimate the amount and distribution of aboveground biomass in the boreal forest of North America. *Canadian Journal of Forest Research*, *45*(7), pp.838-855.

MATLAB and Statistics Toolbox Release 2012, The MathWorks, Inc., Natick, Massachusetts, United States

Matthews, E.R., Schmit, J.P. and Campbell, J.P., 2016. Climbing vines and forest edges affect tree growth and mortality in temperate forests of the US Mid-Atlantic States. *Forest Ecology and Management*, *374*, pp.166-173.

Maynard, R. J., Aall, N. C., Saenz, D., Hamilton, P. S., & Kwiatkowski, M. A., 2016. Road-edge effects on herpetofauna in a lowland Amazonian rainforest. *Tropical Conservation Science*, *9*(1), 264-290.

McConnaughay, K.D.M. and Coleman, J.S., 1999. Biomass allocation in plants: ontogeny or optimality? A test along three resource gradients. *Ecology*, *80*(8), pp.2581-2593.

McPherson, E.G., 2007. Benefit-based tree valuation. *Arboriculture & Urban Forestry 33 (1): 1-11*, *33*(1), pp.1-11.

Medina-Vega, J.A., Bongers, F., Schnitzer, S.A. and Sterck, F.J., 2021. Lianas explore the forest canopy more effectively than trees under drier conditions. *Functional Ecology*, *35*(2), pp.318-329.

Meunier, F., Verbeeck, H., Cowdery, B., Schnitzer, S.A., Smith-Martin, C.M., Powers, J.S., Xu, X., Slot, M., De Deurwaerder, H.P., Detto, M. and Bonal, D., 2021. Unraveling the relative role of light and water competition

between lianas and trees in tropical forests: A vegetation model analysis. *Journal of Ecology*, *109*(1), pp.519-540.

Mohandass, D., Campbell, M.J., Hughes, A.C., Mammides, C. and Davidar, P., 2017. The effect of altitude, patch size and disturbance on species richness and density of lianas in montane forest patches. *Acta Oecologica*, *83*, pp.1-14.

Moorthy, Sruthi M. Krishna, Yunfei Bao, Kim Calders, Stefan A. Schnitzer, and Hans Verbeeck. "Semi-automatic extraction of liana stems from terrestrial LiDAR point clouds of tropical rainforests." *ISPRS Journal of Photogrammetry and Remote Sensing* 154 (2019): 114-126.

Moorthy, Sruthi M. Krishna, Pasi Raumonen, Jan Van den Bulcke, Kim Calders, and Hans Verbeeck. "Terrestrial laser scanning for non-destructive estimates of liana stem biomass." *Forest Ecology and Management* 456 (2020): 117751.

Morsdorf, F., Mårell, A., Koetz, B., Cassagne, N., Pimont, F., Rigolot, E. and Allgöwer, B., 2010. Discrimination of vegetation strata in a multi-layered Mediterranean forest ecosystem using height and intensity information derived from airborne laser scanning. *Remote Sensing of Environment*, *114*(7), pp.1403-1415.

Murphy, P.G. and Lugo, A.E., 1986. Ecology of tropical dry forest. *Annual review of ecology and systematics*, *17*(1), pp.67-88.

Nambiar, E.S. and Sands, R., 1993. Competition for water and nutrients in forests. *Canadian Journal of Forest Research*, *23*(10), pp.1955-1968.

Nelson, R., 2010. Model effects on GLAS-based regional estimates of forest biomass and carbon. *International Journal of Remote Sensing*, *31*(5), pp.1359-1372.

Nelson, R., Margolis, H., Montesano, P., Sun, G., Cook, B., Corp, L., Andersen, H.E., deJong, B., Pellat, F.P., Fickel, T. and Kauffman, J., 2017. Lidar-based estimates of aboveground biomass in the continental US and Mexico using ground, airborne, and satellite observations. *Remote Sensing of Environment*, *188*, pp.127-140.

Newnham, G., Armston, J., Muir, J., Goodwin, N., Tindall, D., Culvenor, D., Püschel, P., Nyström, M. and Johansen, K., 2012. Evaluation of terrestrial laser scanners for measuring vegetation structure. *Australia: CSIRO*.

Nguyen, V.T., Constant, T., Kerautret, B., Debled-Rennesson, I. and Colin, F., 2020. A machine-learning approach for classifying defects on tree trunks using terrestrial LiDAR. *Computers and Electronics in Agriculture*, *171*, p.105332.

Novotny, J., Navratilova, B., Albert, J., Cienciala, E., Fajmon, L. and Brovkina, O., 2021. Comparison of spruce and beech tree attributes from field data, airborne and terrestrial laser scanning using manual and automatic methods. *Remote Sensing Applications: Society and Environment*, *23*, p.100574.

O'Brien, S.T., Hubbell, S.P., Spiro, P., Condit, R. and Foster, R.B., 1995. Diameter, height, crown, and age relationship in eight neotropical tree species. *Ecology*, *76*(6), pp.1926-1939.

Olofsson, K., Holmgren, J., & Olsson, H., 2014. Tree stem and height measurements using terrestrial laser scanning and the RANSAC algorithm. *Remote sensing*, *6*(5), 4323-4344.

Palleja, T., Tresanchez, M., Teixido, M., Sanz, R., Rosell, J. R., & Palacin, J., 2010. Sensitivity of tree volume measurement to trajectory errors from a terrestrial LIDAR scanner. *Agricultural and Forest Meteorology*, *150*(11), 1420-1427.

Paltineanu, C., Septar, L., Gavat, C., Chitu, E., Oprita, A., Moale, C., Calciu, I., Vizitiu, O. and Lamureanu, G., 2016. Characterising root density of peach trees in a semi-arid Chernozem to increase plant density. *International Agrophysics*, *30*(1).

Parolari, A. J., Paul, K., Griffing, A., Condit, R., Perez, R., Aguilar, S., & Schnitzer, S. A., 2020. Liana abundance and diversity increase with rainfall seasonality along a precipitation gradient in Panama. *Ecography*, *43*(1), 25-33.

Pearse, G.D., Dash, J.P., Persson, H.J. and Watt, M.S., 2018. Comparison of high-density LiDAR and satellite photogrammetry for forest inventory. *ISPRS journal of photogrammetry and remote sensing*, *142*, pp.257-267.

Peaucelle, M., Janssens, I.A., Stocker, B.D., Descals Ferrando, A., Fu, Y.H., Molowny-Horas, R., Ciais, P. and Peñuelas, J., 2019. Spatial variance of spring phenology in temperate deciduous forests is constrained by background climatic conditions. *Nature communications*, *10*(1), pp.1-10.

Pérez-Salicrup, D. R., & De Meijere, W., 2005. Number of lianas per tree and number of trees climbed by lianas at Los Tuxtlas, Mexico 1. *Biotropica: The Journal of Biology and Conservation*, *37*(1), 153-156.

Phillips, O.L., Martínez, R.V., Arroyo, L., Baker, T.R., Killeen, T., Lewis, S.L., Malhi, Y., Mendoza, A.M., Neill, D., Vargas, P.N. and Alexiades, M., 2002. Increasing dominance of large lianas in Amazonian forests. *Nature*, *418*(6899), pp.770-774.

Phillips, O.L., Vásquez Martínez, R., Monteagudo Mendoza, A., Baker, T.R. and Núñez Vargas, P., 2005. Large lianas as hyperdynamic elements of the tropical forest canopy. *Ecology*, *86*(5), pp.1250-1258. Pickett, S.T.A. and Kempf, J.S., 1980. Branching patterns in forest shrubs and understory trees in relation to habitat. *New Phytologist*, *86*(2), pp.219-228.

Polgar, C.A. and Primack, R.B., 2011. Leaf-out phenology of temperate woody plants: from trees to ecosystems. *New phytologist*, *191*(4), pp.926-941.

Poorter, L., Bongers, L. and Bongers, F., 2006. Architecture of 54 moist-forest tree species: traits, trade-offs, and functional groups. *Ecology*, *87*(5), pp.1289-1301.

Portillo-Quintero, C.A., Sánchez-Azofeifa, G.A., 2010. Extent and conservation of tropical dry forests in the Americas. Biological Conservation 143, 144–155.

Portillo-Quintero, C., Sanchez-Azofeifa, A. and Culvenor, D., 2014. Using VEGNET in-situ monitoring LiDAR (IML) to capture dynamics of plant area index, structure and phenology in aspen parkland forests in Alberta, Canada. *Forests*, *5*(5), pp.1053-1068.

Pretzsch, H. and Biber, P., 2010. Size-symmetric versus size-asymmetric competition and growth partitioning among trees in forest stands along an ecological gradient in central Europe. *Canadian Journal of Forest Research*, *40*(2), pp.370-384.

Rago, M.M., Urretavizcaya, M.F. and Defossé, G.E., 2021. Relationships among forest structure, solar radiation, and plant community in ponderosa pine plantations in the Patagonian steppe. *Forest Ecology and Management*, *502*, p.119749.

Raumonen, P., Kaasalainen, M., Åkerblom, M., Kaasalainen, S., Kaartinen, H., Vastaranta, M., Holopainen, M., Disney, M. and Lewis, P., 2013. Fast automatic precision tree models from terrestrial laser scanner data. *Remote Sensing*, *5*(2), pp.491-520.

Reich, K.F., Kunz, M. and von Oheimb, G., 2021. A new index of forest structural heterogeneity using tree architectural attributes measured by terrestrial laser scanning. *Ecological Indicators*, *133*, p.108412.

Reis, S.M., Marimon, B.S., Morandi, P.S., Elias, F., Esquivel-Muelbert, A., Marimon Junior, B.H., Fauset, S., de Oliveira, E.A., van der Heijden, G.M., Galbraith, D. and Feldpausch, T.R., 2020. Causes and consequences of liana infestation in southern Amazonia. *Journal of Ecology*, *108*(6), pp.2184-2197.

Reyes-Palomeque, G., Dupuy, J.M., Portillo-Quintero, C.A., Andrade, J.L., Tun-Dzul, F.J. and Hernandez-Stefanoni, J.L., 2021. Mapping forest age and characterizing vegetation structure and species composition in tropical dry forests. *Ecological Indicators*, *120*, p.106955.

Richards, T.J., Karacic, A., Apuli, R.P., Weih, M., Ingvarsson, P.K. and Rönnberg-Wästljung, A.C., 2020. Quantitative genetic architecture of adaptive phenology traits in the deciduous tree, Populus trichocarpa (Torr. and Gray). *Heredity*, *125*(6), pp.449-458.

Rocha-Santos, L., Pessoa, M.S., Cassano, C.R., Talora, D.C., Orihuela, R.L., Mariano-Neto, E., Morante-Filho, J.C., Faria, D. and Cazetta, E., 2016. The shrinkage of a forest: Landscape-scale deforestation leading to overall changes in local forest structure. *Biological Conservation*, *196*, pp.1-9.

Rödig, E., Cuntz, M., Heinke, J., Rammig, A. and Huth, A., 2017. Spatial heterogeneity of biomass and forest structure of the Amazon rain forest: Linking remote sensing, forest modelling and field inventory. *Global ecology and biogeography*, *26*(11), pp.1292-1302.

Rodríguez-Ronderos, M. E., Bohrer, G., Sanchez-Azofeifa, A., Powers, J. S. and Schnitzer, S. A., 2016. Contribution of lianas to plant area index and canopy structure in a Panamanian forest. Ecology, 97: 3271–3277. doi:10.1002/ecy.1597

Rodríguez-Veiga, P., Quegan, S., Carreiras, J., Persson, H.J., Fransson, J.E., Hoscilo, A., Ziółkowski, D., Stereńczak, K., Lohberger, S., Stängel, M. and Berninger, A., 2019. Forest biomass retrieval approaches from earth observation in different biomes. *International Journal of Applied Earth Observation and Geoinformation*, *77*, pp.53-68.

Rosell, J.R., Llorens, J., Sanz, R., Arno, J., Ribes-Dasi, M., Masip, J., Escolà, A., Camp, F., Solanelles, F., Gràcia, F. and Gil, E., 2009. Obtaining the three-dimensional structure of tree orchards from remote 2D terrestrial LIDAR scanning. *Agricultural and Forest Meteorology*, *149*(9), pp.1505-1515.

Rosell, J. R., & Sanz, R., 2012. A review of methods and applications of the geometric characterization of tree crops in agricultural activities. *Computers and Electronics in Agriculture*, *81*, 124-141.

Rouse Jr, J. W., R. H. Haas, D. W. Deering, and J. A. Schell. "Monitoring the vernal advancement and retrogradation (Green Wave Effect) of natural vegetation.[Great Plains Corridor]." (1973).

Rouvinen, S. and Kuuluvainen, T., 1997. Structure and asymmetry of tree crowns in relation to local competition in a natural mature Scots pine forest. *Canadian Journal of Forest Research*, *27*(6), pp.890-902.

Rubio, V.E. and Swenson, N.G., 2022. Functional groups, determinism and the dynamics of a tropical forest. *Journal of Ecology*, *110*(1), pp.185-196.

Rubio, V.E. and Swenson, N.G., 2023. On functional groups and forest dynamics. *Trends in Ecology & Evolution*.

Saarinen, N., Vastaranta, M., Vaaja, M., Lotsari, E., Jaakkola, A., Kukko, A., Kaartinen, H., Holopainen, M., Hyyppä, H. and Alho, P., 2013. Area-based approach for mapping and monitoring riverine vegetation using mobile laser scanning. *Remote Sensing*, *5*(10), pp.5285-5303..

Saarinen, N., Kankare, V., Vastaranta, M., Luoma, V., Pyörälä, J., Tanhuanpää, T., Liang, X., Kaartinen, H., Kukko, A., Jaakkola, A. and Yu, X., 2017. Feasibility of Terrestrial laser scanning for collecting stem volume information from single trees. *ISPRS Journal of Photogrammetry and Remote Sensing*, *123*, pp.140-158.

Sánchez-Azofeifa, G. A., Kalacska, M., do Espírito-Santo, M. M., Fernandes, G. W., & Schnitzer, S., 2009. Tropical dry forest succession and the contribution of lianas to wood area index (WAI). *Forest ecology and management*, *258*(6), 941-948.

Sánchez-Azofeifa, G.A., Castro, K., Wright, S.J., Gamon, J., Kalacska, M., Rivard, B., Schnitzer, S.A. and Feng, J.L., 2009. Differences in leaf traits, leaf internal structure, and spectral reflectance between two communities of lianas and trees: Implications for remote sensing in tropical environments. *Remote Sensing of Environment*, *113*(10), pp.2076-2088.

Sánchez-Azofeifa, A., Portillo-Quintero, C., & Durán, S. M., 2015. Structural effects of liana presence in secondary tropical dry forests using ground LiDAR. *Biogeosciences Discussions*, *12*(20).

Sánchez-Azofeifa, G.A., Guzmán-Quesada, J.A., Vega-Araya, M., Campos-Vargas, C., Durán, S.M., D'Souza, N., Gianoli, T., Portillo-Quintero, C. and Sharp, I., 2017. Can terrestrial laser scanners (TLSs) and hemispherical photographs predict tropical dry forest succession with liana abundance?. *Biogeosciences*, *14*(4), pp.977-988.

Sanchez-Azofeifa, A., Antonio Guzmán, J., Campos, C. A., Castro, S., Garcia-Millan, V., Nightingale, J., & Rankine, C., 2017. Twenty-first century remote sensing technologies are revolutionizing the study of tropical forests. *Biotropica*, *49*(5), 604-619.

Schnitzer, S.A. and Bongers, F., 2002. The ecology of lianas and their role in forests. *Trends in Ecology & Evolution*, *17*(5), pp.223-230.

Schnitzer, S.A., Kuzee, M.E. and Bongers, F., 2005. Disentangling above-and below-ground competition between lianas and trees in a tropical forest. *Journal of Ecology*, *93*(6), pp.1115-1125.

Schnitzer, S.A., 2005. A mechanistic explanation for global patterns of liana abundance and distribution. *The American Naturalist*, *166*(2), pp.262-276.

Schnitzer, S. A., DeWalt, S. J., & Chave, J., 2006. Censusing and Measuring Lianas: A Quantitative Comparison of the Common Methods 1. *Biotropica*, *38*(5), 581-591.

Schnitzer, S. A., & Carson, W. P., 2010. Lianas suppress tree regeneration and diversity in treefall gaps. *Ecology letters*, *13*(7), 849-857.

Schnitzer, S.A. and Bongers, F., 2011. Increasing liana abundance and biomass in tropical forests: emerging patterns and putative mechanisms. *Ecology letters*, *14*(4), pp.397-406.

Schnitzer, S.A., Mangan, S.A., Dalling, J.W., Baldeck, C.A., Hubbell, S.P., Ledo, A., Muller-Landau, H., Tobin, M.F., Aguilar, S., Brassfield, D. and Hernandez, A., 2012. Liana abundance, diversity, and distribution on Barro Colorado Island, Panama. *PloS one*, *7*(12), p.e52114.

Schnitzer, S.A., van der Heijden, G., Mascaro, J. and Carson, W.P., 2014. Lianas in gaps reduce carbon accumulation in a tropical forest. *Ecology*, *95*(11), pp.3008-3017.

Schnitzer, S.A., 2018. Testing ecological theory with lianas. *New Phytologist*, *220*(2), pp.366-380.

Selaya, N.G. and Anten, N.P.R., 2008. Differences in biomass allocation, light interception and mechanical stability between lianas and trees in early secondary tropical forest. *Functional Ecology*, *22*(1), pp.30-39.

Seidel, D., Leuschner, C., Müller, A. and Krause, B., 2011. Crown plasticity in mixed forests—quantifying asymmetry as a measure of competition using terrestrial laser scanning. *Forest Ecology and Management*, *261*(11), pp.2123-2132.

Seidel, D., 2018. A holistic approach to determine tree structural complexity based on laser scanning data and fractal analysis. *Ecology and evolution*, *8*(1), pp.128-134.

Seidel, D., Annighöfer, P., Stiers, M., Zemp, C.D., Burkardt, K., Ehbrecht, M., Willim, K., Kreft, H., Hölscher, D. and Ammer, C., 2019. How a measure of tree structural complexity relates to architectural benefit-to-cost ratio, light availability, and growth of trees. *Ecology and evolution*, *9*(12), pp.7134-7142.

Shenkin, A., Bentley, L.P., Oliveras, I., Salinas, N., Adu-Bredu, S., Marimon-Junior, B.H., Marimon, B.S., Peprah, T., Choque, E.L., Trujillo Rodriguez, L. and Clemente Arenas, E.R., 2020. The influence of ecosystem and phylogeny on tropical tree crown size and shape. *Frontiers in Forests and Global Change*, *3*, p.109.

Shimizu, K., Nishizono, T., Kitahara, F., Fukumoto, K. and Saito, H., 2022. Integrating terrestrial laser scanning and unmanned aerial vehicle photogrammetry to estimate individual tree attributes in managed coniferous forests in Japan. *International Journal of Applied Earth Observation and Geoinformation*, *106*, p.102658.

Shrestha, M., Broadbent, E.N. and Vogel, J.G., 2021. Using GatorEye UAV-Borne LiDAR to Quantify the Spatial and Temporal Effects of a Prescribed Fire on Understory Height and Biomass in a Pine Savanna. *Forests*, *12*(1), p.38.

Smith-Martin, C.M., Xu, X., Medvigy, D., Schnitzer, S.A. and Powers, J.S., 2020. Allometric scaling laws linking biomass and rooting depth vary across ontogeny and functional groups in tropical dry forest lianas and trees. *New Phytologist*, *226*(3), pp.714-726.

Stahl, W. R., 1962. Similarity and Dimensional Methods in Biology: They promise to show quantitative similarities between biological organisms and models of biological systems. *Science*, *137*(3525), 205-212.

Sumida, A., Miyaura, T. and Torii, H., 2013. Relationships of tree height and diameter at breast height revisited: analyses of stem growth using 20-year data of an even-aged Chamaecyparis obtusa stand. *Tree physiology*, *33*(1), pp.106-118.

Sun, G., Ranson, K.J., Kimes, D.S., Blair, J.B. and Kovacs, K., 2008. Forest vertical structure from GLAS: An evaluation using LVIS and SRTM data. *Remote Sensing of Environment*, *112*(1), pp.107-117.

Sun, G., Niu, Z., Gao, S., Huang, W., Wang, L., Li, W. and Feng, M., 2014, November. 32-channel hyperspectral waveform LiDAR instrument to monitor vegetation: design and initial performance trials. In *Multispectral, Hyperspectral, and Ultraspectral Remote Sensing Technology, Techniques and Applications V* (Vol. 9263, p. 926331). International Society for Optics and Photonics.

Thorpe, H.C., Astrup, R., Trowbridge, A. and Coates, K.D., 2010. Competition and tree crowns: a neighborhood analysis of three boreal tree species. *Forest ecology and management*, *259*(8), pp.1586-1596.

Vaaja, M., Virtanen, J.P., Kurkela, M., Lehtola, V., Hyyppä, J. and Hyyppä, H., 2016, June. The Effect of Wind on Tree Stem Parameter Estimation Using Terrestial Laser Scanning. In *International Society for Photogrammetry and Remote Sensing Workshop on Laser Scanning* (pp. 117-122). ISPRS.

Vabalas, A., Gowen, E., Poliakoff, E. and Casson, A.J., 2019. Machine learning algorithm validation with a limited sample size. *PloS one*, *14*(11), p.e0224365.

Van Der Heijden, G. M., & Phillips, O. L., 2009. Environmental effects on Neotropical liana species richness. *Journal of Biogeography*, *36*(8), 1561-1572.

van der Heijden, G. M., Feldpausch, T. R., de la Fuente Herrero, A., van der Velden, N. K., & Phillips, O. L., 2010. Calibrating the liana crown occupancy index in Amazonian forests. *Forest Ecology and Management*, *260*(4), 549-555.

Van der Heijden, G. M., Schnitzer, S. A., Powers, J. S., & Phillips, O. L., 2013. Liana impacts on carbon cycling, storage and sequestration in tropical forests. *Biotropica*, *45*(6), 682-692.

Van Der Heijden, G.M., Powers, J.S. and Schnitzer, S.A., 2015. Lianas reduce carbon accumulation and storage in tropical forests. *Proceedings of the National Academy of Sciences*, *112*(43), pp.13267-13271.

van der Heijden, G.M., Powers, J.S. and Schnitzer, S.A., 2019. Effect of lianas on forest-level tree carbon accumulation does not differ between seasons: Results from a liana removal experiment in Panama. *Journal of Ecology*, *107*(4), pp.1890-1900.

van der Heijden, G.M., Proctor, A.D., Calders, K., Chandler, C.J., Field, R., Foody, G.M., Krishna Moorthy, S.M., Schnitzer, S.A., Waite, C.E. and Boyd, D.S., 2022. Making (remote) sense of lianas. *Journal of Ecology*, *110*(3), pp.498-513.

Van der Zande, D., Hoet, W., Jonckheere, I., van Aardt, J., & Coppin, P., 2006. Influence of measurement set-up of ground-based LiDAR for derivation of tree structure. *Agricultural and Forest Meteorology*, *141*(2), 147-160.

Van der Zande, D., Mereu, S., Nadezhdina, N., Cermak, J., Muys, B., Coppin, P., & Manes, F. (2009). 3D upscaling of transpiration from leaf to tree using ground-based LiDAR: Application on a Mediterranean Holm oak (Quercus ilex L.) tree. *Agricultural and Forest Meteorology*, *149*(10), 1573-1583.

Van Der Sande, M.T., Poorter, L., Schnitzer, S.A., Engelbrecht, B.M. and Markesteijn, L., 2019. The hydraulic efficiency–safety trade-off differs between lianas and trees. *Ecology*, *100*(5), p.e02666.

Van Leeuwen, M., & Nieuwenhuis, M., 2010. Retrieval of forest structural parameters using LiDAR remote sensing. *European Journal of Forest Research*, *129*(4), 749-770.

van Melis, J., Camargo, M. G. G., Carvalho, P. G., Morellato, L. P. C., & Grombone-Guaratini, M. T. (2021). Contrasting edge effect on lianas and trees in a cerrado savanna remnant. *Austral Ecology*, *46*(2), 192-203.

Verbeeck, H., Bauters, M., Jackson, T., Shenkin, A., Disney, M. and Calders, K., 2019. Time for a plant structural economics spectrum. *Frontiers in Forests and Global Change*, *2*, p.43.

Vicari, M.B., Disney, M., Wilkes, P., Burt, A., Calders, K. and Woodgate, W., 2019. Leaf and wood classification framework for terrestrial LiDAR point clouds. *Methods in Ecology and Evolution*, *10*(5), pp.680-694.

Visser, M.D., Muller-Landau, H.C., Schnitzer, S.A., de Kroon, H., Jongejans, E. and Wright, S.J., 2018. A host–parasite model explains variation in liana infestation among co-occurring tree species. *Journal of Ecology*, *106*(6), pp.2435-2445.

Visser, M.D., Detto, M., Meunier, F., Wu, J., Foster, J.R., Marvin, D.C., van Bodegom, P.M., Bongalov, B., Nunes, M.H., Coomes, D. and Verbeeck, H., 2021. Why can we detect lianas from space?. *bioRxiv*, pp.2021-09.

Waite, C.E., van der Heijden, G.M., Field, R., Burslem, D.F., Dalling, J.W., Nilus, R., Rodríguez-Ronderos, M.E., Marshall, A.R. and Boyd, D.S., 2023. Landscape-scale drivers of liana load across a Southeast Asian forest canopy differ to the Neotropics. *Journal of Ecology*, *111*(1), pp.77-89.

Wallace, L., Lucieer, A., Turner, D. and Watson, C., 2011. Error assessment and mitigation for hyper-temporal UAV-borne LiDAR surveys of forest inventory. *Proceedings of Silvilaser*, pp.1-13.

Wallace, L., Lucieer, A., Watson, C. and Turner, D., 2012. Development of a UAV-LiDAR system with application to forest inventory. *Remote sensing*, *4*(6), pp.1519-1543.

Wang, Y., Lehtomäki, M., Liang, X., Pyörälä, J., Kukko, A., Jaakkola, A., Liu, J., Feng, Z., Chen, R. and Hyyppä, J., 2019. Is field-measured tree height as reliable as believed–A comparison study of tree height estimates from field measurement, airborne laser scanning and terrestrial laser scanning in a boreal forest. *ISPRS Journal of Photogrammetry and Remote Sensing*, *147*, pp.132-145.

Wang, Q., Pang, Y., Chen, D., Liang, X. and Lu, J., 2021. Lidar biomass index: A novel solution for tree-level biomass estimation using 3D crown information. *Forest Ecology and Management*, *499*, p.119542.

West, P.W., 2015. *Tree and forest measurement*. Springer.

Wiant Jr, H.V., Wood, G.B. and Williams, M., 1996. Comparison of three modern methods for estimating volume of sample trees using one or two diameter measurements. *Forest ecology and management*, *83*(1-2), pp.13-16.

Wilkes, P., Lau, A., Disney, M., Calders, K., Burt, A., de Tanago, J.G., Bartholomeus, H., Brede, B. and Herold, M., 2017. Data acquisition considerations for terrestrial laser scanning of forest plots. *Remote Sensing of Environment*, *196*, pp.140-153.

de Winter, J.C.F., 2013 "Using the Student's t-test with extremely small sample sizes," *Practical Assessment, Research, and Evaluation*: Vol. 18 , Article 10. DOI: https://doi.org/10.7275/e4r6-dj05

White, J.C., Wulder, M.A. and Buckmaster, G., 2014. Validating estimates of merchantable volume from airborne laser scanning (ALS) data using weight scale data. *The Forestry Chronicle*, *90*(3), pp.378-385.White et al. 2014

Wright, A., Tobin, M., Mangan, S. and Schnitzer, S.A., 2015. Unique competitive effects of lianas and trees in a tropical forest understory. *Oecologia*, *177*(2), pp.561-569.

Wu, X., Shen, X., Cao, L., Wang, G. and Cao, F., 2019. Assessment of individual tree detection and canopy cover estimation using unmanned aerial vehicle based light detection and ranging (UAV-LiDAR) data in planted forests. *Remote Sensing*, *11*(8), p.908.

Xi, Z., Hopkinson, C. and Chasmer, L., 2018. Filtering stems and branches from terrestrial laser scanning point clouds using deep 3-D fully convolutional networks. *Remote Sensing*, *10*(8), p.1215.

Xue, L., Pan, L., Zhang, R. and Xu, P.B., 2011. Density effects on the growth of self-thinning Eucalyptus urophylla stands. *Trees*, *25*(6), pp.1021-1031.

Yang, X., Strahler, A.H., Schaaf, C.B., Jupp, D.L., Yao, T., Zhao, F., Wang, Z., Culvenor, D.S., Newnham, G.J., Lovell, J.L. and Dubayah, R.O., 2013. Three-dimensional forest reconstruction and structural parameter retrievals using a terrestrial full-waveform lidar instrument (Echidna®). *Remote sensing of environment*, *135*, pp.36-51.

Yao, W., Krzystek, P. and Heurich, M., 2012. Tree species classification and estimation of stem volume and DBH based on single tree extraction by exploiting airborne full-waveform LiDAR data. *Remote Sensing of Environment*, *123*, pp.368-380.

Zhang, J., Zhang, Z., Lutz, J.A., Chu, C., Hu, J., Shen, G., Li, B., Yang, Q., Lian, J., Zhang, M. and Wang, X., 2022. Drone-acquired data reveal the importance of forest canopy structure in predicting tree diversity. *Forest Ecology and Management*, *505*, p.119945.

Zotz, G., Cueni, N. and Körner, C., 2006. In situ growth stimulation of a temperate zone liana (Hedera helix) in elevated CO2. *Functional Ecology*, *20*(5), pp.763-769.